Year : 2019

Identification and Isolation of Highly Functional Tumor-Specific CD8 T Cenis for Adoptive Cell Transfer Therapy

Magnin Morgane

Magnin Morgane, 2019, Identification and Isolation of Highly Functional Tumor-Specific CD8 T Cenis for Adoptive Cell Transfer Therapy

Originally published at : Thesis, University of Lausanne

Posted at the University of Lausanne Open Archive http://serval.unil.ch
Document URN : urn:nbn:ch:serval-BIB_E25A9568380B1

UNIL | Université de Lausanne
Faculté de biologie et de médecine

DEPARTEMENT D'ONCOLOGIE

Identification and Isolation of Highly Functional Tumor-Specific CD8 T Cells for Adoptive Cell Transfer Therapy

Thèse de doctorat ès sciences de la vie (PhD)

présentée à la

Faculté de biologie et de médecine
de l'Université de Lausanne

par

Morgane MAGNIN

Ingénieure diplômée de l'INSA de Lyon, Biochimie et Biotechnologies, FR

Jury

Prof. Ping-Chih HO, Président
Dr. Alexandre HARARI, Directeur de thèse
Prof. George COUKOS, Co-directeur de thèse
Dr. Julien SCHMIDT, Superviseur
Prof. Olivier MICHIELIN, expert
Prof. Camilla JANDUS, expert
Prof. Sine REKER HADRUP, expert externe

Lausanne (2019)

UNIL | Université de Lausanne
Faculté de biologie et de médecine

Ecole Doctorale
Doctorat ès sciences de la vie

Imprimatur

Vu le rapport présenté par le jury d'examen, composé de

Président·e	Monsieur	Prof.	Ping-Chih	**Ho**
Directeur·trice de thèse	Monsieur	Dr	Alexandre	**Harari**
Co-directeur·trice	Monsieur	Prof.	George	**Coukos**
Expert·e·s	Madame	Prof.	Camilla	**Jandus**
	Monsieur	Prof.	Olivier	**Michielin**
	Madame	Prof.	Sine	**Reker Hadrup**

le Conseil de Faculté autorise l'impression de la thèse de

Madame Morgane Magnin

Ingénieure en biochimie et biotechnologies,
Institut National des Sciences Appliquées de Lyon, France

intitulée

Identification and isolation of highly functional tumor-specific CD8 T cells for adoptive cell transfer therapy

Lausanne, le 6 décembre 2019

pour le Doyen
de la Faculté de biologie et de médecine

Prof. Ping-Chih Ho

Remerciements

Je tiens premièrement à remercier mon directeur de thèse Alex qui m'a encadrée pendant ces quatre longues années de thèse et m'a fait part de ses brillantes idées et intuitions lors de discussions passionnées. Son exigence et son sens du détail m'ont permis de me surpasser et de comprendre ce que rigueur et précision signifiaient. Je souhaite souligner sa disponibilité permanente, sa patience et la compréhension dont il a fait preuve et qui m'ont apporté un sérieux renfort en périodes de travail soutenues. Merci aussi à mon co-directeur de thèse, Professeur George Coukos, sans qui cette recherche n'aurait pu voir le jour. Un grand merci pour ses analyses et idées ayant fortement inspiré ma thèse. Je souhaite exprimer ma gratitude envers Professeur Immanuel Luescher m'ayant acceptée en stage de master dans son laboratoire et avec qui j'ai beaucoup échangé sur mon sujet.

J'adresse également mes profonds remerciements à Julien qui m'a supervisée tout au long du doctorat et à qui je dois beaucoup. Il a su transmettre avec une grande pédagogie son savoir-faire et connaissances dont j'ai pu bénéficier. Qu'il soit aussi remercié pour sa patience, son honnêteté, sa gentillesse et pour les nombreux encouragements qu'il m'a prodigués. Son aide scientifique, ses nombreux conseils, son humour et son soutien psychologique ont solidement contribué à l'achèvement de ce projet.

Aussi, je voulais remercier la merveilleuse équipe Harari. Un grand merci à Julien, Marie-Aude et Julien qui m'ont assistée à répétition sur les expériences *in vivo*, la culture cellulaire et synthèse de molécules. Sans leur aide précieuse lors des dernières semaines, cette thèse n'aurait sûrement pas aboutir. Un grand merci à Raphael, Lise et Patrick pour leur aide sur le TCR séquençages et les nombreuses discussions et conseils prodigués en biologie moléculaire. Merci à Philippe, Luis et Stéphane pour vos précieux conseils et la synthèse de tetramers et peptides de qualité. Merci à Sara, Petra, Blanca, Valentina, Alex, Marie-Aude, Aymeric et Anne-Christine pour les nombreux échanges scientifiques, votre travail colossal en amont et vos précieux conseils. Enfin, un merci particulier à Marion, Alex, Marie-Aude, Lise, Julien, Margaux, Johanna, Anne-Christine et qui m'ont assisté techniquement et psychologiquement, et surtout qui ont contribué à un environnement de travail d'exception où régnaient rires et entraide. Enfin, merci à la « FACS Facility », particulièrement à Romain et Danny pour leur immense patience face aux innombrables échantillons à trier.

Je tiens à remercier chaleureusement tous les membres de ma famille et particulièrement mes parents et grands-parents qui m'ont considérablement soutenue lors des moments difficiles, ont toujours été à l'écoute, supporté mes humeurs exécrables ou m'ont cuisiné d'innombrables bons petits plats. Un grand merci à mes amis dont le soutien psychologique a été déterminant. Merci pour leur compréhension lors des annulations ou des soirées écourtées. Enfin, je viens exprimer ma profonde gratitude à mon compagnon de vie, Pierre-Joany, ayant partagé avec moi cette aventure et fait preuve d'une immense patience et gentillesse au quotidien. Son écoute, ses conseils, son assistance et son réconfort m'ont permis de résister jusqu'à la fin de ce long parcours, et ont apporté le soutien et la tendresse nécessaire à l'aboutissement de cette thèse.

Résumé large public

Une multitude d'études ont confirmé l'immense potentiel clinique des immunothérapies antitumorales. Ces dernières visent à induire, amplifier ou rediriger le système immunitaire contre la tumeur du patient. Parmi diverses immunothérapies, le transfert adoptif de globules blancs appelés lymphocytes (ACT) se fonde sur i) l'extraction des lymphocytes du système immunitaire d'un patient issues du sang ou la tumeur ii) la sélection des lymphocytes effecteurs dirigés contre la tumeur, iii) leur expansion clonale en laboratoire (*in vitro*), iv) la réinjection des lymphocytes amplifiées dans le patient afin de bénéficier d'un nombre conséquent de cellules pouvant détruire spécifiquement la tumeur. L'ACT repose sur la reconnaissance effective des cellules tumorales cibles, grâce à des éléments protéiques (peptides) présentés à leur surface et appelés antigènes (Ags). Issus de protéines intracellulaires clivées et présentées en surface par des complexes particuliers, les Ags permettent aux lymphocytes T de détecter des anomalies ou des infections virales ayant induit un changement protéique grâce à leur récepteur membranaire unique spécifique d'un Ag (« T cell receptor » : TCR). La force d'interaction entre le TCR (exprimé par les lymphocytes) et l'Ag (présenté par les cellules tumorales) est un paramètre clé corrélant avec la réponse immunitaire antitumorale. Les lymphocytes T sont éduqués dans le thymus pour ne survivre et s'activer qu'en cas d'interaction forte avec des Ags du « non-soi ». Toutefois, les tumeurs présentent fréquemment des Ags du « soi » générant des interactions faibles avec la majorité des TCRs et limitant ainsi les réponses antitumorales. La récente découverte d'Ags issus de mutations tumorales, appelés néoantigènes (NeoAgs), a suscité un nouvel espoir en oncologie. Constituant un élément du « non-soi », la présence de ces NeoAgs et de mutations tumorales ont été corrélés à de nombreux succès thérapeutiques. En revanche, leur supériorité face aux Ags « soi » (TAA) surexprimés par les tumeurs n'a pas été clairement démontrée et l'analyse des interactions entre lymphocytes T et divers Ags tumoraux est nécessaire afin de renforcer leur intérêt et améliorer leur sélection. Ce projet de thèse vise à améliorer l'ACT par l'identification des meilleurs Ags cibles et l'isolation des lymphocytes T les plus fonctionnels. La caractérisation des lymphocytes T ciblant les NeoAgs, TAAs et Ags viraux a été effectuée de manière approfondie. Cette étude a démontré que les cellules T visant les NeoAgs et Ags tumoraux ne sont pas fonctionnellement différentes, à l'inverse des interactions biophysiques, plus élevées pour celles ciblant les NeoAgs. De plus, les lymphocytes T isolés des tumeurs ont présenté une meilleure fonction et affinité d'interaction que les homologues du sang, démontrant la meilleure capacité des cellules hautement fonctionnelles à infiltrer la tumeur et à se multiplier. Enfin, la corrélation entre l'affinité TCR-Ag, la fonction cellulaire et le contrôle tumoral *in vivo* ont prouvé l'intérêt d'utiliser des méthodes biophysiques stables évaluant rapidement le potentiel thérapeutique d'une cellule.

Ces observations ont permis en annexe l'établissement d'outils pour rapidement identifier les lymphocytes T à haut intérêt thérapeutique.

Résumé

Le rôle des lymphocytes T dans le contrôle d'un grand nombre de tumeurs n'est plus à questionner. Cependant, le type d'antigènes permettant au système immunitaire de distinguer les cellules tumorales des cellules saines reste flou. De nombreuses études montrent que des antigènes dérivés de mutations somatiques des tumeurs donnent lieu à des séquences peptidiques nouvelles, appelées neoantigènes (NeoAg), qui sont absentes du génome et du protéome des cellules saines. Ces NeoAg sont donc des antigènes pour cibler spécifiquement les tumeurs et de nombreuses études les associent aux réponses cliniques des immunothérapies.

De surcroit, en plus de leur spécificité tumorale, ces antigènes étant du « non-soi », il n'existe pas de tolérances des cellules les reconnaissant (au même titre que les cellules ciblant des antigènes viraux et donc au contraire des antigènes dérivés d'antigènes associés aux tumeurs (AAT)). Cela suggère que les cellules ciblant les NeoAg devraient être d'avantage fonctionnels que celles ciblant les AAT (pour lesquels les lymphocytes les plus fonctionnels ont été éliminés). Cependant, les différences fonctionnelles entre cellules ciblant les NeoAg ou les AAT n'ont jamais été établies, au même titre que leur autres caractéristiques phénotypiques ou moléculaires. De plus, les paramètres définissant les cellules cliniquement efficaces ou celles infiltrant les tumeurs après un transfert adoptif sont mal connus.

Dans cette étude, nous avons comparé l'affinité structurelle et l'avidité fonctionnelle d'une librairie de lymphocytes spécifiques à plusieurs NeoAg, AAT et antigènes viraux isolés du sang et des tumeurs de patients souffrant de mélanome ou de cancer du côlon, poumon ou ovaire. Pour ce faire, nous avons utilisé des complexes de peptide-MHC réversibles.

Nos analyses montrent que les cellules ciblant les NeoAg ne se distinguent pas de celles ciblant les AAT par leur avidité fonctionnelle mais par leur affinité structurelle. Les cellules hautement fonctionnelles s'accumulent dans les tumeurs alors que les cellules peu fonctionnelles s'accumulent dans le sang, en lien avec le niveau d'expression de molécules de tropisme tumorale. Finalement, nous avons aussi démontré qu'il y a une fourchette optimale de fonctionnalité cellulaire permettant l'infiltration des tumeurs après transfert adoptif ainsi que les contrôle des tumeurs *in vivo*.

Dans l'ensemble, nos études démontrent que des cellules de haute affinité structurelle ciblant des NeoAg s'accumulent dans les tumeurs de patients naïfs à l'immunothérapie.

Ces observations indiquent que des filtres fonctionnels ou des méthodologies permettant un enrichissement en cellules fonctionnelles doivent être considérés dans la panoplie des paramètres pour améliorer les produits cellulaires pour les transferts adoptifs thérapeutiques.

Summary

The clinical relevance of T cells in the control of a diverse set of human cancers is now beyond doubt. However, the nature of the antigens as well as the functional profile of T cells that allow the immune system to efficiently distinguish tumor cells from benign cells has long remained obscure. Growing evidences suggest that such tumor epitopes can derive from antigens known as neoantigens (NeoAg), which have novel protein sequences resulting from tumor-specific somatic mutations and which are consequently absent from the normal human genome and proteome. Targeting such neoantigens is promising and theoretically enables immune cells to distinguish cancer cells from normal cells, leading to cancer rejection. Indeed, several studies confirmed that neoantigens recognition is a major factor in the success of clinical immunotherapies.

Of note, in addition to their tumor-specificity (limiting the risk of autoimmunity), neoantigens also represent very attractive and highly promising targets for immunotherapies since these antigens are non-self and thus are not subjected to negative thymic selection. Consequently, it is generally accepted that the repertoire of T-cell recognizing neoantigens is unbiased and thus composed of high-affinity T cells, comparable to virus-specific T cells and different from T cells directed against shared tumor-associated antigens (TAA) where high-affinity T cells are deleted during thymic selection. However, the functional profile of NeoAg-specific T cells was never comprehensively investigated and it is unclear what distinguishes NeoAg- from other TAA-specific T cells from a functional but also phenotypic or molecular standpoint. In addition to the functional heterogeneity of tumor-specific T cells, which remains to be addressed, the most relevant functional parameter associated with tumor infiltration and clinical efficacy is lacking.

Here, using proprietary pMHC class I reversible multimers (NTAmers), allowing measurement of monomeric pMHC-TCR dissociation kinetics (off-rates) on viable CD8 T cells, we comprehensively profiled the structural affinity (off-rates) and the functional avidity (antigen sensitivity) of peripheral (PBLs) and tumor-infiltrating (TILs) CD8 T cells targeting viral epitopes, TAA, and NeoAgs isolated from immunotherapy-naïve patients with melanoma or ovarian, colorectal or lung cancers. The relative accumulation of T-cell clones in tumors or in blood was associated to functional parameters but also to the expression of tumor homing markers. Finally, the ability of functionally-distinct T-cells to infiltrate and control tumors was evaluated *in vivo*.

Overall, our observations indicated that NeoAg-specific CD8 T cells are superior to TAA-specific T cells with regard to their structural but not functional avidity. High-affinity tumor-specific T cells accumulate in tumors, consistently with their ability to express and upregulate markers of tumor tropism and an optimal range of affinity is required to allow adoptively-transferred T cells to infiltrate and control tumors *in vivo*. Taken together, our data indicate that high structural affinity NeoAg-specific CD8 T cells preferentially accumulate in human tumors.

Our data indicate that structural/functional filters or methodologies to enrich in highly-functional T-cells should be considered in the armamentarium of parameters to improve cellular products for ACT therapies.

Abbreviations

Ab ..... *Antibody*
ACT ..... *Adoptive cell transfer therapy*
Ag ..... Antigen
APC ..... *Antigen presenting cells*
B cells ..... *B-lymphocytes*
CAR-T ..... Chimeric antigen receptor T therapy
CD ..... Cluster of differentiation
CTLA-4 ..... *Cytotoxic T-lymphocyte-associated protein 4*
DCs ..... *Dendritic cells, Dendritic cells*
DNA ..... Deoxyribonucleic acid
IDO ..... *Indoleamine 2,3-dioxygenase*
IFN ..... *Interferon*
Ig ..... Immunoglobulin
IL-2 ..... *Interleukin*
LN ..... *Lymph node*
NeoAg ..... *Neoantigen*
PD-1 ..... *Program cell death -1*
MHC ..... major histocompatibility complex
SLO ..... *Secondary lymphoid organ*
T cells ..... *T-lymphocytes*
T_{CM} cells ..... *Central memory CD8 T cells*
TCR ..... T cell receptor
T_{EM} cells ..... *Effector memory T cells*
Th cells ..... *T helper cells*
TME ..... Tumor micro-environment
Treg ..... *Regulatory T-cell*
T_{RM} ..... Resident memory T cells
TSA ..... *Tumor specific antigens*
T_{SCM} ..... *Stem cell-like CD8+ T cell*

Table of contents

Remerciements *3*

Résumé large public *5*

Résumé *7*

Summary *9*

Abbreviations *11*

Table of contents *12*

General introduction *14*

A. The immune system: **14**

1. Cellular elements of the adaptive immune system 14
2. T cell development 16
3. CD8 T cell response 18
4. TCR Signaling 20
5. CD8 T cell dysfunction 22
6. Peripheral tolerance of T cells 23

B. Cancer and immune system interactions **26**

1. Cancer development 26
2. Cancer antigens 29
3. Cancer immunotherapy 32

C. Identification, isolation and characterization of antigen-specific T cell **40**

1. Antigen-specific T cell identification 40
2. Antigen-specific T cell characterization 41

General aims *43*

Thesis work *44*

High Structural Affinity Neoantigen-Specific CD8 T Cells Preferentially Accumulate in Human Tumors *45*

A. Aim **45**

B. Introduction **46**

C. Materials and Methods **47**

D. Results **54**

E. Discussion **65**

General conclusion *74*

Perspectives *74*

Appendix *76*

A. Supplementary figures **76**

B. Side project: TCR repertoire subtraction assay: a new method for rapid identification of highly potent tumor-specific TCRs **86**

1. Aim 86
2. Results 87
3. Discussion 93

References *96*

C. Book chapter **115**

General introduction

A. The immune system:

Throughout their history, living beings have never stopped adapting to a changing environment. Among other things, advanced vertebrates have evolved through the elaboration of complex means of defense (*6*).The immune system is defined as the body's natural defense, aiming to fight against infections, noxious substances and diseases such as cancer. It is composed of a collection of specific tissues, cells and soluble molecules and is divided in three main structures: i) the epithelial barriers, representing the first physical protective fence, ii) the innate immune system, inherited from a primitive version of the defense mechanisms, iii) the adaptive immune system, resulting from a more sophisticated evolution of the means of protection. Besides physical barrier, immune system is mainly based on the distinction between "self" and "non-self" through the detection of cell surface molecules or pathogen specific structures called "antigen" (Ag). Their recognition is based on immune receptor proteins that specifically bind to a portion of these ligands called epitope, triggering different pathways to attack and eliminate the non-self aggressors. The innate immune system constitutes the second line of defense when invaders breach the skin and mucous membrane. It generates a general response within a few hours against a broad variety of pathogens through recognition of conserved primitive Ags (*7*). However, when pathogens escape the short term innate immune response, long term specific adaptive immune response is required for their eradication.

1. Cellular elements of the adaptive immune system

The adaptive immune system constitutes the last line of defense against microbial infection or altered self-cells. By contrast with the immediate innate immune response, the adaptive response is highly specific and necessitates several days after the beginning of an infection to be launched. Indeed, starting with really low number of pathogen-specific cells, huge proliferation is needed to limit the infection or the proliferation of abnormal cells. This long-term process generates highly potent immune responses coupled with the formation of an immune memory allowing stronger and faster immune control in case of second encounter with a particular Ag. Memory is engendered by long-lived latent cells endowed with the capacity to recover effector functions, even decades after the first activation (*8, 9*).

The key components of the adaptive immune system are T-lymphocytes (T cells) and B-lymphocytes (B cells). B cells are professional Ag presenting cells responsible for the humoral immunity. They produce several types of antibodies (Ab), known as immunoglobulins (Ig), able to recognize unique Ags and to serve different functions supporting the innate immune system, such as i) agglutination of infectious elements, ii) activation of the complement generating inflammation and cell lysis, iii) opsonization of Ags to increase

phagocytosis, iv) neutralization of bacteria and viruses and v) activation and support of antibody-dependent immune cells (*10-12*). Ag-specific recognition is made through the B cell receptor: a cell-linked antibody that specifically binds to the native form of an Ag. BCRs are randomly generated and constitute highly diversified B cell repertoires with around 3.5×10^6 different cell-surface antibodies (*13*) eventually receive further activation signal from T helper cell to which the Ag is presented, and differentiate into effectors cells, so called plasma cells, able to secrete different classes of Ig (IgA, IgG, IgE or IgD). Generated by class switching during differentiation, they are more adapted than the initial B cell's IgM for the specific pathogen eradication. After 2-3 days, the major proportion of plasma cells declines, but 10 % persist as long-life memory B-cell, allowing stronger and faster immune reaction upon second pathogen invasion (*14, 15*).

T lymphocytes are the core of adaptive cellular immunity. They are divided in two main cell types: CD4 and CD8 T lymphocytes; named from their cell surface co-receptor glycoproteins: cluster of differentiation (CD) 4 and 8 (CD4 and CD8). CD4 T cells, composed of helper (Th cells) and regulatory T-cells (Treg), act as the principal immune response mediators. Despite their low cytotoxic effect, they significantly support (Th) and regulate (Treg) the existing innate and adaptive responses by i) emphasizing the inflammation and activation signals via the secretion of diverse cytokines leading to B- and T-cell responses amplification and mononuclear phagocytes activation (*16, 17*) ii) driving the maturation of B cells into plasma cells through the secretion of diverse cytokines and their direct binding using specific cell surface ligands/receptors (*18, 19*) iii) downregulating the activation and proliferation of effector T cells via the expression of inhibitory biomarkers and the production of inhibitory or suppressor cytokines (*20*). CD8 T cells or cytotoxic T-lymphocytes play a dominant role in adaptive immune response through their direct cytotoxic function on virus-, pathogen-infected cells and altered-self cell with the release of cytotoxic effector molecules (*14, 15*). As B cells, Ag-specific recognition by T cells is made through a specific receptor: the T cell receptor (TCR). This complex of integral membrane proteins located on CD8 and CD4 T cells specifically binds to Ags presented at the cell surface by major histocompatibility complex (MHC) I or II, respectively. MHC class I complexes are expressed at the surface of most cells, and MHC class II have a more restricted distribution on professional Ag presenting cells (APC), like dendritic cells (DCs), monocytes/macrophages, or B lymphocytes. MHC class I and class II molecules bind 8–12 and 12-20 residues long Ag derived peptides, respectively (*21*). For MHC I, the peptides are derived from endogenous proteins cleaved by the proteasome into short fragments that can be both "self" peptides derived from their own proteins, and "non-self" peptides originating from invading pathogens or mutated peptide derived from somatic deoxyribonucleic acid (DNA) mutations. For MHC II, the peptides are derived from endocytosed exogenous protein cleaved by proteases in intracellular vesicles (*22, 23*). Both CD8 and CD4 T cells express highly varied TCRs repertoire allowing to target a broad panel of unique Ags (*24, 25*). After recognition of their cognate Ag and additional activation signals,

CD4 and CD8 T cells are able, as B cells, to activate, proliferate, and differentiate to eradicate target cells and generate an immune memory. Altogether, components of the adaptive system form a coherent whole to generate a strong, specific and durable response, by cooperating and reinforcing the innate immune response (Figure 1).

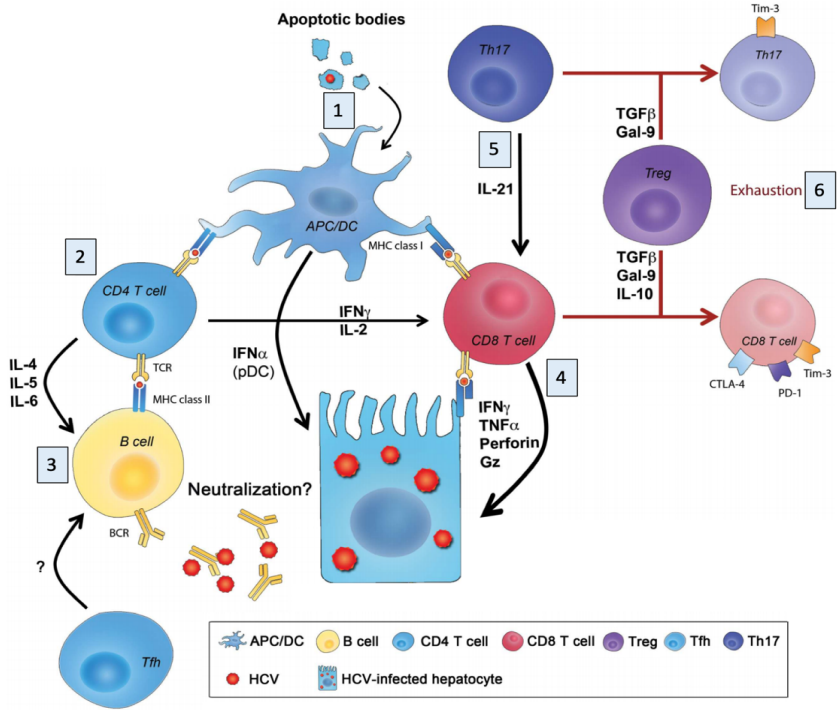

Figure 1: Schematic overview of the adaptive immune response. (adapted from (26))

2. T cell development

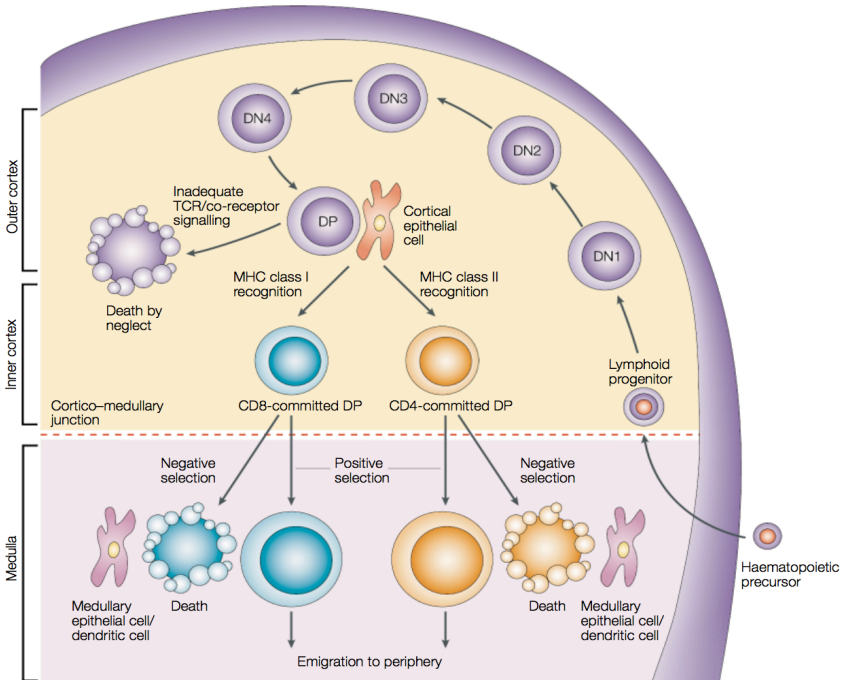

Figure 2: Schematic drawing of T cell maturation in the thymus. Adapted from (4).

CD8 and CD4 T cells originate from hematopoietic stem cells found in the bone marrow (*27*). Progenitors called thymocytes migrate to the thymus where they undergo a succession of maturation phases characterized by the expression of specific cell surface markers. Initially, thymocytes do not express CD4 or CD8 coreceptor and are called double-negative (DN). They undergo 4 differentiations associated with defined expressions of CD25 and CD44: i) $CD44^+$ $CD25^-$, ii) $CD44^+$ $CD25^+$, iii) $CD44^-$ $CD25^+$ iv) $CD44^-$ $CD25^-$ (*28*). Steps iii) and iv) are accompanied with somatic rearrangement of TCR β and α chain respectively, generating late stage thymocytes which express mature TCRs and CD4 CD8 coreceptors (Figure 2)(*4, 29, 30*). TCR somatic recombination is key to produce large TCRs repertoire. Diversity is generated by rearrangement of TCR genes composed of variable (V), diversity (D), joining (J), and constant I fragment, which initially includes 85 V and 71 J segments. These single fragments are randomly assembled to create mature VαJα chains and VβDβJβ chains (Figure 3) (*31*).

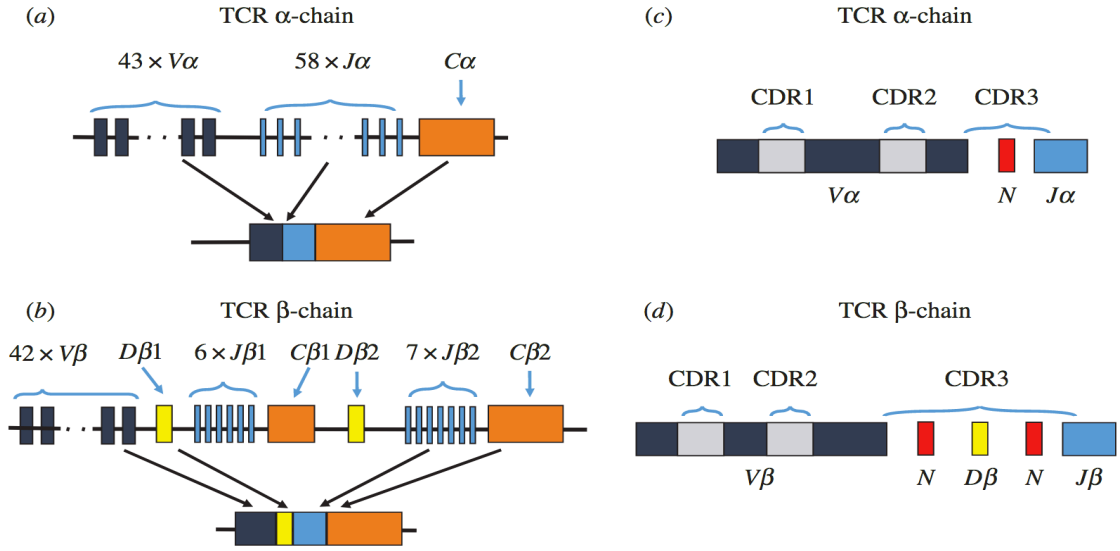

Figure 3: Schematic representation of TCR gene recombination. (a-b) α- and ß-chain gene rearrangement. (c-d) α- and ß-chain hypervariable regions. Adapted from (1)

To do so, the recombination-activating gene 1 and 2 (RAG1 and RAG2) enzymes cleave the DNA nearby the V, D, and J segments (*32*). Their association is then performed by a group of DNA repair enzymes also recruiting terminal deoxynucleotidyl transferase which adds further nucleotides at the VDJ junctions. This step allows a huge increase in the junctional diversity of α and β sequences by generating hypervariable region called CDR3 (*33*). Altogether, up to 10^{15} TCRs combinations are achievable (*34*). However, only a certain fraction leads to functional and useful TCRs. To ensure the immune safety and efficiency of generated T cells, clonal selection occurs in the thymus by deleting altered or harmful self-reactive thymocytes before they reach the periphery. This process is divided in two steps: first, the positive thymic selection occurs in the thymic cortex. Epithelial cells present self-Ags through pMHC I or II. Thymocytes are positively selected on their capacity to bind self pMHC I or II. If thymocytes bind with sufficient affinity to pMHC I or II, they maintain respectively CD8 or CD4 coreceptor expression, and repress the second one. Following this lineage choice, single

positive CD8/CD4 T cells receive survival signals and migrate to the thymic medulla where negative selection occurs in order to prevent autoimmunity: DCs and macrophages present self pMHC I or II to T cells which are negatively selected if their TCR has too high affinity for self-Ags. In both cases, T cells rejected by positive or negative thymic selection are deleted by apoptosis (Figure 2) (*4, 35*). For CD4 T cells, intermediate level of self-reactivity are associated with survival signal and upregulation of forkhead box P3 (FOXP3) expression to generate Treg (*36*). Finally, mature CD4/CD8 T cells can migrate to the periphery where they will support the adaptive immune system.

3. CD8 T cell response

Naïve CD8 T cells are characterized by CD45RA^{high},CD45RO^{low} (marker of the memory CD8 T cell subset), CCR7^{high} and CD62L^{high} (associated with the ability to home to the lymph-node (LNs) and CD44^{low} (known as activation marker). When naïve CD8 T cells reach the periphery, they require Ag priming by DCs to acquire their effector functions. As the frequency of a CD8 T cell specific for a given Ag ranges is between $1/10^4$ and $1/10^6$ among all the CD8 T cell, they constantly circulate between secondary lymphoid organs (SLOs) via the blood and the lymph vessels to scan for their cognate peptides (*37*). CD8 T cells can enter the LNs via the high endothelial venules expressing CD34, the ligand of lymphocyte's CD62L adhesion molecule (*38*). In parallel, immature DCs encapsulate exogenous Ags at the site of inflammation which triggers their maturation in pro-inflammatory DCs migrating to LNs where they present Ags to T cells through their MHC complex (*39*).

In the lymph node paracortex, Ag recognition by a CD8 T cell TCR initiates the CD8 T cell response. In order to properly prime CD8 T cells, three particular signals are required: i) the specific pMHC-TCR binding reinforced and stabilized by the CD8 coreceptor (*40*), ii) the costimulatory signal provided by CD80 or CD86 expressed on DCs surface which bind to the stimulatory receptor CD28 on CD8 T cell membrane (*41*), and iii) the secretion of cytokines by DCs which drives CD8 T cells differentiation into the appropriate effector phenotype. After activation, naïve CD8 T cells undergo a massive expansion phase (up to 20 consecutive divisions), during which differentiation initiates their acquisition of effector functions (*42*). This is reflected through the secretion of cytokines such as, tumor necrosis factor receptor α and β (TNF-α, TNF-β) and interferon (IFN) γ (IFN-γ). This latter increases pMHC-TCR effective recognition and invaders eradication by inhibiting viral replication and boosting the expression of MHC I and Ag processing genes. IFN-γ also supports the innate immune system activation via improvement of macrophages activity and promotion of natural killer cells (NK cell) function. TNF-α and -β reinforce the process of macrophage activation and also bind to the tumor necrosis factor receptor (TNF-R) in order to induce apoptosis of targeted cells (*13*). Moreover, effector CD8 T cells produce important cytotoxic molecules as granzyme B and perforin, the core of the granule-mediated killing pathway by CD8 T cells (*43*).

After differentiation, CD8 T cells migrate to the site of infection where they start their cytotoxic duty (*44*). Upon pMHC I recognition at the surface of infected or altered-self cell, CD8 T cells release lytic granules containing perforin and granzyme B. On targeted cells, perforin polymerizes and produces transmembrane pores, allowing granzymes B to enter the cytosol, where these highly cytotoxic serine proteases trigger cell apoptosis (*45*). Finally, as CD8 T cells express Fas ligand, they can induce targeted cells apoptosis through the Fas pathway by specifically binding to cells expressing death receptors Fas (*46*).

After removal of the targets, 90 to 95% of effector CD8 T cells are deleted by apoptosis during the contraction phase. The phenotype of these short-lived effector cells (SLECs) is $CD127^{low}$ (IL-7 receptor subunit-α) and $KLRG1^{high}$ (killer cell lectin-like receptor G1). Only 5 to 10 % of CD8 T cells, originating from cells having a memory-precursor effector (MPECs) phenotype ($CD45RO^{high}$, $CD127^{high}$ and $KLRG1^{low}$), subsist as long-lived memory T cell population. They are able to rapidly proliferate and differentiate into effector cells upon second encounter with their cognate Ag, even years avec the first exposure (Figure 4) (*44*).

.

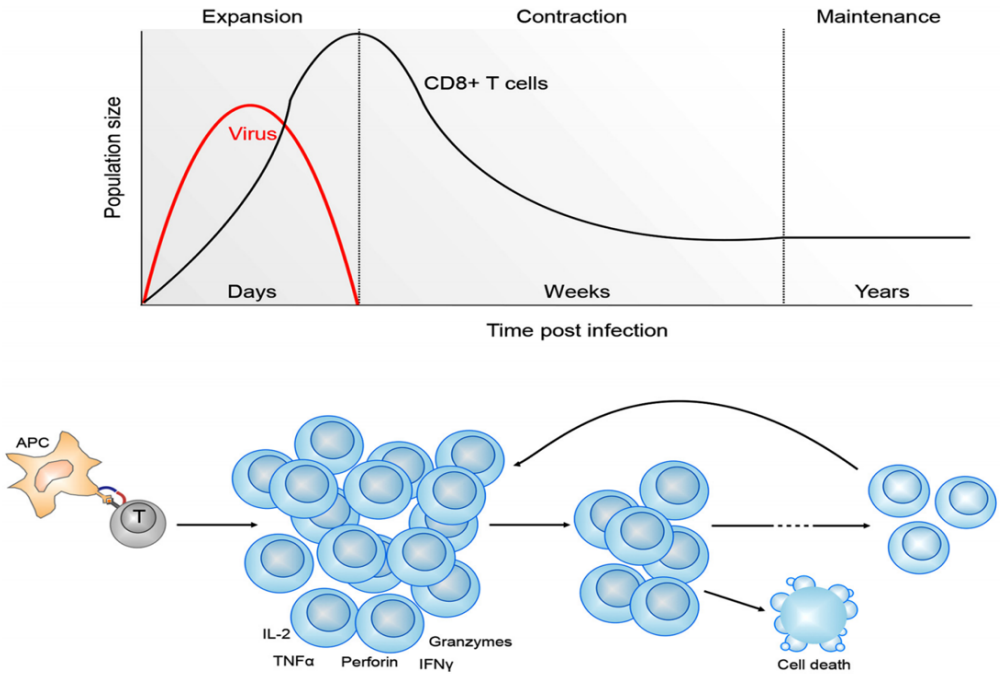

Figure 4: Kinetic of CD8 T cell response upon viral infection. Following the beginning of an infection, pathogen-specific effector CD8 T cells clonally expand (expansion phase). After the pathogen eradication, most of the CD8 T cells disappear (contraction phase). Only a small fraction of these cells survive as memory cells (maintenance). Adapted from (3)

As opposed to effector cells, memory CD8 T cells do not necessitate TCR or interleukin-2 (IL) signaling but relies on IL-15 and IL-7 for persistence and self-renewal (*47*). Memory CD8 T cells are composed of four main subsets with distinct levels of differentiations, meaning different capacity of migration, self-renewal and proliferative potential (Figure 5)(*48, 49*). First, central memory CD8 T cells (T_{CM} cells) are localized in SLOs. They have large proliferative capacity and are able to produce great amount of IL-2 upon Ag re-challenge (*50*). Their

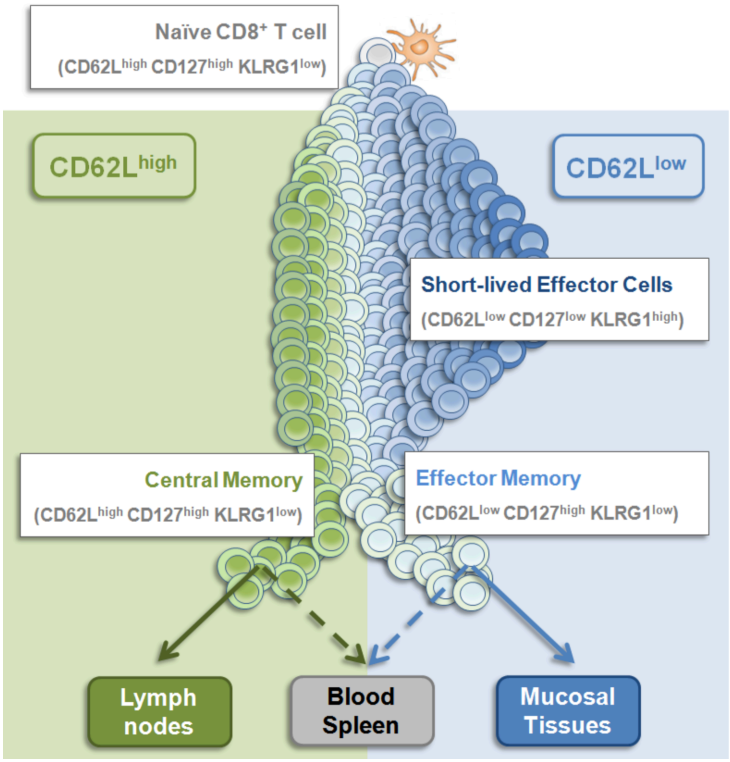

Figure 5: Phenotypes of CD8 T cell subsets. Upon antigen recognition, undifferentiated CD8 T cells downregulate CD127 and CD62L. The majority will upregulate KLRG1 by terminal differentiation and become SLEC. Others cells upregulate CD127 to become T_{CM} and T_{EM} residing in SLOs and the peripheral tissue, respectively. (2)

phenotype is: $CD62L^{high}$ associated with the ability to move to the LNs, $CD127^{high}$ and $CD44^{high}$ known as activation markers. Secondly, effector memory T cells (T_{EM} cells), also $CD127^{high}$ and $CD44^{high}$, have an inferior proliferative capacity than T_{CM} cells but have immediate available effector capacity upon Ag re-exposure. Being $CD62L^{low}$, which reduces the lymph node mobilization, T_{EM} recirculate from SLOs and can migrate to the peripheral tissues (*48*). Despite their differences, T_{EM} and T_{CM} can generate secondary effector and memory CD8 T cell upon Ag re-challenge. Another subset of memory T cells called resident memory T cells (T_{RM}) are kept at the site of infection in mucosal tissues and cannot recirculate in SLOs or at the periphery. Characterized by the expression of CD69 (early activation marker) and CD103 (intraepithelial homing receptor), they can generate direct response upon Ag re-encounter and attract innate and adaptive immune cells through the release of diverse cytokines and chemokines (*51, 52*). The last memory T cell subset discovered is stem cell-like CD8+ T cells (T_{SCM}). They interestingly have a naïve-like phenotype: $CD62L^{high}$, $CD44^{low}$, $CD45RA^{high}$, $CD122^{high}$ (a subunit of IL-15 receptor). T_{SCM} can proliferate upon IL-7 and IL-15 stimulation and are capable of differentiation into other memory subsets and effector cells (*53*) . Generally, establishment of memory CD8 T cell subsets is predetermined during the course of the initial immune response and is conditioned through signals received by naïve CD8 T cells (*54*).

4. TCR Signaling

CD8 T cell activation is triggered after TCR engagement by its cognate MHC inducing a cascade of signaling pathways, whose intensity depends on the CD8 T cell differentiation state, the presence of co-stimulatory molecules, and the pMHC-TCR binding strength. TCR signaling machinery first comprises the TCR directly coupled with the CD3 co-receptor, a transmembrane protein composed of three pairs of dimeric chains (εγ, εδ, ζζ) whose cytoplasmic domains contain immunoreceptor tyrosine activation motifs (ITAMs)(*55*). When the CD8 T cell TCRs bind to their cognate pMHC, TCRs segregate in the immune synapse

between the T cell and APC, and bigger cell surface molecules such as CD45 (receptor-like protein tyrosine phosphatase) are rejected from the synapse (*56*). CD45 rejection provokes the activation of the SRC family tyrosine kinase Lck bound to the CD8 coreceptor intracellular domain. CD8 coreceptor binding to MHC I molecule brings Lck into close proximity with ITAMs, leading to their phosphorylation (*57*). This process induces the recruitment of the zeta-chain-associated protein kinase 70 (ZAP70) to the phosphorylated ITAMs of the TCR, which is in turn phosphorylated by Lck (*58*). The activated ZAP70 phosphorylates the transmembrane protein linker of activated T cells (LAT) and the cytoplasmic adaptor phosphoprotein SLP-76, triggering TCR signaling cascade governing cell adhesion, cytoskeleton rearrangements and gene expression. This latter is controlled through three main pathways involving transcription factors nuclear factor-kappa B (NF-κB), activator protein 1 (AP-1) and nuclear factor of activated T-cells (NFAT) known to be activated by calcium release from the endoplasmic reticulum (*59, 60*). The main TCR signaling pathways implied in T cell activation are illustrated in Figure 6.

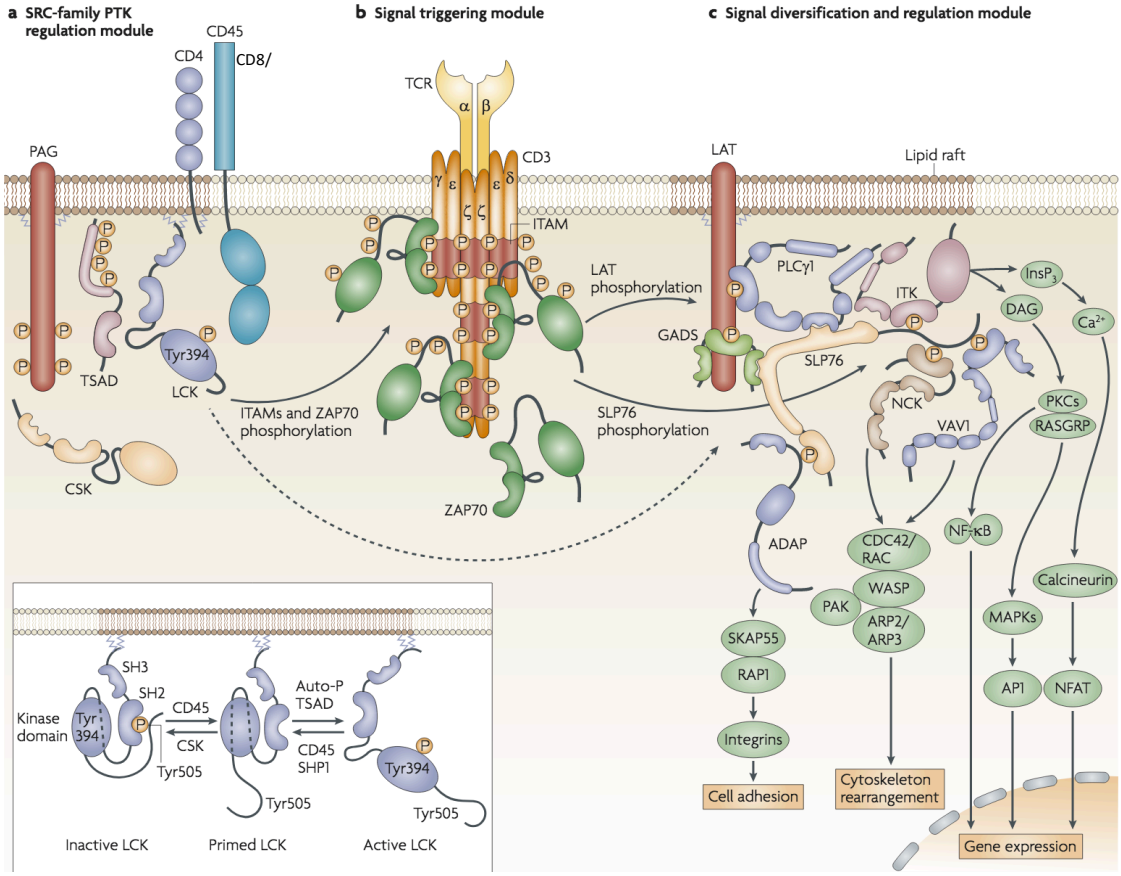

Figure 6: Illustration of the main TCR signaling pathways. CD8/CD4 T cell activation is triggered upon antigen recognition through the TCR signaling machinery. It is composed of a. the SCR-family PTK regulation module b. the signal triggering module and c. the signal diversification and regulation module controlling cell adhesion, cytoskeletal rearrangements and gene expression. Adapted from (61).

5. CD8 T cell dysfunction

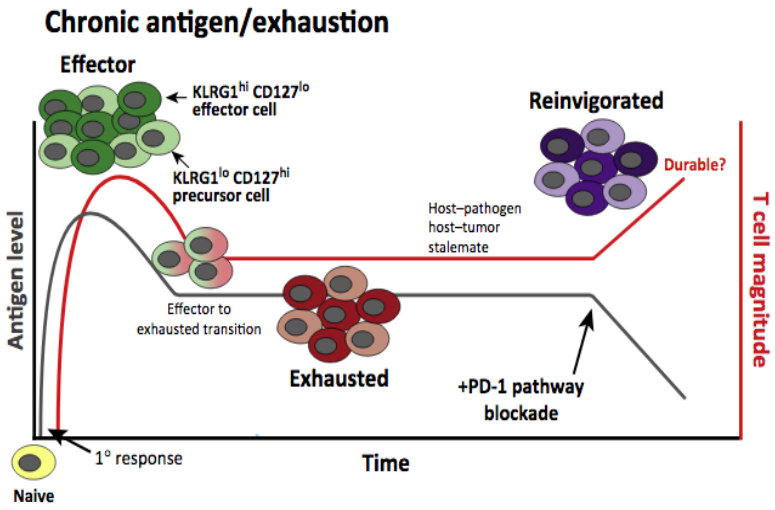

	Memory	Exhausted	Reinvigorated
Proliferative potential	+++	+/–	++
Cytokine production	+++	+	++
Killing capacity	+++	+/–	++
Dependence on antigen for persistence	–	+++	?
Responsiveness to IL-7/IL-15	+++	–	?

Figure 7: Dynamic of an immune CD8 T cell response during (A) acute and (B) chronical infection. (C) Characteristics of memory, exhausted, and anti-PD-L1-treated "reinvigorated" CD8 T cells. Adapted from (5)

Upon chronic stimulation with a particular Ag, CD8 T cells function become progressively impaired and are unable to provide an efficient cytotoxic response. So called "exhausted" CD8 T cells are characterized by the upregulation of cell surface inhibitory receptors such as program cell death-1 (PD-1), lymphocyte activation gene 3 (Lag3), cytotoxic T-lymphocyte-associated protein 4 (CTLA-4), T cell immunoglobulin-3 (TIM3), B- and T-lymphocyte attenuator (BTLA) and co-inhibitory SLAM family member 2B4 (CD244)(*62*). Reduced effector functions are the consequence of lower cytokines production (IFN-γ, TNFα and IL-2) and impaired proliferative potential (Figure7)(*63*). Also, exhaustion level is correlated with the lack of CD4 Th cells and the duration of Ag exposure. Principally, this dysfunctional state has a preventive role in T cell related immunopathology and highly exhausted CD8 T cells can be removed by apoptosis in case of severe chronic infection (*64*). As opposed to the first theories, exhausted T cell are not all terminally differentiated and can generate immune memory. Indeed, it was shown that murine adoptive transfer of exhausted CD8 T cells into naïve host is coupled with secondary cell proliferation upon re-infection by the Ag of interest, highlighting the existence of an exhausted memory CD8 T cells population (*65*)

Similarly with chronic infection, cancer patient's tumor-infiltrated lymphocytes (TILs) frequently display an exhausted phenotype, equally in mice and human. They express diverse inhibitory receptors besides PD1, such as TIM3, CTLA4, LAG3 and BTLA, in accordance with the several stratagems displayed by the tumor micro-environment (TME) to escape immune-mediated tumor control (*66*). Among other upregulated inhibitory receptors, PD1 has shown to have a key role in CD8 T cell exhaustion (*67*). Its expression is considerably upregulated upon TCR-mediated CD8 T cell activation and its signaling directly affects effector function,

proliferation and survival of CD8 T cell (*68*). PD1 signaling is triggered upon binding of PD-L1 ligand, potentially expressed on tumor cells, APCs, T lymphocytes and several tissues such as muscles and nerves (*69, 70*). As observed in a murine model of chronic infection, PD-L1 blockade can restore the function of exhausted CD8 T cells (Figure 7)(*71*). Generally, IFN-γ release can trigger the upregulation of PD-L1 expression in diverse type of cells (*72*). In tumor cells, intrinsic signaling like hyperactive PI3K pathway, can also increase PD-L1 expression (*73*). Finally, PD1 signaling can also be induced by PD-L1 in APCs, affecting their maturation, thus disturbing T cell priming (*74*).

In line the previous observations, a new subset of exhausted CD8 T cells has been recently discovered upon chronic infection. So-called memory-like CD8 T cells have a hybrid phenotype between central memory cells and exhausted effector CD8 T cells. They express Burkitt lymphoma receptor 1 (BLR1) and other costimulatory molecules, such as CD28. They are required for T cell proliferation when exposed to inhibitory receptor blockade antibody (*75*). Indeed, this PD-1^{high} population can experience secondary proliferation but relies on transcription factor TCF-1 expression (*76*). For a long time, this dysfunctional state of CD8 T cells has been a burden for treatment of chronical disease like chronic infection and cancer. Thanks to new recent findings, it is now possible to release the breaks of this biological pressure and to target this "exhausted" state as an opportunity for several immunotherapies.

6. Peripheral tolerance of T cells

Immune tolerance is a collection of mechanisms leading to immune unresponsiveness against potentially immunogenic Ags and there are several strategies to repress autoreactive responses causing autoimmune dysfunctions. This phenomenon is initiated and sustained centrally and peripherally, by means of different strategies restraining self-reactivity (*77*). in the thymus where self-reactive T cells are deleted during the negative selection (*35*) are expressed by thymic cells, central tolerance is not fully successful and several self-reactive T cells can reach the periphery and get activated upon recognition of cognate Ag. Peripheral tolerance then comes into play to delete or repress the activity of these auto-reactive T cells in SLOs and peripheral tissues. The different mechanisms will be discussed in this chapter.

a) Peripheral clonal deletion

Peripheral clonal deletion is characterized by T cell death following chronic activation by self-Ag. Based on activation-induced cell death (AICD), this phenomenon can be triggered through different pathways. Activated T-cells normally secrete IL-2 and express its specific receptor IL-2R for autocrine support of proliferative capacities (*78, 79*). Nevertheless, IL-2R upregulation also plays important role in AICD upon chronic infection, preventing autoimmune and lymphoproliferative diseases (*80, 81*). Also, activation-mediated upregulation of "death ligand" such as Fas ligand, members of the Bcl-2 family or TNF-α on

CD8 T cell increase their death through apoptosis. Hence, AICD can be properly triggered depending on the intensity of the costimulatory support, abolishing adequately the autoimmune response to maintain cellular integrity (*82-84*).

b) Tolerogenic APCs

In the absence of chemical danger signal during self-Ag uptake by DCs, toll-like receptor (TLR) and cytokine receptor-mediated activation of NF-kB pathways are repressed, preventing the complete maturation of DCs and their expression of costimulatory molecules such as CD80/86 (*85*). Because so called tolerogenic DCs are not totally mature, they cannot provide the second co-stimulatory signal when they present self-Ag to auto-reactive CD8 T cells. Receiving only the first activation signal, CD8 T-cells are not properly primed and apoptosis signals are sent to eradicate them from the periphery. Also, tolerogenic DCs can express PD-L1 and PD-L2, governing the equilibrium between CD8 T cell activation and tolerance (*86*).

c) Anergy

Anergy is an essential mechanism of peripheral tolerance. When CD8 T cells are primed without correct co-stimulation by tolerogenic APCs, instead of receiving apoptotic signals, CD8 T cells can fail to divide, secrete cytokines and acquire effector functions: they are called anergic (*87, 88*). This inactive state prevents T cell activation but can interestingly be reversible upon IL-2 treatment (*89*).

d) Ignorance and Immune privilege

Some auto-reactive CD8 T cells can get activated *in vitro* upon cognate Ag encounter. However, this rarely occurs *in vivo* as CD8 T cells ignore certain self-Ags. In some locations, ignorance happens when Ag has low cell surface expression leading to low pMHC-TCR binding avidity and, thus, low immunogenicity (*90*). In immune-privileged sites, such as the eyes, the central nervous system or the testicles, the introduction of immunogenic Ag does not generate a specific inflammatory immune response (*91*). This phenomenon is principally guided by active processes, such as the absence of lymphatic vessels, the downregulation of MHC molecules expression, the direct secretion of immunosuppressive cytokines, the constitutive surface expression of FasL, or the natural presence of immune regulatory cells such as Treg or natural killer T cells (NKT) (*92*).

e) Autoimmune regulator (AIRE)

Autoimmune regulator (AIRE) is a transcription factor implicated in many central and peripheral tolerance processes (*93*). In central tolerance mechanism, it regulates the gene expression of tissue-specific Ags (TSAs) in medullary thymic epithelial cells (mTECs), removing self-reactive T cells and inducing Treg generation (*94*). In the periphery, AIRE is expressed in SLOs and tissues such as the liver, testis, ovary, and also cells like monocytes/macrophages and DCs, increasing the TSAs expression in order to contribute to immune tolerance by

deleting self-reactive T cells (*95*). Furthermore, AIRE downregulates the expression of TLRs on APCs, disturbing the recognition of patterns associated with pathogens, senescent cells, or altered self-cells (*96*). Importantly, AIRE can influence the DCs maturation by regulating the expression of costimulatory molecules such as CD40 and CD86 (*95, 97*). Finally, AIRE-overexpressing DCs can inactivate and induce apoptosis of self-reactive CD4 T cells and guide their differentiation toward immunoregulator Treg and Th2 subsets (*98*).

f) Immune Regulation by Tregs

The majority of immune regulation is accomplished by Tregs, Foxp3-expressing CD4 T cells maintaining peripheral tolerance. They block or downregulate priming and proliferation of CD8 T cells using several immunosuppressive mechanisms such as the secretion of inhibitory cytokines (*20, 99*), the modulation of APCs activation and function, and direct cell-cell contact. Tregs specifically recognize self-Ag with moderate affinity. In the periphery, self-pMHC/TCR binding is determinant for their proliferation and/or preservation (*100, 101*). Thus, AIRE-mediated expression of TSAs leads to Tregs accumulation exclusively at sites where the TSAs are overexpressed (*102*). Furthermore, Tregs can secrete granzyme B inducing apoptosis of effector CD8 T cells (*103*). Another major suppressive process is based on blockade of co-stimulatory signal on CD8 T cells with Tregs CTLA-4 which compete with CD28 for binding to CD80 and CD86 on APCs (*104*). Also, their direct interaction with DCs can induce the secretion of immunosuppressive indoleamine 2,3-dioxygenase (IDO) by DCs, promoting their immunosuppressive function (*105, 106*). Also, through the conversion of ADP and ATP to AMP, and AMP to adenosine Tregs create an adenosine-driven immunosuppressive milieu evolving in coordination with the pathological context (*107*). In addition, Tregs express and upregulate the co-inhibitory receptors LAG3 and T cell Ig and ITIM domain (TIGIT) which directly interact with DCs to maintain immune homeostasis (*106, 108*). Finally, using IL-2R to sense the environmental IL2 indicating the proximal and high function of effector T cell, Tregs can activate and generate a suppressive response against highly activated CD8 T cells (*109*). Besides feedback loop, IL2 molecule binds to Tregs IL-2R with higher affinity than effector T cells IL-2R, which sufficiently deprive effector T cells from IL-2 to inhibit their function (*110*)(Figure 8).

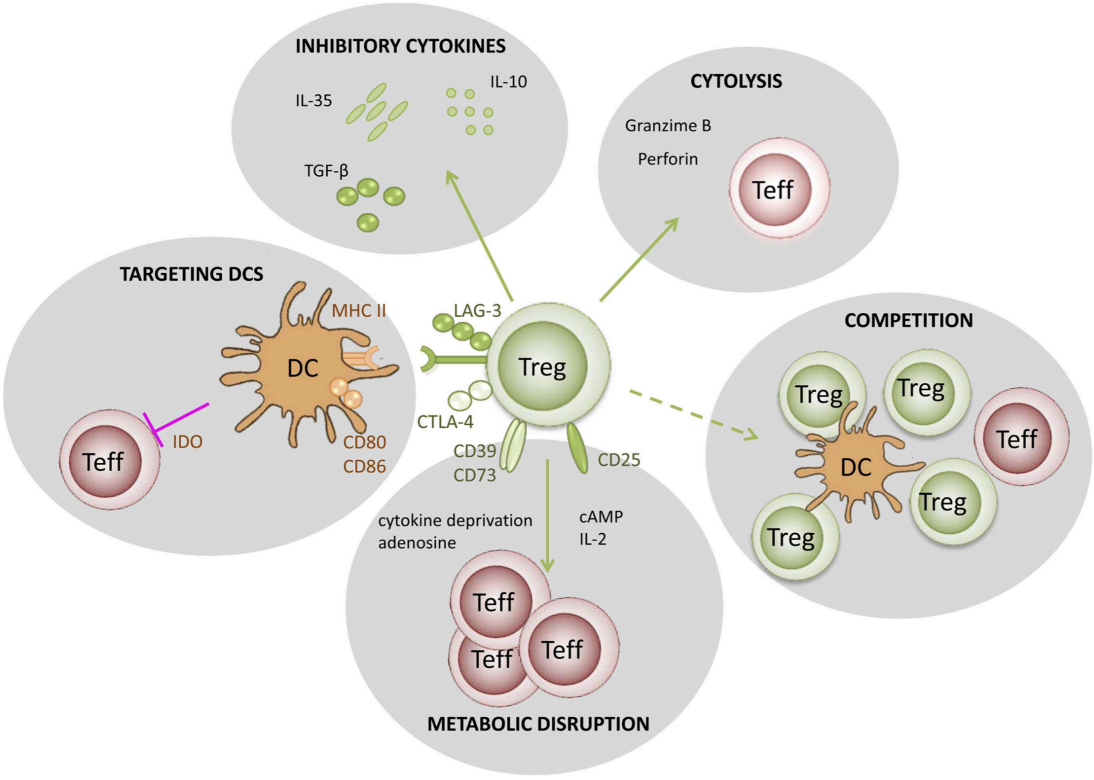

Figure 8: Schematic overview of the immune regulation processes mediated by Tregs, adapted from (111).

B. Cancer and immune system interactions

1. Cancer development

Cancer is characterized by abnormal cell growth with the potential to invade or spread to other parts of the body, which finally disturbs the integrity and the function of the invaded tissues. Cancerous cells formation is the result of several DNA mutations accumulation being either inherited (germline mutations) or appearing after birth in the somatic tissues (somatic mutations)(*112*). Somatic mutations are induced by errors of DNA replication or several environmental factors comprising three main mutagens categories: i) the chemical carcinogens such as polycyclic aromatic hydrocarbons, nicotine or alcohol, ii) the physical carcinogens such as UV rays, ionizing radiation or mechanical irritation and iii) the biological carcinogens such as oncoviruses or bacteria (*112-115*). Each cancer has unique mutation signatures, meaning an association of mutations types resulting from precise mutational processes. While mutation signatures can be associated with age, failures in DNA repair, or exposure to specific carcinogens, numerous signatures still have unidentified origins (*116*).

Cancer cells transformation happens gradually and diverse “competences” are required to generate a tumor. Named the “hallmarks of cancer”, ten major capabilities describe not only the tumor cells characteristics, but also the stromal cells particularities (*117*). These normal cells (mainly fibroblasts, macrophages, B cells and T cells) recruited at the tumor site constitute the tumor microenvironment and strongly contribute to the tumor growth

(*118*). The main characteristic of cancer cell is the capacity to maintain proliferative signaling. As opposed to normal cells whose proliferation is controlled by many checkpoints to prevent altered-cell propagation, mutation-mediated oncogenes are constitutively expressed and stimulate the cell cycle. In addition, resistance to cell death through altered apoptosis signaling pathway is a key factor to generate cancers. Also, cancer cells are able to escape growth suppressors such as p53, which normally repress cell division by limiting the advancement through the cell cycle. Furthermore, cancer cells are endowed with replicative immortality, expressing an enzyme maintaining telomere length which normally regulates cells lifespan by gradually shortening upon each division. Another hallmark of cancer is the high angiogenesis activity ensuring abundant oxygen and nutrients intake supporting tumorigenesis. Finally, the activation of invasion and metastasis is a key parameter to distinguish between benign tumors which cannot spread over the body and malignant tumors, whose threat is related to their capacity to migrate through the blood or lymphatic vessels to generate secondary tumors, called metastases (*119*). Recently "emerging hallmarks" have been integrated in the cancer features: they comprise i) the genome instability and mutation, ii) the faculty to dysregulate cellular energetic, iii) the ability to promote tumor inflammation and iv) the capacity to escape immune responses, which is essential to sustain cancer development (*117*).

a) Immunosurveillance

The immune system is a major actor in cancer development and prevention of tumor formation, which dynamically eradicates mutant altered-cells, supports cellular transformation, controls tumor cells proliferation and shapes the tumor immune landscape. These diverse and contradictory functions depend on the temporal aspect of cancer development, the origin of the altering manifestation, the specific elements implied in the immune response, and the type of tumor specific antigens (TSA) presented at the tumor cell surface (*120*). As part of the immune functions, cancer immunosurveillance is defined as the immune capacity to restrain and delay tumor development (*121*). Lymphocytes are central components in cancer immunosurveillance and actively patrol over the body to prevent tumor promotion by suppressing mutated altered cells (*122*). Also, the innate immune system components such as NK and NK T cells cooperate in the defense against cancerous cells, in particular NK cells mediating tumor control in response to IL-12 (*123*). Furthermore, while it can sometimes promote cancer evolution, IFN-γ has shown to be a key mediator of tumor control (*124*). IFN-γ increases the immunogenicity of cancerous cells through the upregulation of MHC class I expression and the generation of a suitable inflammatory environment stimulating the immune system (*125, 126*). However, the role of IFN-γ in immunosurveillance has been controversial since it occasionally supports the tumor immune resistance via PDL-1 upregulation which inhibits tumor-specific CD8 T cells activity (*127, 128*). To conclude, despite the contradictory role of certain actors, immunosurveillance includes many players of the

innate and adaptive immune system which actively cooperate to prevent tumor formation and preserve human body integrity.

b) *Immunoediting*

Despite an effective immunosurveillance, tumor development and progression frequently occur. This phenomenon is underlined in the particular dynamic process called "immunoediting", where the immune system inhibits tumor emergence and also shapes the immune landscapes of growing tumors. It was first highlighted in a study where tumors generated in immunodeficient mice progressed slower when transferred in immunocompetent mice, as opposed to tumors generated in immunocompetent mice, being more hazardous after transplantation (*129*). Immunoediting consists of three steps: elimination, equilibrium, and escape (*130*). During the elimination phase, the adaptive and innate immune system recognize and eradicate tumor cells through the generation of local inflammation at the emerging tumor site, the recruitment of immune cells, and the production of specific cytokines and chemokines to maintain immunosurveillance (*131*). Nevertheless, if the lesions persist and develop, tumors must be dynamically controlled by the immune system. During the phase of equilibrium, tumors evolve and adapt due to their genetic instability and the stress induced by the immune system initiating the survival of immune-resistant cells, for instance by downregulating MHC I expression. Consequently, besides the prevention of neoplasm development, the immune pressure induces their shaping by selecting immune-resistant tumor cells variants with the accumulation of tumor-promoting mutations, providing better resistance to the immune response (*131*).

c) *Tumor escape*

Due to high immunoediting rate, a large diversity of immune-resistant tumor cells is generated. The last phase called tumor escape occurs when cancer cells are no longer beyond the control of immunosurveillance. Consequently, cancers can progress and generate primary tumor and metastases (*132, 133*). Many strategies are developed by tumors cells or by their supportive stroma to disrupt their immune-mediated rejection. Often, tumor-derived DCs do not receive immunogenic signals and preserve their tolerogenic phenotype, provoking T cell anergy instead of their efficient priming (*134*). Also, myeloid-derived suppressor cells (MDSC) actively support local immunosuppression. These cells originating from the myeloid lineage quickly invade the tumor and accomplish their functions by secreting immunosuppressive cytokines such as TGF-β and IL-10 and by expressing Arginase 1, depleting L-Arginine supplies. Their cytotoxic role is ensured by the expression of iNOS enzyme producing nitric oxide (*135*). Other lymphoid cells participate in immunosuppression, such as Treg recruited by tumors to generate a tolerogenic environment (*136*). Also, besides its constitutive expression by tumors and the supportive stroma, PD-L1 is further induced by the presence of IFN-γ during T cell response to promote their dysfunction. Additional factors, such as IDO expressed by the tumor

and myeloid cells, support tumor immunosuppression by recruiting MDSC and by reducing L-tryptophan supplies essential for effector T cell survival (*137*). Similarly, FasL is overexpressed in the tumor endothelium when encountering other immunosuppressive factors, inducing the death of tumor-infiltrated T cells (*138*). Tumor escape is also reinforced by the interaction between adaptive and innate immune system, where the production of blocking Ab precludes the complement components production and activation. Some Ab can even protect tumor cells by preventing Ag recognition (*139*). Finally, tumors can modulate the Ags presentation to avoid immune recognition, provoking their translocation from the surface to the cytoplasm (*140*). Downregulation of Ag-processing machinery, such as β2m or HLA expression loss heavily contribute as well to tumor escape (*141*).

2. Cancer antigens

In tumors, peptides displayed at the cell surface by MHC class I molecules originate from a large diversity of intracellular altered or abnormally expressed proteins, allowing tumor-specific immune recognition (*142*). Tumor Ags are divided in two main categories having a huge repercussion on therapeutic strategies: Ags with high tumor specificity and Ags with low tumor specificity. The latter class, "the tumor associated Ags", is composed of Ag derived from genes overexpressed in tumors and differentiation Ag (*143*). Differentiation Ags are expressed predominantly on tumor cells, but their expression is detected on some healthy cells as well. In melanoma cells for instance, most of the proteins of interest are implicated in the melanosome biogenesis or the melanin biosynthesis. Despite their "self-nature", peptides originating from proteins such as tyrosinase, Melan-A/MART-1, or gp100/pmel17 often induced spontaneous T cell responses in healthy donors and melanoma patients, highlighting the deficiencies in central tolerance to these Ags (*144-147*). Therefore, differentiation Ag-specific T cell responses can frequently trigger diverse autoimmune-related adverse event such as vitiligo in melanoma patients, while being often related to good prognosis (*148*). Overexpressed Ags have also low tumor specificity but have been used in the elaboration of immunotherapeutic vaccines. These Ags are expressed in healthy tissue, but to a lesser extent than in the tumor cells. Many immunogenic peptides have been described as "overexpressed", such as peptides derived from PRAME, which is overexpressed in many tumors but having low levels of expression in normal tissues (*149, 150*). When used as immunotherapeutic targets, the main limitation of these Ag is the quality of the quantification of their cell surface density in tumor and normal cells, used to define a threshold of expression over which Ag-recognition by T cells can occur. Since these Ags are shared by many cancer types, they became attractive targets for immunotherapy. However, due to their detectable expression in healthy cells, they might initiate autoimmune side effects. Indeed, attempts to increase pMHC-TCR affinity to improve CD8 T cell response by making TCR engineering on

TAA-specific CD8 T cells led to severe autoimmune events limiting the translational potential of this strategy (*151*).

Others adequate Ags candidates for immunotherapies is the class of "tumor-specific Ags". TSAs have various origins as they are exclusively expressed on the tumor cell surface (*143*). First, in the case of virus-induced cancers such as cervical carcinoma, hepatocarcinoma, and some leukemias, TSAs can be viral Ags. These mutated Ags derive from viral proteins inside the tumor cells, which are the result from infection with tumorigenic transforming virus (*152*). Moreover, Ags derived from cancer-germline genes represent a fundamental resource of TSA, including the melanoma-Ag encoding (MAGE) genes or LAGE/NY-ESO1 (*153, 154*) Apart from trophoblastic and germline cells, these genes are not expressed in normal healthy tissue, but are found in many tumor types (*155*). Cancer-germline genes expression originates from the demethylation of the promoter sequence, as the one occurring in male germline cells (*156*). However, as trophoblastic and male germline cells do not present cell surface MHC I molecules, germline self Ag are not loaded on cells in normal conditions (*157*). Therefore, these highly tumor-specific Ag might be used as relevant and safe targets for immunotherapies. Recently, other abnormal transcripts absent in normal cells but expressed in tumors have been identified, such as peptide deriving from cyclin-A1, a proliferative and anti-apoptotic protein expressed only in acute myeloid leukemia and testis (*158-160*). Also, oncofetal Ag have fetal tissues- and tumor cells-specific expression. Alphafetoprotein and carcinoembryonic Ag are the most studied. They are constitutively formed in the primary steps of embryogenesis and decrease over the immunity development, preventing self-tolerance when expressed on tumor-cell surface (*161*). Post-translationally altered Ags constitute an important source of TSA, since post-translational mutations, such as tumor-associated alterations in glycosylation or ubiquitination, create unique novel Ags (*162*). Last but not least, neoantigens (NeoAg) arise as a consequence of tumor-specific somatic mutations that are naturally acquired during tumor development and progression. Frequently, the mutation impacts a unique amino acid (AA), producing a new Ag recognized by CD8 T cells or allowing the peptide to bind to the MHC class I molecule. Rarely, the mutation engenders a frameshift producing new Ags (*163*). Some neoAgs arise from passenger mutations which are not altering cell fitness and are therefore mostly unique among different patients as they are not driving the hallmarks of cancer. Thus, the resulting neoAgs called "private neoAg" are exclusive to the patient in which they are isolated. However, a limited fraction of CD8 T cells recognizes "public neoAgs" resulting from frequently mutated genes, such as P53 or KRAS. Most of the public NeoAg-specific CD8 T cells were discovered with the reverse instead of the direct immunology approach, meaning that these public neoAgs might have low immunogenicity (*164, 165*). The pipeline for Ag discovery relies on technologies exploiting genomic, transcriptomic and immuno-peptidomics data (DNA/RNA/peptide sequencing respectively) to identify mRNA splicing, somatic mutations, their expression level and their HLA restriction in the tumor (*166*). The analysis of the differences between cancer and germline DNA allows the detection of

tumor-specific DNA mutations being the potential source of TSA recognized by the immune system. Exome sequencing can be performed on cancer and healthy tissue to identify somatic mutations, even though it requires large tumor fraction with low heterogeneity to provide an adequate coverage (*167*). Gene products such as mutated Ag, gene fusions or tumor-specific splice variants are identified by RNA sequencing. However, these technics cannot surely identify processed and immunogenic Ags. Therefore, *in silico* algorithms are constantly evolving to predict peptide-MHC binding affinities, stability and immunogenicity to refine peptide hits (*168*). Recent developments imply machine learning technology, such as neural networks like NetMHC (*169*) or hidden Markov models (*170*). Large database of pMHC are used to train these algorithms, permanently improving and extending to new type of HLA alleles (*171*). In order to filter the predictions of MHC ligand, peptide-MHC binding affinity and stability assay are performed *in vitro*. It includes biochemical technics measuring peptide-MHC binding such as the peptide-rebinding assay (*172*) or the refolding assay (*173*). However, these technologies might identify unprocessed peptides or fail to discover peptides altered by proteasomal reverse splicing or containing post-translational modifications (*174, 175*). Immunopeptidomics circumvent these defects by first isolating pMHC molecules from cells, then by isolating and analyzing the peptides by liquid chromatography and mass spectrometry (LC-MS)(*176*). Immunoaffinity purification of pMHC complexes (using pan anti-human leukocyte antigen (HLA) I or II antibodies) allows HLA isolation and peptides recovery. Then, MS/MS spectra are aligned to theoretical spectra of different sequences of peptides using search engines such as MaxQuant to finally deduce the sequence of the peptide of interest (*177*). Comparison with databases from genomic and transcriptomic analysis allows the identification of peptides sequences not referenced in protein sequence databases (*178*). Despite the high accuracy and sensitivity of LC-MS analysis, 1 gram of tumor or 1-5x10^8 cells originating from tumor cell lines are required for detailed immunopeptidome analysis allowing the discovery of thousands of Ags (*179*). Once peptides of interest are identified, *in vitro* validation of immunogenicity is performed using APCs pulsed with synthetic peptides or RNA encoding for mutated peptides. Following validation, immunogenic peptides are used to build pMHC multimers for the isolation of Ag-specific T cells. This validation is still tedious, costly and error prone (impurities within synthetic peptides, MHC restriction, precursors frequencies…) and many developments such as in-house high-throughput *in vitro* peptide binding assay are ongoing to improve the Ag validation and discard non-binders.

Several preclinical and clinical studies have put neoAgs' clinical relevance beyond doubt showing their successful implication in immune-mediated rejection of melanoma, lung cancer, leukemia and gastrointestinal cancers (*180-182*). These tumors having high mutational rate are expected to contain more neoAg inducing their higher immunogenicity. The first evidence that neoAgs were recognized by the immune system was shown by Wölfel et al. where anti-tumor response in a melanoma patient was mainly driven by autologous T cells directed against neoAgs (*183*). They also detected neoAg-specific CD8 T cells in *in vitro*

expanded TILs coming from a melanoma patient who underwent a total tumor regression after adoptive cell transfer therapy (ACT) (*184*). Furthermore, correlations between neoAgs load or clonal neoAgs burden and clinical benefit were revealed in many recent clinical trials (*185-187*). Advantages of neoAg-specific CD8 T cells towards others Ags are that i) neoAgs are specific targets of tumor cells and ii) neoAgs, as non-self Ags, are not affected by thymic selection and thus, neoAg-specific T cells are expected to be of higher avidity and endowed with better tumor killing capacity.

3. Cancer immunotherapy

Traditional cancer treatments, including surgery, chemotherapy and radiation therapy, have only limited efficacy in late-stage cancer patients. Immunotherapy is the treatment of diseases by inducing, enhancing or suppressing an immune response. Cancer immunotherapy is intended to improve clinical outcome by destroying tumors while preventing detrimental side effects on healthy tissues. Five principal immunotherapies have been developed and approved in the clinical use. They comprise active and passive immunotherapies, or the combination of both. The first type aims at manipulating the immune system to target TAAs or TSAs (carbohydrates or proteins) on tumor cells surface. The passive approach boosts the existing antitumor immune responses by exploiting diverse antibodies, cytokines and lymphocytes (*188*). Undoubtedly, despite highly variable response, clinical outcome of patients greatly depends on the tumor type, stage, the expression of key biomarkers and predictive factors of response (*189*).

a) Antibodies

Monoclonal Abs therapy is an active therapy which aims at targeting specific Ags at the tumor cell surface. They can be used alone or conjugated with therapeutic drugs enhancing the tumor-specific cytotoxicity of the treatment *(190)*. This strategy was used in numerous tumor types such as breast, lymphoma, and colorectal cancer *(191)*. Monoclonal Abs specifically target an Ag sequence or epitope exclusively present on malignant cells to trigger their death or inhibit their function. Different mechanisms of action are exploited: i) blockade of an essential receptor for the survival or growth of the cancerous cells, ii) antibody-dependent cell-mediated cytotoxicity via the Fc portion, or iii) immunomodulation of T cell activity. Unfortunately, many limitations are related to this therapy, inducing highly variable response rate. The major cause is the high specificity of Ab recognition. Indeed, unique Abs can recognize only one single Ag, preventing epitope recognition and binding in case of point mutations generating similar isoforms (*192*). Secondly, the targeted Ag must be expressed on the tumor cell surface, homogeneously and at high levels. Despite several successful clinical trials and FDA approvals for the first line cancer treatment, such as Cetuximab or Trastuzumab (*193-195*), the characteristics of monoclonal Abs directly inflict the high variability in patient's clinical outcome, being inappropriate for standard for clinical use.

In order to improve the chance of tumor-recognition, diminish the non-specific toxicity or attract immune compounds to the TEM, bispecific antibodies (targeting two Ags) have been developed. Some, such as blinatumomab, already showed promising results in the clinic, and several others have been under clinical investigations (*196-199*).

b) Immune checkpoints blockade

The first passive immunotherapeutic approach having shown long term remission in advanced cancer patients aimed at restoring the activity of preexisting exhausted cancer-specific T cells by blocking inhibitory immune checkpoints (*200, 201*). Under normal conditions, these checkpoints counteract autoimmune events resulting from over-activation of CD8 T cells by weakening their activity. Cancerous cells are able to exploit this phenomenon to protect themselves from CD8 T cell attack by inactivating TILs. Two of the key immune checkpoint ligands are PD-L1 or PD-L2 and their respective receptor PD-1 and PD-2. As PD-L1 is overexpressed on the tumor cell surface and on myeloid cells in the TME, upon binding to tumor, activated CD8 T cells expressing PD-1 convert into an inactive phenotype, profoundly disturbing their function (*202*). Also, another inhibitory receptor, CTLA-4, acts by competing with CD28 costimulatory molecule on CD8 T cell surface to bind to the ligands CD80 and CD86, diminishing T cells activity. Immune checkpoint inhibitors are antagonist antibodies blocking immune checkpoint receptors which allow T cells to recover their tumoricidal function and to promote inflammation. Besides that role, it was shown that blocking immune checkpoint receptors also abrogates Treg suppressive activity (*191*). The FDA approved molecules are anti-PD-L1 and anti-CTLA-4. Anti-CTLA-4 called ipilimumab was first used in phase III clinical trial in metastatic melanoma patients. It significantly augmented overall survival and progression-free survival. In this study, 18% of the patients survived after two years upon ipilimumab treatment, as opposed to 5% receiving the vaccine only (*200*). Two anti-PD-L1 have been developed: nivolumab and pembrolizumab. They were first shown to have an antitumor effect in advanced melanoma, where PDL-1 tumoral expression was associated with better patient survival (*203*). Currently, pembrolizumab is studied in more than 400 clinical trials for numerous different cancer types such as breast, lymphoma, melanoma and lung cancer (*204*). In a recent phase III clinical trial against advanced melanoma, it induced better tumor control and induced fewer serious adverse events than ipilimumab (*205*). Furthermore, it was proved to surpass chemotherapy in patients having ipilimumab-refractory melanoma (*206*). The main advantage of these therapies comes from the distinct inhibitory pathways of PD-1 and CTLA-4, allowing better response in advanced melanoma patients when treated with nivolumab and ipilimumab in combination, as compared to monotherapy (*68, 207*). The exceptional success of these molecules encouraged the FDA to approve these therapies for numerous tumor types such as, kidney cancer, Hodgkin lymphoma, non-small-cell lung cancer, and bladder cancer (*208-211*). In 2018, thanks to the growing interest in this therapy and the positive clinical outcome, Jim Allison received the Nobel Prize in Physiology or Medicine for his work on

Immune checkpoint blockade (*212*). Nevertheless, clinical outcome is highly variable even among patients bearing the same tumor type and efforts are put to define the best predictive marker of response and to combine its action with other therapies to improve clinical response (*189*). Recently, studies have shown the importance of the gut microbiota composition and diversity in regulating immune response to anti-PD-1 in melanoma patients. Patients with varied microbiota composition showed better response to immune checkpoint blockade than others. The presence of Faecalibacterium and Clostridiales phyla's species was associated to an increase in tumor-specific CD8 T cells number, suggesting that some bacteria would contribute to increase objective tumor response, while some might have a negative impact (*213*).

c) Therapeutic Cancer vaccines

The second active therapy focused on the development of cancer vaccines to generate immune-mediated tumor control, which have shown promising clinical results (*214-216*). Vaccines are immunogenic biological concoctions inducing an active acquired immunity against a specific Ag. Against many diseases, vaccines are used in prevention to generate a pathogen-specific immune memory and avoid disease development upon real pathogen encounter. However, prophylactic vaccines cannot be envisaged for the majority of cancers, except for virus related tumors, such as the human papilloma virus (HPV) causing cervical cancer (*217*). Cancer vaccines usually implicate conventional vaccination procedures to trigger or enhance a preexisting antitumor immune response when the tumor is already existent (*218*). Current therapies are based on many strategies affecting the type of responses. They are designed depending on the tumor manifestation (local or systemic) and on the diversity of Ag-specific responses.

Peptide-based and adjuvant-based cancer vaccines intend to mount an immune response against one defined Ag. Nevertheless, this approach expects that the tumor is uniform and the majority of the expressed Ag is reachable by APCs. Furthermore, many attempts were directed against TAAs, having low affinity and being tolerized as "self" Ags. Therefore, the TAA-directed vaccines did not generally mount a sufficient immune response to induce tumor regression in clinical trials (*219*). In many cases, targeting a specific TAA led to significant collateral damages associated with autoimmune response to healthy cell expressing the same Ag (*151*). Thus, the choice of the appropriate Ag appears to be determinant in cancer vaccine success. Mutated Ag, neoAgs and cancer germline Ags are the most attractive candidates for therapeutic vaccines. For peptide-based vaccines, the use of long peptides provided better clinical success. As opposed to short peptides able to bind exclusively to MHC-class I, and to only prime CD8 T cell, long peptides can mediate CD4 and CD8 T cell responses, further developing immune memory and improving clinical outcome (*220*). Overall, the clinical responses of peptide vaccines used as unique therapy were limited, even exploiting synthetic long peptides (SLP). However, Ott et al. have shown highly promising

results when exploiting neoantigenic SLPs in a phase I clinical trial in melanoma patients, where significant immune responses and tumor reduction or no recurrence were observed (*216*). These results highlight the clinical importance of the selection of the Ag of interest.

The second type of vaccines is DNA and RNA vaccines, where Ags are generated following the administration of their genetic sequence. Here, DNA can directly be administered as "naked DNA" by intramuscular injection. However, DCs have low cellular uptake of DNA, encouraging the development of techniques and formulations to increase the cellular uptake using vectors to administer the gene of interest, such as delivery by nanoparticles, microneedle arrays, gene gun, *in situ* electroporation, bacterial and viral plasmids that considerably improved DNA transfection (*221*). Cells, such as APCs, are able to capture the DNA and to express the peptide of interest. Also, oncolytic viral vectors were developed, benefiting from their direct virulence to tumor and the generation of inflammatory environment improving the immune response (*222*). Despite a generally low success for DNA vaccine, a recent phase IIb trial have proved for the first time the efficiency of a cervical cancer DNA vaccine (*223*). It is generally accepted that RNA cancer vaccines offer clear advantages over DNA vaccines as RNA cannot enters the genome and it only needs to reach the cytoplasm to be effective, as opposed to DNA that needs to enter the nucleus (*224*). The major part of RNA vaccines exploit mRNA, but RNA replicons have been lately studied (*225*). They can self-replicate, persist longer than mRNA, and thus need lower vaccination doses. Like DNA, despite rare convincing clinical studies using RNA vaccines, a phase I trial showed encouraging tumor regression and T cell response in advanced melanoma patients exploiting mRNA vaccine expressing 4 TAAs complexed in a liposomal formulation (*226*). Also, Sahin et al. tested RNA vaccines with neoAgs and have shown highly promising results in a phase I clinical trial in melanoma patients, where significant immune responses and tumor reduction or no recurrence were observed, suggesting again the great potential of neoAgs (*215*).

Whole tumor cell vaccines have been developed to bypass the difficulty of the identification of the Ag of interest. Autologous tumor lysates comprise the whole repertoire of TA and NeoAg while preventing their identification. So far, this method had limited clinical success, despite the small improved antitumor response as compared to single peptide vaccines: 8.1% versus 3.6% objective clinical response in 173 clinical trials (*227*). It is noteworthy that the exploitation of allogeneic tumor cell lines provided comparable efficacy than autologous tumor lysates, suggesting that allogeneic tumor cell lines are an appropriate source of Ags and their exploitation would allow their genetic modification to improve their transport in the tumor site, and would prevent many constraints inflicted by personalized immunotherapy, such as high costs and logistic limitations. Regrettably, no clinical benefit was observed with this approach yet (*228*).

In order to improve single Ag and whole tumor lysate vaccine efficacy, APCs have been used as vector for tumor Ag. Ag presentation is induced *in vitro* by maturation and pulsing APCs with the peptides of interest. Often, there was a limited efficacy of this approach despite

the stimulation of immune responses (*229, 230*). Recent advances allowed to slightly but significantly improve their clinical efficacy (*231-233*).

Despite all the efforts, a few clinical trials induced important objective clinical responses. Facing the numerous limitations offering current tumor vaccine strategies, such as intra and inter-patient's Ags variability, tumor heterogeneity or hostile TME, many lessons have been learned and today allow an improvement of clinical outcomes. Thus, the new strategies consider the necessity of various immunogenic Ags or neoAgs, the importance of the vaccine vectors and the TME-mediated immunosuppression. Last approaches exploit the most appropriate vectors and use multimodal therapy, such as the combination with immune checkpoint blockade therapies or chemotherapy (*218, 230, 234, 235*).

d) Cytokine mediated immunotherapy

In healthy individuals, cytokines directly impact immune responses, modulating the expression and activity of the immune system's effector proteins. Immunotherapies permanently exploit cytokines alone or in combination with others therapies to boost the existing immune response, commonly with IL-2 and IFN-α (*236*). IFN-α is an immune stimulator activating DCs and thus promoting Ag presentation, CD8 and CD4 T cell activity, encouraging the Th1 response and the NK cells cytotoxic activity (*232*). Likewise, IL-2 increases the CD8 and CD4 T cells activity (particularly TILs) and promote NK cell cytotoxic activity (*237*). IL-12 have also been used to stimulate NK cells activity and support Th1 cells differentiation. Due to severe adverse event in the initial clinical trials, local IL-12 expression in the TME has been developed and offered promising results when combined with other therapies (*238*). Despite significant clinical responses, cytokine mediated immunotherapy is limited by the necessity for patients to have a preexistent vigorous immune system to be efficient, contributing to the great variability in the response rates.

e) Adoptive cell transfer

Finally, adoptive cell transfer therapy (ACT) is based on the administration to cancer patients of natural or genetically engineered autologous or allogenic *in vitro* expanded immune cells to target tumor Ags, such as vascular Ags, cancer germline Ags or neoAgs (Figure 9) (*191*). Once the cells are administrated into the patient, cytokines such as IL-2 are often injected in combination to improve the results of ACT (*236*). One of the cell-based strategy relies on the administration of particular artificial cells called chimeric Ag receptor T cells (CAR-T cells). It implicates the adoptive transfer of ex vivo genetically engineering T cells directly targeting tumor cells surface Ags independently of the MHC presentation. The potential "chimeric-like" Ags are proteins, glycolipids and carbohydrates, which provide a large advantage in case of immune evasion through the loss of HLA molecule (*239*). The chimeric Ag receptor comprises two segments: i) The extracellular domain containing the scFv of an Ab specific for a chimeric-like extracellular TSA and ii) the intracellular domain composed of CD3ζ

signaling domain and a unique or multiple costimulatory domain, depending on the CAR generation (Figure 9). So far, clinical trials showed undoubtable outcomes for the treatment of hematological malignancies and especially for acute lymphocytic leukemia with up to 92% of full recovery (*240-242*). However, the treatment of solid tumors with CAR therapy is challenging and did not show highly promising immune response yet, mainly due to the difficult identification of the appropriate Ags preventing off-target toxicity, and therapeutic complications such as CAR T-cell division, traffic, and persistence inside solid tumors (*241, 243*).

Another strategy focused on adoptive transfer of patient's tumor TILs. However, the chronic exposure to tumor Ags and to the immunosuppressive TME exhaust TILs, diminishing their function. TILs isolation and *in vitro* expansion allow their extensive proliferation and reactivation, isolating them from the destructive TME and providing adequate inflammatory signals. Re-infusion via an intravenous injection is generally carried out after irradiation or pretreatment with lymphodepletion-inducing chemotherapy. So far, ACT of TILs has been an effective treatment for some late-stage cancer patients, particularly with metastatic melanoma (*244-246*). While TIL therapy has shown objective clinical response rates of 50% in stage IV melanoma patients in several clinical trials, it appears that the majority of disease progression is correlated with low frequencies of T cells reactive against known melanoma-associated Ags (*247*). Recently, Kelderman and colleagues showed that ACT of enriched tumor-specific CD8 T cells gives better pre-clinical responses than conventional TIL transfer (*248*). Thus, next generation TIL therapies might be focused on the transfer of a cell-based product enriched in TAA, TSA or neoAg-specific T cells. The first evidence of tumor rejection by neoAg-specific CTLs was brought by Tran et al, exhibiting significant tumor regression in patient with metastatic cholangiocarcinoma, following two ACTs of autologous CD4 TILs recognizing a tumor neoAg arising from ERBB2 protein. This study highlighted the great neoAg potency and confirmed, as others reports, that both CD8 and CD4 T cells are important in immune-mediated tumor rejection (*249-251*). However, TILs therapy is restricted by numerous factors limiting its systematic use: i) tumors need to be accessible to surgical resection, ii) high levels of TILs are required in the TME, with optimal affinity to tumor Ag, and iii) the host needs to stand the lymphodepletion and resist the delay imposed by the preparation of TILs infusion (*252*).

Thereby, another type of ACT has been developed: the adoptive transfer of TCR-transgenic T cells. This relies on the transfer of T cell transduced with genetically engineered or natural TCR targeting tumor Ag with optimal affinity. For a matter of accessibility and optimal cellular functionality, PBMCs are exploited to be genetically modified. Indeed, the best antitumor responses have been driven by engineered cells having less differentiated state.

Upon stimulation, naïve, T_{SCM}, T_{CM} and T_{EM} cells showed sustained cytokine release, better proliferation and differentiation into T_{eff} cells than more differentiated phenotypes (*253, 254*). Clinically relevant TCRs can be either designed *in silico*, or selected from autologous

or allogeneic populations having high affinity CD8 T cell targeting a private or shared Ag respectively, or sometimes can be selected from mouse model (*255*). Retro- or lentiviruses are used as the vector of choice to introduce DNA into the host cells for the expression of the new TCR (*256, 257*). Then transduced PBMCs are expanded *in vitro* before being infused into a lymphodepleted cancer patient (*255*). In 2006, the first cases using this approach performed ACT on melanoma patients, with engineered T cells bearing TCR targeting the HLA-A2 restricted MART-1 Ag, isolated from autologous TILs. Objective tumor regression without severe side effects confirmed the therapeutic potential and the safety of this strategy (*258, 259*). Another study on metastatic melanoma patients using higher avidity TCRs targeting the MART-1_{27-35} Ag or the $gp100_{154-162}$ Ag showed better objective responses. Indeed, tumor regression was observed in 30% and 19% of the patients, respectively. However, autoimmune related side effects were superior than those obtained with TILs therapy, suggesting that high avidity TAA-specific T cells might not be the appropriate targets for ACT (*260*). Several TAA-specific TCRs have been used for ACT in patients with other tumor types such as colorectal cancer. They have shown variable objective clinical responses but often off- and on-target toxicity associated to the TAA expression on healthy tissue (*151, 261, 262*). This highlighted the need to transduce TCR specifically targeting TSAs. In this regard, Robbins et al exploited TCRs targeting the NY-ESO6 Ag for the treatment of metastatic synovial cell sarcoma or melanoma, leading to objective clinical responses in most of the patients, without TCR-related adverse event (*263*). New approaches now focus on the isolation of neoAg-specific TCRs to improve ACT clinical outcomes without generating off-target toxicity. The TCR identification can be performed by TCR sequencing after i) T cell sorting with neoAg-specific pMHC multimers and ii) sorting of TILs expressing PD-1 and/or activation markers such as CD137 and CD134, co-culture with APCs pulsed with neoAgs, and FACS sorting of the activated clones (*264*). One interesting study demonstrated the possibility to isolate neoAg specific-TCRs from healthy donors to overcome the limitations inherent to the use of autologous TILs (*265*). Finally, as private neoAg identification still remains tedious and challenging, newly identified shared neoAgs arising from “hot spot” mutations emerge as new attractive candidates for ACT, being a rapid approach to screen neoAg-specific T cells. A recent study focused on patients with epithelial cancer bearing shared “hot spot” p53 mutations. Here, 39% of the TILs isolated from patients targeted p53 hot spot mutations, being either CD8 or CD4 T cells. Engineered PBLs transduced with 9 TCRs targeting 7 shared p53 neoAgs highlighted the capacity of these cells to recognize the Ags of interest *in vitro*, to release proinflammatory cytokines and to degranulate. However they did not demonstrate yet if these cells are able to mediate tumor control *in vivo* (*266*). Of note, as others immunotherapies, many efforts are put into combining ACT with other therapies to improve general clinical outcome by preventing tumor immune escape and deleterious TME (*267-271*). It seems indeed indispensable to restore immune function by blocking immunosuppressive factors or cells and reversing CD8 T cell tolerance. Teague et al. reversed the tolerance on CD8 T cells by delivering

pro-inflammatory cytokines such as IL-15 (*272*). Also, the combination with PD-1 blockade therapy led to specific expansion of high functional avidity T cell in another study from Zhu and colleagues, demonstrating the requirement for combination with other treatments for successful ACT (*273*). So far, despite huge advances in this domain, only the CAR-T cells have obtained FDA approval to treat B-cell malignancies. In 2017, tisagenlecleucel (Kymriah, Novartis, Switzerland) was the first anti-CD19 CAR T-cell having been approved to treat pediatric and young adult patients having relapsed and/or refractory B-cell precursor acute lymphoblastic leukemia (*274*). Later in 2017, axicabtagene ciloleucel (Yescarta, Kite Pharma, USA) was also approved by the FDA to treat adults with relapsed or refractory large B-cell lymphoma who received two or more lines of therapy. Both were approved in Europe in 2018. Indeed, along with the low availability and high cost of these highly personalized therapies, ACT has been associated with moderate and severe toxicities due to the infused cell product or to the associated medication and chemotherapy. Toxicities related to TIL therapy are mainly due to the complementary treatment and are often transitory, low grade and manageable, when providing adapted supportive care. On the contrary, despite many advantages, ACT exploiting transduced T cells with non-natural TCRs presents a higher risk of cell product-mediated off- and on- target toxicity. In order to control these hazardous side effects, patients must be treated in highly specialized centers, making challenging to integrate these therapies in conventional cancer care (*275*). Regarding CAR therapy, there is a lower risk of cross-reactivity as CARs bind to larger Ags. (*276*). This restrains the principal toxicity risk of this therapy to the concomitant medication and chemotherapy. Together with its high rate of clinical success, the risk/benefit ratio justified its approval by the FDA. Of note, toxicity is a real challenge for the establishment of ACT, since T cells can persist for up to ten years or more, which promotes long-term surveillance or eradication of remaining cancerous cells, but increases the risk of potential long-term toxicity (*277, 278*). The challenge remains to make these therapies safe enough for a larger number of patients for their use in conventional cancer care. It still requires a global consensus for side effect management and prevention. Altogether, despite the current difficulties, the improvement of ACT protocols, the future development of innovative high throughput technologies for cells infusion production, the patients selection, the side effect prediction and management might lead to a general improvement of the clinical outcome, and could tilt the benefit-risk balance in favor of the TIL or engineered T cell ACT approval.

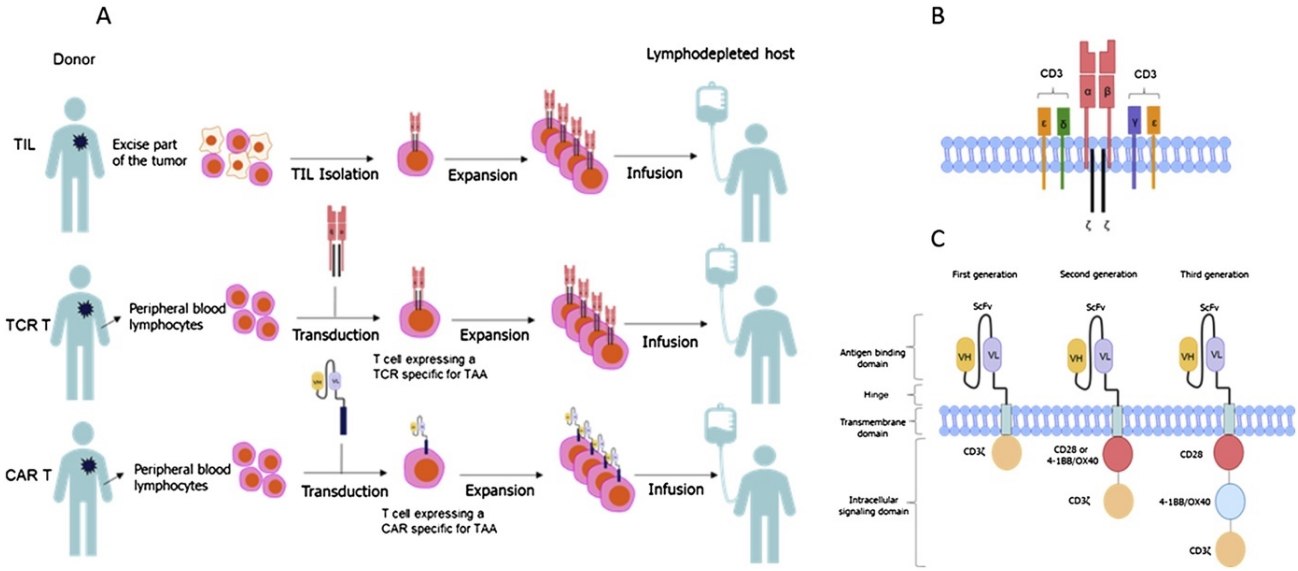

Figure 9: Adoptive cell transfer therapy: the basics. (A) Description of adoptive transfer of primary TILs, TCR engineered T cells and CAR T cells. (B) Representation of a TCR. (C) Representation of the different generations of CAR.

C. Identification, isolation and characterization of antigen-specific T cell

Detection and characterization of human Ag-specific CD8 and CD4 T cells is a major concern in cancer research to follow the course of an immune response or to identify T cells of interest for immunotherapies. The technologies developed to either quantify or functionally profile Ag-specific CD8 and CD4 T cells are discussed in this chapter.

1. Antigen-specific T cell identification

Several methods allow the detection of Ag-specific T cells among immune cells samples and are mostly based on functional readouts or staining with recombinant pMHC multimers (*279*). Functional assays following stimulation with cognate Ag such as cytokine release assay, proliferation assay (*280*), intracellular staining (ICS) (*281*) or cytolytic assays are highly sensitive to detect and/or quantify Ag-specific T cells in a sample and allow multiplex analyses on large samples libraries. In particular, IFN-γ-ELISpot assay quantifying the release of IFN-γ upon TCR engagement by cognate pMHC is one of the gold standards readout of T cell functionality. It is routinely used to measure the frequency of Ag-specific T cells within a sample and to monitor the efficiency of vaccination and other tumor immunotherapy trials (*282, 283*). Main drawback of this assay is its unability to recover cells of interest even if alternatives strategies exist (i.e IFN-γ catch assay). Also, a major drawback of the functional assays is their dependence on the functional state of the interrogated cells. Indeed, the frequency of exhausted, functionally deficient, T cells can be highly underestimated. To prevent such limitations, pMHC multimers have been used since decades to identify and isolate Ag-specific T cells by flow cytometry (*284, 285*). Several strategies have been developed for the high-throughput synthesis and multimerization of pMHC monomers using

multiple scaffolds in order to improve their sensitivity. Recent technological advances in the field of pMHC multimers are discussed in the book chapter in Annex 2 (*286*).

2. Antigen-specific T cell characterization

Besides isolation of Ag-specific CD8 T cells, there is a growing interest for their comprehensive characterization as immunotherapies rely on the induction of optimal T cell responses. Several assays can be exploited for a deep profiling of Ag-specific CD8 T cells. Phenotypic analysis and recent transcriptomic, metabolomic and proteomic technologies allow the measurement of several parameters related to gene expression which are correlated to the T cell potency.

Functional avidity, also referred to as Ag sensitivity, of T cells is a major parameter to evaluate T cell potency *in vitro*. Immune assays based on cytokine release quantification upon stimulation with increasing concentrations of the cognate Ag have been developed to directly gauge T cell functionality. Among other techniques evaluating the CD8 T cell killing potency, an historical method developed at the Ludwig institute directly assess the Ag-specific CD8 T cell frequency and potency through the measurement of target cell lysis using ^{51}Cr-release assay. This method offers high sensitivity levels with a detection limit superior to 1 in 20,000 T lymphocytes (*287*). However, this method became controversial due to the hazardous manipulation of radioactive isotopes. In order to avoid this major drawback, more recent techniques exploited a specific ELISpot detecting with high sensitivity cytolytic molecules such as granzyme B and perforin secreted by activated T cells (*288*) and assessed their sensitivity to incremental amount of Ag, reflecting their functional capacity. However, functional assays are not perfectly suitable for the prediction of *in vivo* efficacy (*289*). For this purpose, many studies highlighted the importance to consider the magnitude of the T cell response, its functional avidity, and its polyfunctionality (*290*). The two first parameters can be determined by cytokine release assay (amplitude of the signal and EC_{50} respectively), but they do not provide information on the T cell polyfunctionality. Nevertheless, it was shown that EC_{50} values are highly variable and mostly depend on the T cell's state of activation.

The pMHC-TCR binding strength (pMHC-TCR affinity, related to the dissociation constant K_D) also defined as structural affinity, is known to be a robust and reliable marker of T cell potency. Indeed, this parameter has shown to correlate with CD8 T cell responsiveness and with improved clinical outcomes (*291-294*). The binding strength of a TCR to its cognate pMHC indirectly regulates the inherent functional avidity of cytotoxic T cells by influencing CD8 T cells priming and differentiation through its action on the TCR signaling pathway (*295, 296*). Many studies highlighted that, within a range of physiological affinities (K_D 100-1 µM), TCR-pMHC affinity or structural affinity correlate with T cell functional avidity (*293, 297*). Regrettably, the majority of these studies exploited artificial models. In particular, using T cells transduced with engineered TCRs of incremental affinity, numerous studies have underlined that optimal T cell response happens within a defined window of TCR-pMHC affinity over

which cells start to gradually lose their functional capacity (*297-300*). Also, when exploiting engineered TCRs specifically targeting TAAs, the superior physiological affinity range often induces high functional avidity but cross-reactivity with self-derived peptides, potentially leading to self-immune response (*291, 301*).

Allard et al. showed on primary TAA- and virus-specific CD8 T cells that monomeric TCR-pMHC off-rate is closely related to the different features of CD8 T cell functions such as CD107a mobilization, cytokine release, cytotoxic function, proliferation, the modulation of coreceptor and polyfunctionality (*302*). Other *in vitro* studies and mathematical models also emphasized k_{off} as the best biophysical readout for prediction of CD8 T cells potency (*303, 304*).

Furthermore, pMHC-TCR binding strength proved *in vivo* to be a good predictor of efficient tumor eradication. ACTs with high affinity TCR are associated with increased antitumor response, better tumor infiltration and survival, but frequently coupled with concomitant autoimmunity when targeting TAAs (*260, 291, 303, 305*). Conversely, weak TCR-pMHC interactions are appropriate to prime naïve CD8 T cells, but usually do not support tumor eradication (*305*). Few clinical trials demonstrated better antitumor response provided by TCRs of higher affinity (*258, 260, 306*). However, when targeting TAAs, these high affinity tumor infiltrated CD8 T cells were highly susceptible to tolerization, reflected by the reduction of CD107a mobilization and IFN-γ expression (*273, 307*). Low affinity CD8 T cells presented indeed less susceptibility to tolerization, but did not support an effective antitumor response, due to ineffective priming and suboptimal functional potency (*308*). However, some studies supported their role in immune tumor control concerning the polyvalent responses (*309*). Altogether, these evidences support the need to select CD8 T cells of optimal affinity targeting for improved clinical outcomes.

General aims

Based on many clinical successes, immunotherapy is now the most innovative and promising strategy to fight cancer. Despite the high efficacy of ACT against metastatic melanoma and hematologic malignancies, it exhibited significantly lower objective clinical response against solid tumor. Kelderman et. al recently highlighted *in vivo* the significance to enrich T cells infusions in tumor-reactive T cells. Tumor-specific CD8 T cells are known to be critical for tumor growth control, as their infiltration into the tumor site better predict clinical outcome. Nevertheless, as tumor Ags are highly diverse, tumor-specific CD8 T cells are functionally heterogeneous (*310*), and the parameters associated with stronger CD8 T cell antitumor response are not fully understood yet, we expect that next-generation ACT will require optimal high-throughput methodologies to identify and isolate highly functional tumor-specific CD8 T cells or their TCR.

My PhD thesis addresses these issues to optimize ACT and comprises i) the comprehensive analysis and the designation of the most relevant antigenic target for ACT, ii) the determination of reliable parameters predicting antitumoral CD8 T cell potency, and iii) the development of reliable methodologies allowing the identification, selection and isolation of clinically relevant clones or TCR.

Recently, tumor neoAgs emerged as highly promising targets for ACT and are associated with many clinical benefits. Higher clinical relevance of neoAg-specific CD8 T cells over that of TAAs is hypothesized to be associated with their potential high affinity TCR since they escape central tolerance, but their direct superior antitumor activity has not been comprehensively assessed so far. Furthermore, many controversial studies supported or refuted the relationship between pMHC-TCR affinity and CD8 T cells functional avidity, and little is known about their correlation with *in vivo* efficacy (*302, 304, 311, 312*). To strengthen the current knowledge about these questionable assumptions and to clearly identify the factors predicting CD8 T cell potency, our main project comprehensively analyses structural affinity (monomeric pMHC-TCR off-rate) and functional avidities of peripheral and tumor-infiltrating CD8 T cells targeting viral epitopes, TAA and neoAgs. Then, to confirm the selection criteria for isolation of highly functional tumor-specific CD8 T cells, TAA-specific CD8 T cells of different structural affinities were used for tumor-control *in vivo*. In parallel, we aimed at developing tools to identify and isolate tumor-specific CD8 T cell of high clinical interest. In particular, we propose a high throughput method for indirect identification of highly potent tumor-specific TCRs based on the correlation between CD8 T cell functional avidity and their susceptibility to apoptosis following stimulation with cognate Ags. The comparative analysis of TCRs repertoires of bulks previously Ag-overstimulated or not will allow the identification of high affinity TCRs.

Thesis work

- **Main project: High Structural Affinity Neoantigen-Specific CD8 T Cells Preferentially Accumulate in Human Tumors**

- **Side project (Appendix): TCR repertoire subtraction assay: a new method for rapid identification of highly potent tumor-specific TCRs**

High Structural Affinity Neoantigen-Specific CD8 T Cells Preferentially Accumulate in Human Tumors

A. Aim

As previously described, the main goal of my PhD is to acquire a deeper understanding of TAA- and neoAgs-specific T cells functional and structural characteristics to improve the identification and isolation of the most clinically relevant ones. Regarding neoAgs, there are two issues emerging in our group: i) how can we improve the identification of neoAgs and ii) are all neoAgs-specific CD8 T cells equivalent and beneficial for ACT? i) for neoAgs, most mutations will not lead to processed peptides or to MHC ligands that are immunogenic. The group of Dr. Harari is currently focused on the development of tools and knowledge allowing the identification, profiling, filtering and isolation of neoAg-specific T cells for mutanome-based personalized immunotherapies. The pipeline for Ag discovery (Figure 10) relies on genomic, transcriptomic and immuno-peptidomics data (Dr. Bassani's group) (DNA/RNA sequencing and peptide analysis, respectively) to identify somatic mutations or mutated peptides (*166, 313*). Then, *in silico* predictions of peptide-MHC binding affinities are performed to refine peptide hits as well as, when applicable, *in vitro* peptide-MHC micro-scale refolding assay in order to eliminate non-binding peptides. Next, *in vitro* validation of immunogenicity is performed using APC pulsed with synthetic peptides or RNA encoding for mutated peptides. Following validation, immunogenic peptides are used to synthetize pMHC multimers for the isolation of Ag-specific T cells. This validation is tedious, costly and error prone (impurities within synthetic peptides, MHC restriction, precursors frequencies…). ii) My project addresses the second issue: as structural and functional profiles of neoAg-specific CD8 T cells remain poorly defined, the main objectives of my PhD are to perform complete profiling and comprehensive characterization of neoAg-specific CD8 T cells a) to further define the range of functional and structural avidity of neoAg specific CD8 T cells derived from PBLs or TILs in different types of cancer b) to compare them with other classes of Ag and c) to define the most clinically-relevant parameters allowing the identification of highly tumoricidal CD8 T cells.

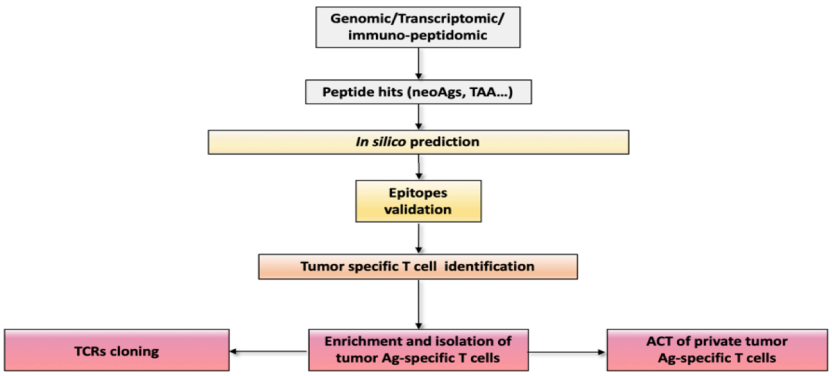

Figure 10: General pipeline for neoepitope discovery and validation

B. Introduction

The clinical relevance of T cells in the control of a diverse set of human cancers is now beyond doubt. However, the nature of the antigens as well as the functional profile of T cells that allow the immune system to efficiently distinguish tumor cells from benign cells has long remained obscure. Growing evidences suggest that such tumor epitopes can derive from Ags known as neoantigens, which have novel protein sequences resulting from tumor-specific mutations and which are consequently absent from the normal human genome and proteome. Targeting such neoAgs is promising and would enable immune cells to distinguish cancer cells from normal cells, leading to cancer rejection. Indeed, several studies confirmed that neoAgs recognition is a major factor in the activity of clinical immunotherapies.

Of note, in addition to their tumor-specificity (limiting the risk of autoimmunity), neoAgs also represent very attractive and highly promising targets for immunotherapies since these Ags are non-self and thus are not subjected to negative thymic selection. Consequently, it is generally accepted that the repertoire of T-cell recognizing neoAgs is unbiased and thus composed of high-affinity T cells, comparable to virus-specific T cells and different from T cells directed against shared tumor-associated antigens (TAA) where high-affinity T cells are deleted during thymic selection.

However, the functional profile of neoAg-specific T cells was never comprehensively investigated and it is unclear what distinguishes neoAg- from other TAA-specific T cells from a functional but also phenotypic or molecular standpoint. In addition to the functional heterogeneity of tumor-specific T cells, which remains to be addressed, the most relevant functional parameter associated with tumor infiltration and clinical efficacy is lacking.

Here, using proprietary pMHC class I reversible multimers (NTAmers), allowing measurement of monomeric pMHC-TCR dissociation kinetics (off-rates) on viable CD8 T cells, we comprehensively profiled the structural affinity (off-rates) and the functional avidity (Ag sensitivity) of peripheral (PBLs) and tumor-infiltrating (TILs) CD8 T cells targeting 5 viral epitopes, 6 TAA, and 7 neoAgs isolated from patients with melanoma or ovarian, colorectal or lung cancers. The relative accumulation of T-cell clones in tumors or in blood was associated to functional parameters but also to the expression of tumor homing markers. Finally, the ability of functionally-distinct T-cells to infiltrate and control tumors was evaluated *in vivo*.

Overall, our observations indicated that neoAg-specific CD8 T cells are superior to TAA-specific T cells with regard to their structural affinity but not functional avidity. High-affinity tumor-specific T cells accumulate in tumors, consistently with their ability to express and upregulate markers of tumor tropism and an optimal range of affinity is required to allow adoptively-transferred T cells to infiltrate and control tumors *in vivo*.

Taken together, our data indicate that high structural affinity neoAg-specific CD8 T cells preferentially accumulate in human tumors.

C. Materials and Methods

Ethics statement

Patients under study had stage III/IV metastatic melanoma, ovarian, non-small cell lung cancer and colorectal cancer and had received several lines of chemotherapy (Table 1). They were enrolled under protocols approved by the respective institutional regulatory committees at the University of Pennsylvania (Penn), USA, and Lausanne university hospital (CHUV), Switzerland. In particular, none of the subjects had any underlying infection or inflammatory condition at the time of study enrollment. Patients and healthy donors' recruitment, study procedures, and blood withdrawal were done upon written informed consent. All immune analyses were conducted at the Lausanne Branch of the Ludwig Institute for Cancer Research (LLB).

Identification of non-synonymous tumor mutations

Genomic DNA from cryopreserved tumor tissue and matched PBMC was isolated using DNeasy kit (Qiagen) and subjected to whole exome capture and paired-end sequencing using the HiSeq2500 Illumina platform. Data analysis was performed at the Vital-IT Systems Biology Division, Swiss Institute of Bioinformatics (SIB), Lausanne. Somatic variants were called from exome reads and the reference human genome hg19 by using a software pipeline composed of a genome mapping tool, fetchGWI (*314*), followed by a detailed sequence alignment tool, align0. Non-deterministic predictors of any kind were avoided and the route of minimizing false negative was prioritized and a cross-comparison with GATK as consensual variant detection/prediction method reached over 96% agreement. Variations present in the tumor samples and absent from the corresponding blood samples were assumed to be somatic.

Neoantigen prediction and in vitro validation

Binding predictions to class-I HLA alleles for all candidate peptides incorporating somatic non-synonymous mutations were performed using the netMHC algorithm v4.0. Candidate neoAg-epitope peptides (*i.e.* mutant 9mer and 10mer peptide sequences containing the somatically altered residue at each possible position) with a predicted binding affinity lower than 500 nM were synthesized. CD8 T cells (10^6 mL^{-1}) isolated (Dynabeads, Invitrogen) from cryopreserved PBMC were co-incubated with autologous irradiated CD8 and CD4-depleted PBMCs and peptides (1 µg mL^{-1}, single peptide, or pools of ≤ 50 peptides) in RPMI supplemented with 8 % human serum and IL-2 (20 IU mL^{-1} for 48 h and then 100 IU mL^{-1}). IFN-γ Enzyme-Linked ImmunoSpot (ELISpot) and peptide-MHC multimer staining assays were performed at day 12. T cell reactivity for every neoAg was validated by ≥ 2 independent experiments.

ELISpot assays were performed using pre-coated 96-well ELISpot plates (Mabtech) and counted with Bioreader-6000-E (BioSys). We considered as positive conditions those with an average number of spots higher than the counts of the negative control (No Ag) plus 3 times the standard deviation of the negative. TILs were generated from tumor enzymatic digestion by plating total dissociated tumor in p24-well plates at a density of $1x10^6$ cells/well in RMPI

supplemented with 8 % human serum and hrIL-2 (6000 IU/mL) without (conventional) or with (primed) 1µM of predicted peptides (in pools). After 2-4 weeks, TILs were collected and a fraction of the cultures underwent a rapid expansion (REP) for 14 days. T-cell reactivity against predicted neoantigens was tested by IFN-γ ELISpot on pre-REP TILs when available and post-REP TILs as described above. Positivity was confirmed in 2 independent experiments.

Isolation and expansion of antigen-specific CD8 T cells

Circulating and tumor-infiltrating Ag-specific CD8 T cells were FACS sorted using conventional or reversible NTAmers, and were either used for TCR sequencing or expanded or cloned by limiting dilution. To this end, cells were plated in Terasaki plates or 96-well plates and stimulated with irradiated feeder cells (PBMC from two donors) in RPMI supplemented with 8 % human serum, phytohemagglutinin (1 µg mL^{-1}) and IL-2 (150 U mL^{-1}). At the end of the REP, multimer-positive cells were > 95 % pure.

Peptides synthesis

Peptides were produced by the Peptides and Tetramers Core Facility (PTCF) of the University of Lausanne, were HPLC purified (>90 % pure), verified by mass spectrometry and kept lyophilized at -80°C. (table 1.)

Peptide-MHC multimers and NTAmers

Conventional pMHC multimers and NTAmers were synthesized by the Peptide and Tetramer Core Facility of the University of Lausanne. NTAmers are composed of streptavidin-phycoerythrin (SA-PE; Invitrogen) complexed with biotinylated peptides carrying four Ni^{2+}-nitrilotriacetic acid (NTA_4) moieties and non-covalently bound to His-tagged pMHC monomers. For pMHC-TCR dissociation kinetics experiments, pMHC monomers were refolded with Cy5-labeled β2m. Briefly, β2m containing the S88C mutation was alkylated using Cy5-maleimide (Pierce), purified and used for further refolding assay.

Dissociation kinetic measurements and data analysis

Ag-specific CD8 T cell clones (200 000 cels) were incubated for 40 minutes at 4°C with cognate NTAmers containing streptavidin-phycoerythrin and Cy5-labeled pMHC monomers in 50 µL FACS buffer (PBS supplemented with 0.5% BSA and 2 mM EDTA). After washing, cells were suspended in 500 µL FACS buffer at 4°C and cell surface-associated mean fluorescence was measured under constant temperature using a cooling device (4°C) on a SORP-LSR II flow cytometer (BD Biosciences) following gating on living cells. PE-NTA_4 and Cy5-pMHC monomer fluorescence was measured before (during 30 seconds; baseline) and during 10 minutes after addition of imidazole (100 mmol/L). FACS data were processed using the FlowJo software (v.9.6, Tree Star, Inc.). After gating on living cells, PE or Cy5 mean fluorescence intensity was derived using the kinetic module. Gates of 6 seconds period were created following addition of imidazole at the following time points: 15 seconds, 30 seconds, 45 seconds, 60 seconds, 90 seconds, 120 seconds, and then every minute for 10 minutes. Geometric MFI was measured

at each time point. Irrelevant NTAmer was used to measure background signal and values were systematically subtracted for each time points. Specific gMFI values were plotted and analyzed using the GraphPad Prism software (v.7, GraphPad) fitting a one phase exponential decay model.

Functional avidity

Functional avidity of Ag-specific CD8 T-cell responses was assessed by performing *in vitro* IFN-γ Enzyme-Linked ImmunoSpot (ELISpot, Mabtech) assay with limiting peptide dilutions (ranging from 10 µg/ml to 0.1 pg/ml). The peptide concentration required to achieve a half-maximal cytokine response (EC_{50}) was determined and named as the functional avidity.

CD8 T cells tropism assay

PBMCs, primary CD8 T cells clones, or primary CD8 T cells transduced with engineered TCR specific for NY-ESO-1 restricted by HLA-A0201 were distributed in 48 well plates (600 000/well) in RPMI supplemented with 8 % human serum and IL-2 (150 U/mL). Cells were stimulated at 37°C under 5 % CO_2 either with culture medium alone, phytohemagglutinin (PHA; Oxoid, 1 mg/mL), OKT3 antibody (plate precoated with 30 ng/mL, 5 ng/mL, or 1 mg/mL in PBS), or 200000 T2 cells pulsed with cognate peptide (at 1 mM or 1nM). After 48 h, cells were washed and replaced in culture for 48 h at 37°C under 5 % CO_2 in RPMI supplemented with 8 % human serum and IL-2 (150 U/mL). Half of the cells were analyzed by flow cytometry using the following panel of antibodies: Zombie Aqua™ dye (biolegend), Pacific Blue™ anti-human CD8 antibody (SK1, biolegend), PE-Texas Red anti CD3d antibody (7D6, Invitrogen), Brilliant Violet 650™ anti human CX3CR1 antibody (2A9-1, biolegend), Brilliant Violet 605™ anti human CD194 (CCR4) antibody (L291H4, biolegend), Brilliant Violet 711™ anti human CD197 (CCR7) antibody (G043H7, biolegend), FITC anti human CD49b antibody (P1E6-C5, biolegend), PerCP/Cy5.5 anti human CD195 (CCR5) antibody (HEK/1/85a, biolegend), Brilliant Violet 650™ anti human CD196 (CCR6) antibody (G034E3, biolegend), PE anti human CD49a antibody (TS2/7, biolegend), PE/Cy7 anti human CD103 (Integrin αE) antibody (Ber-ACT8, biolegend), Brilliant Violet 510™ anti human CD183 (CXCR3) antibody (G025H7, biolegend). After 5 days of resting, the cell leftover was also characterized with the same panel.

Flow cytometric assay for TCR-induced apoptosis

From day 12 after REP, virus-, TAA- and neoAg-specific CD8 T-cell clones were washed twice in PBS and were fluorescently labelled with cell proliferation dye eFluor™ 450 or eFluor™ 670 (at 0, 2 µM and 0.1 µM in PBS respectively) for 10 min at 37 °C. After 3 washes with RPMI medium supplemented with 8% human serum, cells were transferred in 96 well plates (50000 cells of each CD8 clone/100 µl RPMI medium supplemented with 8% human serum). Peptide-MHC stimulation was performed in parallel with irrelevant or cognate unlabeled pMHC tetramers (1 µg/ml) during 1, 2, 4, 5 and 24 h at 37°C under 5 % CO_2. TCR-induced cell death was assessed on a SORP-LSR II flow cytometer (BD Biosciences) using annexin V (BD

biosciences) staining. Flow-cytometric–based data were processed using the FlowJo software (v.9.6, Tree Star, Inc.).

TCR-induced apoptosis

From day 12 after REP, virus-, TAA- and neoAg-specific CD8 T-cell clones were transferred in 96 well plates (50000 cells/100 µl RPMI medium supplemented with 8% human serum). Peptide-MHC stimulation was performed with both irrelevant and cognate unlabeled pMHC tetramers (1 µg/ml) during 4 h at 37°C under 5 % CO_2. TCR-induced cell death was measured on a SORP-LSR II flow cytometer (BD Biosciences) using annexin V (BD biosciences) and DAPI (Thermo Fisher Scientific) staining on CD8 T cell clones. Flow-cytometric–based data were processed using the FlowJo software (v.9.6, Tree Star, Inc.). Cell death was considered for annexin V^{pos} and $DAPI^{pos}$ cells. The relative percentage of apoptotic cells has been calculated by subtracting the cell death induced by irrelevant pMHC tetramers.

TCRα and TCRβ Repertoire Sequencing

mRNA was isolated using the Dynabeads mRNA DIRECT purification kit (Lifetechnologies) and was then amplified using the MessageAmp II aRNA Amplification Kit (Ambion) with the following modifications: *in vitro* transcription was performed at 37°C for 16h. First strand cDNA was synthesized using the Superscript III (Thermofisher) and a collection of TRAV/TRBV specific primers. TCRs were then amplified by PCR (20 cycles with the Phusion from NEB) with a single primer pair binding to the constant region and the adapter linked to the TRAV/TRBV primers added during the reverse transcription. A second round of PCR (25 cycles with the Phusion from NEB) was performed to add the Illumina adapters containing the different indexes. The TCR products were purified with AMPure XP beads (Beckman Coulter), quantified and loaded on the MiniSeq instrument (Illumina) for deep sequencing of the TCRα/TCRβ chain. The TCR sequences were further processed using *ad hoc* Perl scripts to: (i) pool all TCR sequences coding for the same protein sequence; (ii) filter out all out-frame sequences; (iii) determine the abundance of each distinct TCR sequence. TCR with a single read were not considered for the analysis.

Clone TCRα and TCRβ Sequencing

mRNA was isolated using the Dynabeads mRNA DIRECT purification kit (Lifetechnologies). First strand cDNA was synthesized using oligo dT and the Superscript III (Thermofisher). Second strand was performed using a collection of TRAV/TRBV specific primer (1 cycle with the Phusion from NEB). TCRs were then amplified by PCR (20 cycles with the Phusion from NEB) with a single primer pair binding to the constant region and the adapter linked to the TRAV/TRBV primers added during the reverse transcription. A second round of PCR (25 cycles with the Phusion from NEB) was performed to add the Illumina adapters containing the different indexes. The TCR products were purified with AMPure XP beads (Beckman Coulter), quantified and loaded on the MiniSeq instrument (Illumina) for deep sequencing of the TCRα/TCRβ chain. The TCR sequences were further processed using *ad hoc* Perl scripts to: (i)

pool all TCR sequences coding for the same protein sequence; (ii) filter out all out-frame sequences; (iii) determine the abundance of each distinct TCR sequence. TCR with a single read were not considered for the analysis.

TCR-pMHC structure modeling

The protocol used to model the TCR-p-MHC complexes was adapted from our TCRep 3D approach (*315*). Starting from V and J segment identifiers and from the CDR3 sequences, the full sequence of the constant and variable domains of TCRα and TCRβ were reconstituted based on IMGT/GENE-DB reference sequences (*316*). Homology models of the TCR-p-MHC complexes were obtained using the Modeller (*317*) program, version 9. Template experimental structures were taken from the Protein Data Bank (*318*), and selected based on the sequence similarity to the different components of the complexes, i.e., peptide, MHC, β-microglobulin, TCRα, and TCRβ. Sequence alignments between the target and template proteins were obtained using the MUSCLE program (*319*). A total of 500 models were produced for each TCR-p-MHC complex, and ranked according to the Modeller Objective Function. The best ranked model was selected for CDR loop refinement. The later was performed by creating 4×500 alternative loop conformations using the "loop modeling" module of Modeller. During this refinement, loops were treated by pairs, as follows: TCRα CDR1 and CDR3 were optimized simultaneously by creating 500 loop conformations (whereas other CDR loops were held fixed), followed by TCRα CDR1 and CDR2, TCRβ CDR1 and CDR3 and finally TCRβ CDR1 and CDR2, in this order. After each of these four loop refinement steps, all models were ranked according to the Molecular Mechanics—Generalized Born Surface Area (MM-GBSA) score we used previously to perform TCR engineering (*297, 320, 321*). The total energy of the system was calculated using the CHARMM2749 force field, and the CHARMM v39 molecular mechanics package50. The electrostatic solvation free energy was calculated using the GB-MV251 implicit solvent model, with a dielectric of 1 and 80 for the protein and solvent, respectively, and no cutoff on the non-bonded terms. The non-polar solvation energy was estimated by weighting the solvent accessible surface area calculated analytically with CHARMM (with a probe radius of 1.4 Å) by a 0.0072 kcal/mol/Å2 surface tension. After each step of loop refinement, the model with the most favorable MM-GBSA energy was selected for the next step. Molecular graphics and analyses were performed with the UCSF Chimera package (*322*).

PRediciton of IMmunogenic Epitopes: PRIME

Immunogenic (n=1'266) and non-immunogenic (n=3'601) peptides were collected from many recent studies (*215, 216, 323-326*), and comprise both viral epitopes and cancer neoantigens. Only peptides with reported HLA restriction were considered. 8-mer peptides that could not be mapped back to a reference proteome were excluded (13 peptides in total), since NetChop predictions could not be performed on them. Non-immunogenic peptides were defined as peptides for which CD8 T cell reactivity could not be observed in the experiment where they had been tested.

Autoimmune epitopes were downloaded from IEDB (Feb 2019), restricting to class I linear (8- to 12-mers) epitopes in human with information about the allele restriction. A total of 204 epitopes could be obtained.

To disentangle the influence of affinity to HLA-I molecules from other parameters, we first annotated positions with minimal impact on affinity for each HLA-I allele, using our set of HLA-I binding motifs derived from unbiased MS data. We next trained a logistic regression taking as input the predicted affinity of the peptides to the HLA-I molecules and the amino acid frequencies at positions with minimal impact on affinity (i.e., 21-dimensional input vector), using glmnet R package v2.0.16 (alpha=0 and lambda=1). Affinity predictions were performed with MixMHCpred v2.0.1 (*327*) or NetMHCpan-4.0 (*328*). 2'800 (i.e., 50 per allele present in our data) additional negatives randomly selected from the human proteome were added to the training set in order to better match the real situation where non-immunogenic peptides are in strong excess compared to immunogenic ones. To validate our predictions and ensure that our results are not biased by one specific study, we used a leave-one-sample-out cross-validation strategy. Each sample with more than five immunogenic and more than 5 non-immunogenic peptides were iteratively removed from the training of the predictor and used to benchmark its accuracy. The area under the receiver operating curve (AUC) was used to assess the prediction accuracy. Comparisons were performed with affinity predictors (MixMHCpred2.0.1 (*327*) and NetMHCpan-4.0 (*328*)), cleavage site predictions (NetChop-3.0 (*329*)) and the immunogenicity predictor implemented on IEDB website (http://tools.iedb.org/immunogenicity/) (*325*).

Combinations of any of the features previously tested were further explored using the logistic regression based on glmnet). Neural networks with 2, 5, and 10 hidden nodes were also used to combine amino acid frequencies at positions with minimal impact on affinity with predicted affinity (MixMHCpred2.0.1), using the nnet R package (v7.3.12, decay=0.001).

Adoptive T cell transfer in immunodeficient IL2 NOG mice

IL2 NOG mice (Taconic) were maintained in a conventional animal facility at the University of Lausanne under specific pathogen–free status. Six- to nine-week-old female mice were anesthetized with isoflurane and subcutaneously injected with 10^6 HLA-A2/NY-ESO-$1_{157–165}$–positive human melanoma Me275 tumor cells (grown in DMEM medium supplemented with 10 % FCS). Once the tumors became palpable (around day 7), 2 to 5 million human tumor-specific CD8 T cell clones bearing TCRs of incremental affinity (kind gift from Dr Nathalie Rufer, (*310*)) were injected intravenously in the tail vein. Tumor volumes were measured by caliper twice a week and calculated as follows: volume = length x width x width/2. Mice were sacrificed by CO_2 inhalation before the tumor volume exceeded 1,000 mm^3 or when necrotic skin lesions were observed at the tumor site. When sacrificed, tumors were harvested, processed at the Tumor Processing Facility of the University of Lausanne. Immunofluorescence *in situ* labeling was performed by the Immune Landscape Laboratory. This study was approved by the Veterinary Authority of the

Statistical analysis

Statistical analyses were performed with the GraphPad Prism software. Correlation analyses were performed using Pearson or Spearman (Fig. 5) coefficient r. The associated P value (two-tailed, a 1⁄4 0.05) quantifies the likelihood that the correlation is due to random sampling.

Peptide-driven refolding assay

Refolding with heavy chains carrying a C-terminal BirA substrate peptide (BSP), biotin-labeled β2m and a test peptide were performed essentially as described (Guillaume, 2003 JBC). Human β2m was mutated S88 to C and after refolding alkylated with maleimide-PEG_2-biotin (Pierce, ThermoFisher Scientific) in PBS at pH 7.4. Refolding reactions were performed in 96 well plates at 4°C for 72 h in the presence of 10 µM peptide. Incubation without peptide and with reference peptides for each allele served as negative and positive controls, respectively. After centrifugation (4'000 rpm, 5 min), the reaction mixtures were transferred into 96 well plates coated with anti-BSP antibody. Amount of refolded pMHC complexes were detected by ELISA using streptavidin-alkaline phosphatase and following manufacturer's instructions (Sigma). All measurements were performed in triplicates and data processed using Excel (Microsoft).

D. Results

Neoantigen-specific CD8 T cells are superior to TAA-specific T cells with regard to structural affinity but not functional avidity

NeoAg-specific T cells are associated to the clinical efficacy of immunotherapy. However, it is unclear whether these cells functionally or phenotypically differ from TAA and, in particular, what is driving their superior efficacy. We sought to comprehensively investigate the functionality of neoAg-specific T cells together with that of other classes of Ags such as TAA and viral Ags. To this end, we generated a library of CD8 T-cell clones from 18 unique and distinct specificities (7 Neo, 6 TAA and 5 virus epitopes) isolated from patients with Melanoma or with ovarian, lung or colorectal cancer **(Tables 1-2)**. NeoAgs were *in silico* predicted from non-synonymous point mutations as described in the methods section. NeoAg-, TAA- and virus-specific T cells were identified in peripheral blood (PBL) and TIL and were then isolated by FACS sorting using multimeric pMHC complexes and cloned *in vitro* by limiting dilution.

We first looked at the functional avidity (or Ag sensitivity) determined as the antigenic dose (*i.e.* peptide concentration) able to mobilize half of the maximal T-cell response measured by IFN-γ ELISpot. As shown in the representative examples as well as in the cumulative data, a large breadth of functional avidities was observed within each class of Ag (neo vs TAA vs viral) but also within each single specificity (**Figure 11 A-B and S1**). Of interest, virus-specific CD8 T cells were highly functional and were significantly superior to neoAg- and TAA-specific CD8 T cells (**Figure 11 C**). No significant difference, however, was observed between neoAh- and TAA-specific CD8 T cells (**Figure 11 C**). The two above conclusions were not biased by the different HLA class I restrictions and remained valid when exclusively HLA-A*0201-restricted T-cells were considered (**Figure 11 C**). Still, taken together, these data indicate that neoAg-, virus- and TAA-specific CD8 T cells partially overlap regarding their functional avidity but also that only virus-specific CD8 T cells are composed of significant fraction of highly functional cells (with an $EC_{50}<10^{-10}$ M) while neoAg- and TAA-specific CD8 T cells are mostly composed of average or low functionality ($EC_{50}>10^{-10}$ or $>10^{-7}$ M, respectively) T cells (**Figure 11 D**).

Given the fact that functional avidity is a parameter requiring a functional T-cell response (e.g. cytokine secretion), it is influenced by the affinity of pMHC-TCR interactions but it is also potentially biased by the activation/exhaustion state of cells. To circumvent this potential bias, and to more comprehensively investigate pMHC-TCR interactions, we analyzed the structural affinity of the library of 18 Ag-specific T cells using reversible multimeric pMHC molecules, named NTAmers (*330*), and determined their off-rate (K_{off} or $\ln(2)/T_{1/2}$). As shown in the representative examples as well as in the cumulative data **(Figure 11 E-F and S2**), a large breadth of structural affinity was observed within each class of Ag (neo vs TAA vs viral) but also within each single specificity. Of interest, unlike for the functional avidity, neoAg-specific CD8 T cells were superior to TAA-specific CD8 T cells with regard to structural affinity and were

not significantly different from virus-specific CD8 T cells **(Figure 11 G)**. In contrast, when only HLA-A*0201-restricted CD8 T cells were considered, neoAg-specific T cells remained superior to TAA-specific T cells but were also lower than virus-specific T cells **(Figure 11 G)**.

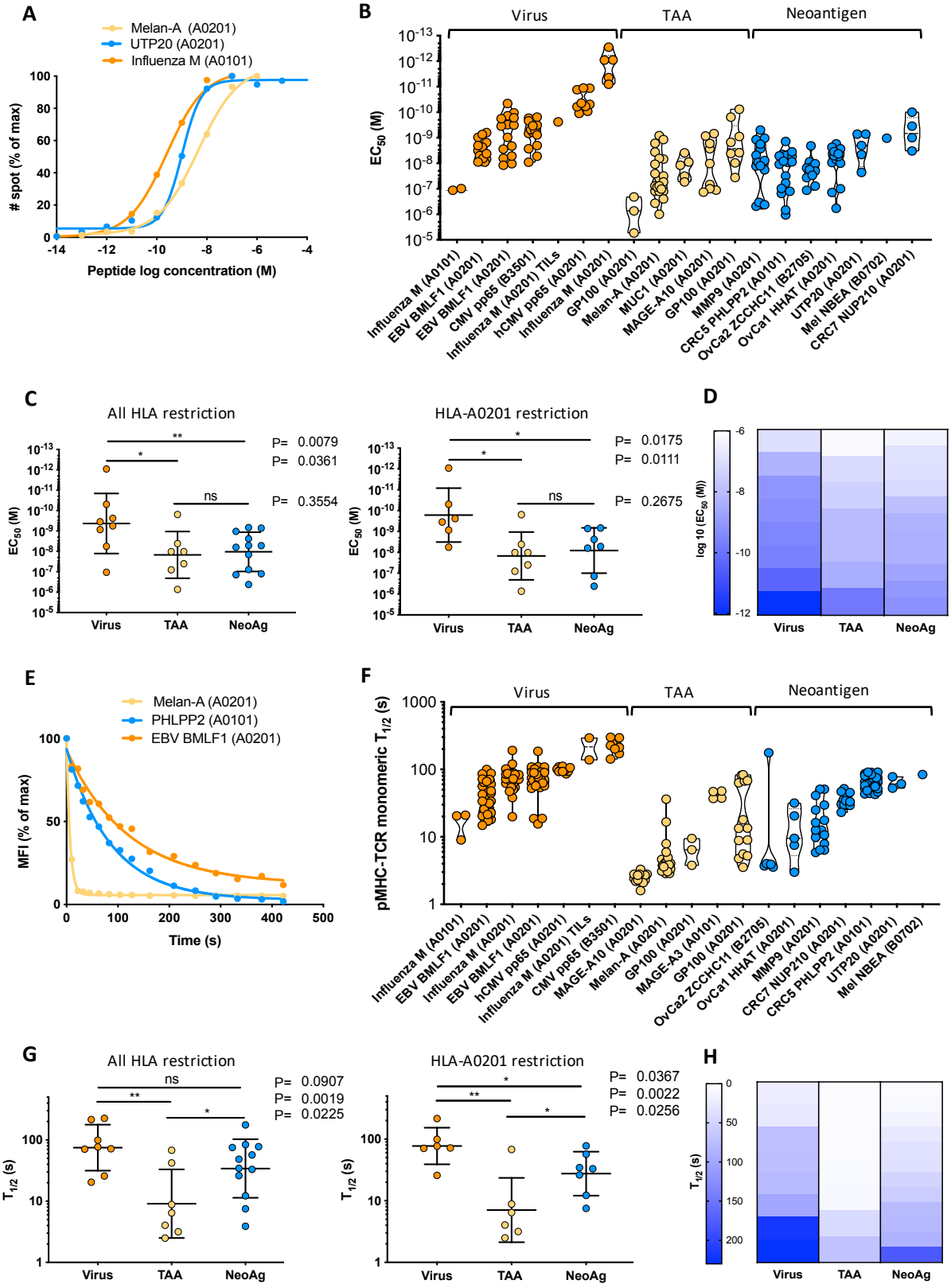

Figure 11: Functional and structural avidity of neoAg-, TAA- and virus-specific CD8 T cells. A. Representative examples of the functional avidity of virus-, TAA- or neoAg-specific primary CD8 T-cells. Cells were stimulated with serial dilutions of

*cognate peptides and functional responses were assessed by IFN-γ ELISpot assay. B Functional avidity (EC_{50}, M) of individual virus-, TAA- and NeoAg-specific CD8 T-cells measured by IFN-γ ELISpot assay (median with 95% CI). C. Medians of the functional avidity (EC_{50}, M) of all HLA class I- (left) or HLA-A*0201- (right) restricted virus-, TAA- and NeoAg-specific CD8 T-cells. D. Average composition of virus-, TAA- and NeoAg-specific CD8 T-cells of different ranges of functional avidity. E. Representative examples of monomeric pMHC-TCR dissociation kinetics of virus-, TAA- or NeoAg-specific CD8 T-cells. NTAmers were used to measure monomeric pMHC-TCR $T_{1/2}$ (s). F. Structural affinity (monomeric pMHC-TCR dissociation kinetics: $T_{1/2}$ (s)) of individual virus-, TAA- or neoAg-specific T-cells (median with 95% CI). G. Medians of the structural affinity ($T_{1/2}$ (s)) of all HLA class I- (left) or HLA-A*0201- (right) restricted virus-, TAA- and neoAg-specific primary CD8 T-cell clones. H. Average composition of virus-, TAA- and NeoAg-specific CD8 T-cells of different ranges of structural affinity.*

These data indicate that virus-specific T cells were exclusively composed of high (>75s) and intermediate (10-75s) affinity cells in contrast to TAA-specific T cells which were mostly composed of low (<10s) affinity cells and that NeoAg-specific T cells had an intermediate profile with high, intermediate and low affinity cells **(Figure 11 H**). Taken together, our observations indicate that neoAg-specific CD8 T cells are superior to TAA-specific T cells with regard to their structural affinity but not functional avidity.

High affinity neoantigen-specific CD8 T cells reside in tumors

Given the large breadth of structural affinity and functional avidity observed among the different Ag-specific CD8 T cells, we asked whether these would be associated to the affinity of peptides for cognate HLA alleles or with any common *in silico* predictor of peptide-MHC stability or processing, or, in the case of neoantigen, to the distance to self (*171, 328, 331, 332*). Our data indicate that none of these parameter (pMHC affinity and stability, prediction of processing as well as distance to self) did correlate with either the functional nor the structural avidity (**Figure S6**).

The lack of significant correlation between *in silico* predictors of pMHC interactions and T-cell functionality across distinct epitopes is consistent with the fact that a large functional diversity was also observed within each epitope-specific T-cell population. Indeed, several neoAg- (but also TAA- and virus-) specific T cells recognizing the same epitope were functionally heterogeneous, suggesting that pMHC features may influence but do not dictate T-cell functionality.

In this regard, we previously reported in ovarian cancer patients that neoAg-specific TIL were of higher functional avidity than blood counterparts (PBL) targeting the same neoAg (*324*). We thus sought to determine whether this preliminary observation could be confirmed also for neoAg-specific T cells isolated from patients with melanoma or lung or colorectal cancer but also whether this would also hold true for other classes of Ags. In addition, the ranges of functionality of neoAg-specific T cells was never comprehensively compared to that of TAA- or virus-specific T cells. Figure 12 A shows a representative example of the functional avidity of PHLPP2-specific T-cell clones isolated from tumor or blood of patient CRC5 with colorectal cancer. As expected, PHLPP2-specific TIL were superior to blood counterpart by more than one order of magnitude (**Figure 12 A**). Of interest, the superior average functional avidity of TIL relative to cognate PBL was also confirmed in melanoma, CRC or NSCLC patients for 3 neoAgs as well as three TAA (**Figure 12 B and S3**). However, for one additional neoAg

(ZCCHC11 from OvCa patient 19809-304), PBL were superior to TIL and this outlier (with the highest off-rates among all tumor-reactive TCRs seen in TIL) will be discussed below. Interestingly, the breakdown of data between PBL and TIL for each classes of Ags confirmed that virus-specific T cells are more functional than both neoAg- and TAA-specific T-cells (which are not different from each other) and this for both circulating or tumors-infiltrating cells (**Figure 12 C**).

We then asked whether similar differences would be seen with regard to structural affinity. As shown for PHLPP2-specific T-cell clones, but also for the entire panel of neoAg- and TAA-specific T-cell clones, the average structural affinity of TILs was consistently higher than that of cognate PBL, including for the aforementioned ZCCHC11-specific T cells which is showing the most striking difference between PBL and TIL (**Figure 12 D-E**). The breakdown of data between PBL and TIL for each classes of Ag indicated that neoAg-specific TILs were of high structural affinity, almost in the same range than virus-specific TIL but also that high affinity TAA-specific TIL could be identified (although the overall number of TAA precluded major conclusions since average values of multiple different T-cell clones were considered) (**Figure 12 F**).

To clarify the dynamic between neoAg-specific PBL and TIL at the clonotypic level, we repeated FACS sorting of PBL and TIL recognizing the same neoAg in the same patients using pMHC multimers and performed a comprehensive TCRα and TCRß sequencing on purified Ag-specific PBL and TIL (**Figure 12 G**). These analyses indicated that neoAg-specific PBL and TIL were both oligoclonal, with only some shared TCRs found between cells isolated in blood and tumors (**Figure 12 G-H and S5**). Of interest, the relative clonal dominance in PBL and TIL was discordant and inverted between both compartments. In patient SCC001, the dominant UTP20-specific TCR Cl1 from TIL (70%) was contributing to only 1% of the PBL repertoire. The TCR Cl25 from TIL was also 10-fold lower in PBL. In contrast, Cl24 and Cl48 TCR representing 0,1% and 8% of UTP20-specific TIL, respectively, were 3-6 fold enriched in PBL (**Figure 12 H)**. Furthermore, several unique TCRs were mostly identified in PBL relative to TIL. Similar experiments were performed on three additional neoAgs and confirmed that neoAg-specific TILs are mostly composed of shared TCR (i.e. also found in PBL) while neoAg-specific PBL are more balanced and composed of unique and shared TCRs (**Figure 12 H**). To understand how these observations relate to the overall higher affinity of TIL compared to PBL discussed earlier (**Figure 12 A-F**), we determined the structural affinity of Cl1, Cl25 and Cl48 TCRs and observed the following hierarchy Cl1 > Cl25 > Cl48. Molecular modeling analyses also confirmed that the CL1 TCR was making more favorable interaction with the UTP20 pMHC than the Cl48 TCR, consistently with k_{off} data (**Figure 12 I and S4**). The ranges of affinity determined for Cl1, Cl25 and Cl48 TCRs thus indicated that among the distinct TCRs found in UTP20-specific cells, there was a direct positive correlation between the structural affinity and the relative clonal dominance in TIL while, conversely, these parameters negatively correlated in PBL (where low affinity TCR accumulate, **Figure 12 J**). Finally, a positive correlation was observed between the

clonal dominance of UTP20-specific TCR and their structural affinity in TIL, while the correlation was inversed in PBL (**Figure 12 K**). These data indicate that high- and low-affinity neoAg-specific CD8 T cells are preferentially found in tumors and in peripheral blood, respectively.

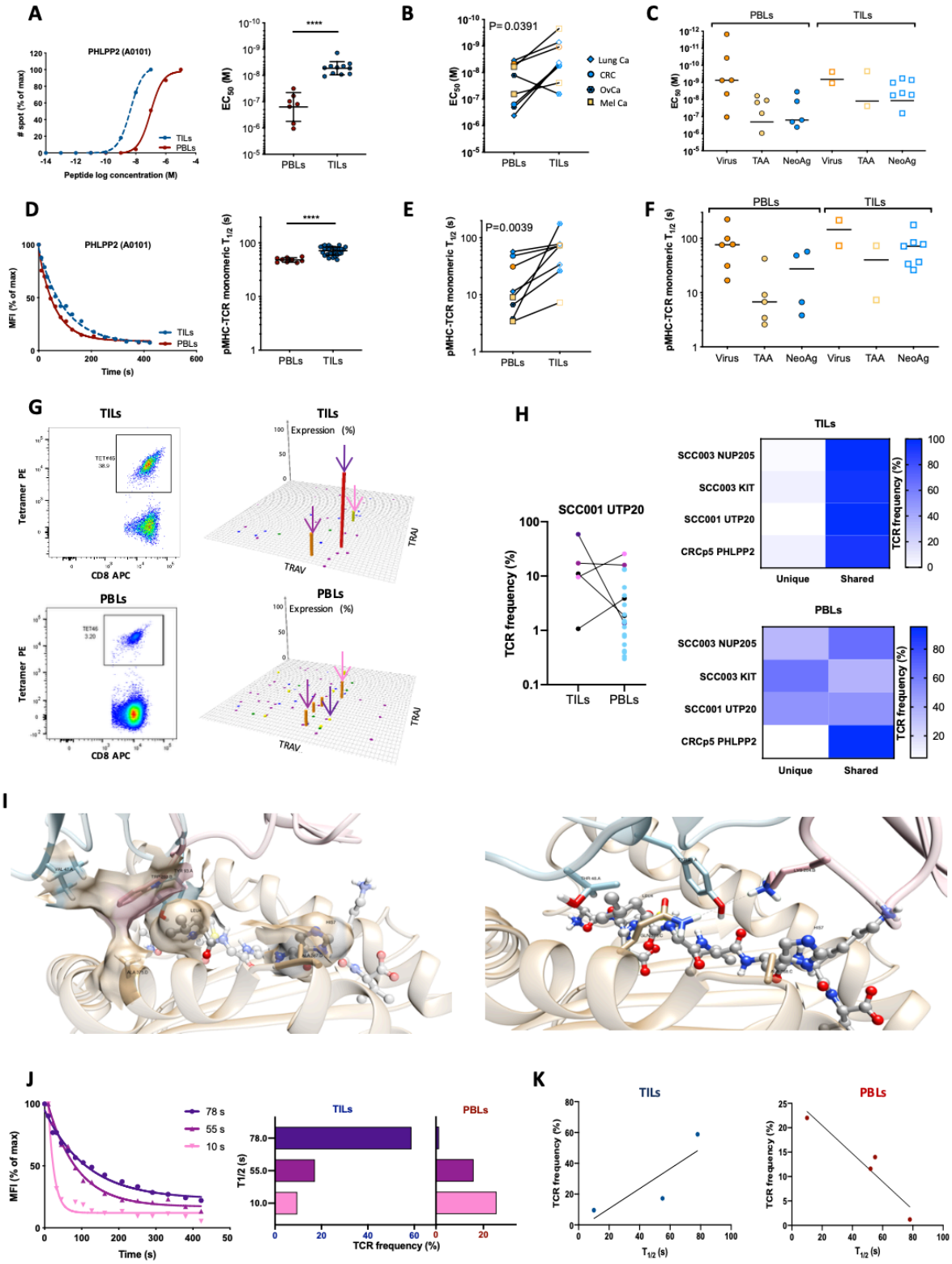

Figure 12: Functional and structural avidity of NeoAg-specific PBLs and TILs. A. Representative examples (left) and cumulative analyses (mean ± SD) (right) of the functional avidity of NeoAg-specific PBLs (red lines) and TILs (blue dotted lines) assessed by IFN-γ ELISpot assay. PHLPP2-specific TILs and PBLs were isolated from patient CRCP5. B. Comparison of

the functional avidity (EC_{50}, M) of eight pairs of PBL and TIL each recognizing the same epitopes. C. Median of the functional avidity (EC_{50}, M) of each virus-, TAA- and NeoAg-specific PBLs (filled circles) and TILs (empty squares). D. Representative examples (left) and cumulative analyses (right) of the monomeric pMHC-TCR dissociation kinetics of NeoAg-specific PBLs (red lines) and TILs (blue dotted lines) assessed with NTAmers. E. Comparison of the structural affinity ($T_{1/2}$ (s)) of eight pairs of PBL and TIL. F. Median of the structural affinity ($T_{1/2}$ (s)) of each virus-, TAA- and NeoAg-specific PBLs (filled circles) or TILs (empty squares). G. Dot plot of the pMHC multimer sorting of UTP20-specific CD8 T cells from PBLs and TILs from patient SCC001 (left). TCR repertoire of the sorted UTP20-specific PBLs and TILs. H. TILs and PBLs TCR repertoires comparison: frequency of shared (black and purple) and unique (blue) TCRs found in Ag-specific PBLs and TILs of patients SCC001 (left). Heat map of the frequency of shared and unique TCRs found in Ag-specific PBLs or TILs from patients SCC001, SCC003 and CRC5 (right panel). I. In silico analysis of the molecular interaction between TCR-pMHCs for UTP20-specific TCR derived from TILs (left) and PBLs (right). TCRα ribbon is coloured in light blue, with residues displayed in sticks and coloured according to the atom types carbon coloured in light blue. TCRβ is coloured in pink, with residues displayed in sticks and coloured according to the atom types, with carbon coloured in pink. MHC is coloured in brown, with residues displayed in sticks and coloured according to the atom types, with carbon coloured in brown. The peptide is shown in grey ball and stick and coloured according to the atom types and carbon coloured in grey. Residues are labelled in black. For the TIL Cl1 we observe more polar and apolar contacts between the TCRs and the peptide, as described in Table 4-7. For TIL the hydrophobic residue LEU4 is in a cloud of non-polar contacts that include VAL47.A, TYR93.A and TRP203.B, involving therefore CDR3a and CDR3β. HIS7 of the peptide is also involved in apolar contact but mainly with MHC. For a better comprehension of the apolar interactions around these residues, we have highlighted them in surface representation. LEU4 in PBL is less involved in apolar contacts and interacts mainly with THR48.A. In the PBL, (when compared to TIL), the CDR3b loop is shifted to the C-terminal region of the peptide, presenting a hydrogen bond with CDR1a TYR28 that also presents a hydrogen bond with GLN387 from MHC. The peptide is less involved in interactions with TCR in the PBL structure supporting the lower mean half-life for PBL. J. Structural affinity and TCR frequency of CD8 T cells from TILs or PBLs: Representative examples (left panel) of the monomeric pMHC-TCR dissociation kinetics of UTP20-specific CD8 T cell clones assessed with NTAmers. TCR frequency (right panel) of functionally characterized UTP20-specific CD8 T cell clones derived from PBLs and TILs bulks (left). K. Correlation between the structural affinity ($T_{1/2}$ (s)) and TCR frequency of UTP20-specific PBLs and TILs.

High-affinity T cells preferentially express tissue (tumor) homing receptors

Having established that high-affinity CD8 T cells preferentially reside in tumors, we then hypothesized that these cells may better express tissue homing receptors since several studies reported that key combinations of chemokine receptors and integrins, such as CXCR3 and CD103, may be required to allow tumor infiltration (*333*). To address this question, we analyzed the expression of relevant chemokine receptors and integrins on Ag-specific T-cells of low and high avidity, either directly or after short-term stimulations. Representative examples of FACS profiles are shown in **Figure 13 A**. As shown in these examples, high-avidity T-cells express higher level of CXCR3, but also of VLA-1 and VLA-2, relative to low avidity T-cells (recognizing the same epitopes) (**Figure 13 A-B**). No significant difference was observed, in contrast, for chemokine receptors that are not known to be involved in tumor infiltration or retention, such as CCR4 or CCR6 (**Data not shown**). Furthermore, high-avidity T-cells were also endowed with the ability to more strongly upregulate CXCR3 and CD103 than low-avidity cognate T-cell clones (**Figure 13 C-E**). The latter observation was specific to tumor-related molecules since no significant difference was observed for other chemokine receptors on the same panel of Ag-specific T-cells (e.g. CCR4 or CCR6) which are not implied in tumor infiltration (data not shown). Taken together, these observations suggest that high-affinity T cells preferentially express tissue (tumor) homing receptors.

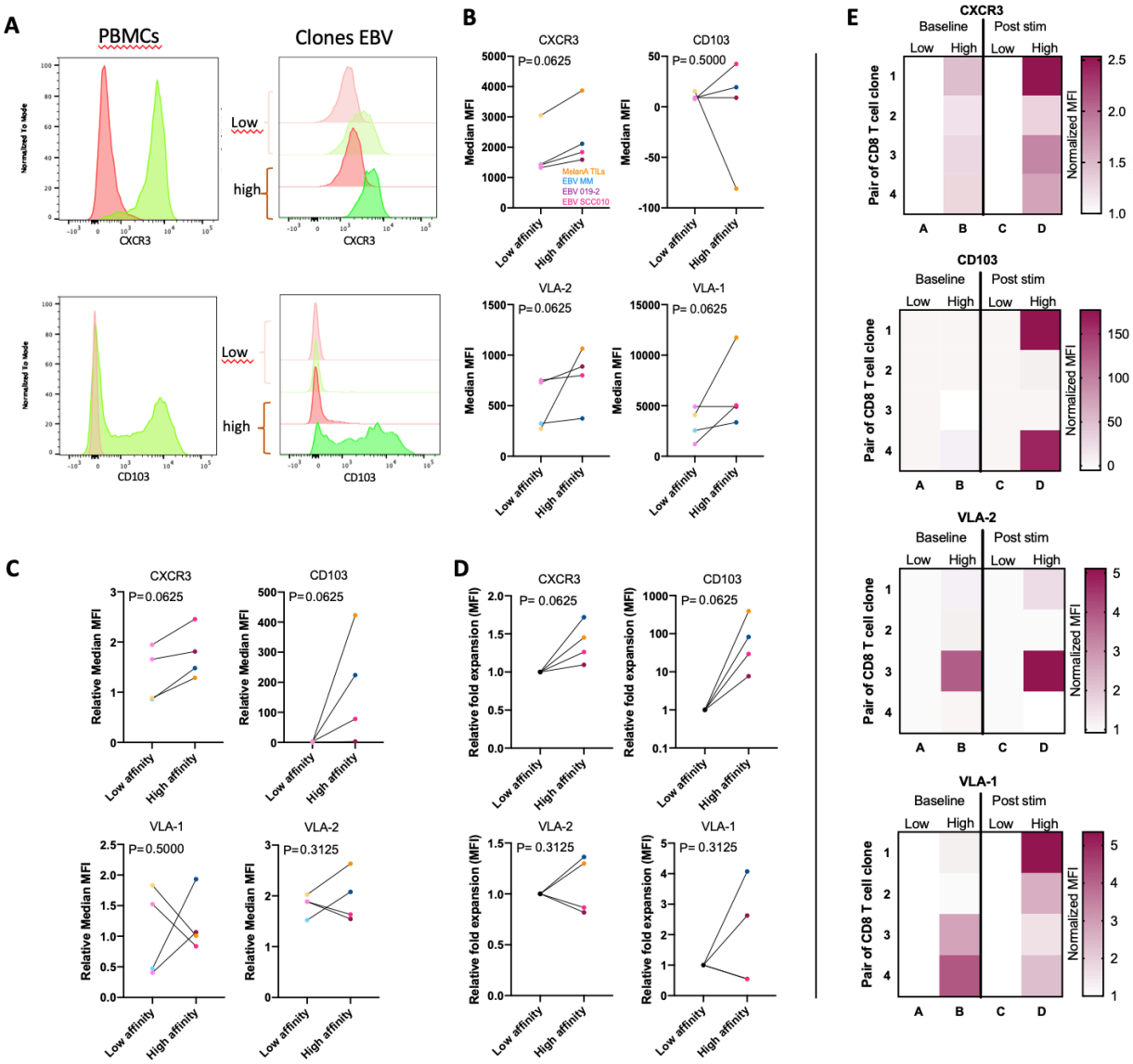

Figure 13: Expression of tissue (tumor) homing receptors on high- and low-affinity T cells. A. FACS analysis of the expression of chemokine receptors and integrins on ex vivo PBL (left panel) from a healthy donor stimulated (red) or not (green) with OKT3 for 48h followed by 48h of resting, or on EBV BMFL1-specific CD8 T-cells of low- (light color, $T_{1/2}$=18s) and high- (dark color, $T_{1/2}$=45 s) structural affinity stimulated (red) or not (green) with T2 loaded with 1 µM of EBV peptide (GLCTLVAML) for 48h followed by 48h of resting. The histograms represent the relative fluorescence intensity (MFI) of cells stained with different anti-integrin or chemokine receptor antibodies. B. Comparison of the basal expression of cell surface homing receptors in pairs of virus- and TAA-specific CD8 T-cells derived from the same donor. The median MFI corresponding to each chemokine receptor and integrins expression is represented for each pair of Ag-specific CD8 T-cells of low (light) and high (dark) structural affinity. C. Cell surface homing receptor expression in pairs of virus- and TAA-specific CD8 T-cells derived from the same donor after 48h of stimulation with T2 pulsed with 1µM of cognate peptide followed by 48h of resting. The median MFI is normalized to the baseline expression for each pair (left). D. TCR-pMHC structural affinity-dependent homing receptor upregulation after 48h of stimulation with T2 pulsed with 1µM of cognate peptide and 48h of resting. The median MFI is normalized for each virus- and TAA-specific CD8 T cells pair to the homing receptors upregulation of the low structural affinity clone. E. Heat map representing the TCR-pMHC structural affinity-dependent cell surface homing receptor expression either without (left) or after (right) TCR-dependent stimulation for each pair of T-cells. The median MFI corresponding to each marker is normalized for each pair to that of low avidity CD8 T-cells.

Adoptively-transferred low-affinity T cells do not infiltrate tumors

Having determined that high-affinity T cells preferentially express but also upregulate markers of tumor tropism after cognate T-cell stimulation, we sought to validate the relevance of these makers as predictors but also mediators of tumor infiltration. To this end, we focused on a well established in-house model of primary CD8 T cells transduced with distinct NYESO-1 TCRs covering a 4-log range of functional and structural avidity (*297, 310, 334*). The panel of TCR variants of progressive affinities was established by *in silico* modelling. Computational approach (MM-GBSA) was applied to the wild type TCR BC1, to evaluate the contribution of each AA to the interaction energy with A2/NY-ESO$_{157–165}$ and identify the substitutions that would impact the binding. Then, binding free energy evaluation with crystal structure of the closely associated TCR 1G4 (T95Q, S96T, N97A, & T98A) complexed with A2/NY-ESO-1$_{157–165}$, allowed to design four TCR variants of incremental affinity (including DMB). V49I and wtc51 mutants were identified by phage-display screening of a 1G4 TCR-based library. TCR-pMHC affinity parameters were validated by biacore.

After transduction, the DMB and V49I transduced primary CD8 T cells have a pMHC-TCR dissociation $T_{1/2}$ of 252 s and 7 s, respectively, and the maximal functional capacity (assessed by IFN-γ release assay) of DMB mutant is 15 fold superior to the one of the V49I mutant (**Figure 14 A**). Of interest, upon adoptive transfer of primary T cells transduced with either DMB or V49I into IL2 NOG mice bearing the autologous Me275 tumor, only DMB-, but not V49I-transduced T cells successfully infiltrated tumors (**Figure 14 B-C**). These data indicate that adoptively-transferred low-affinity T cells do not infiltrate tumors.

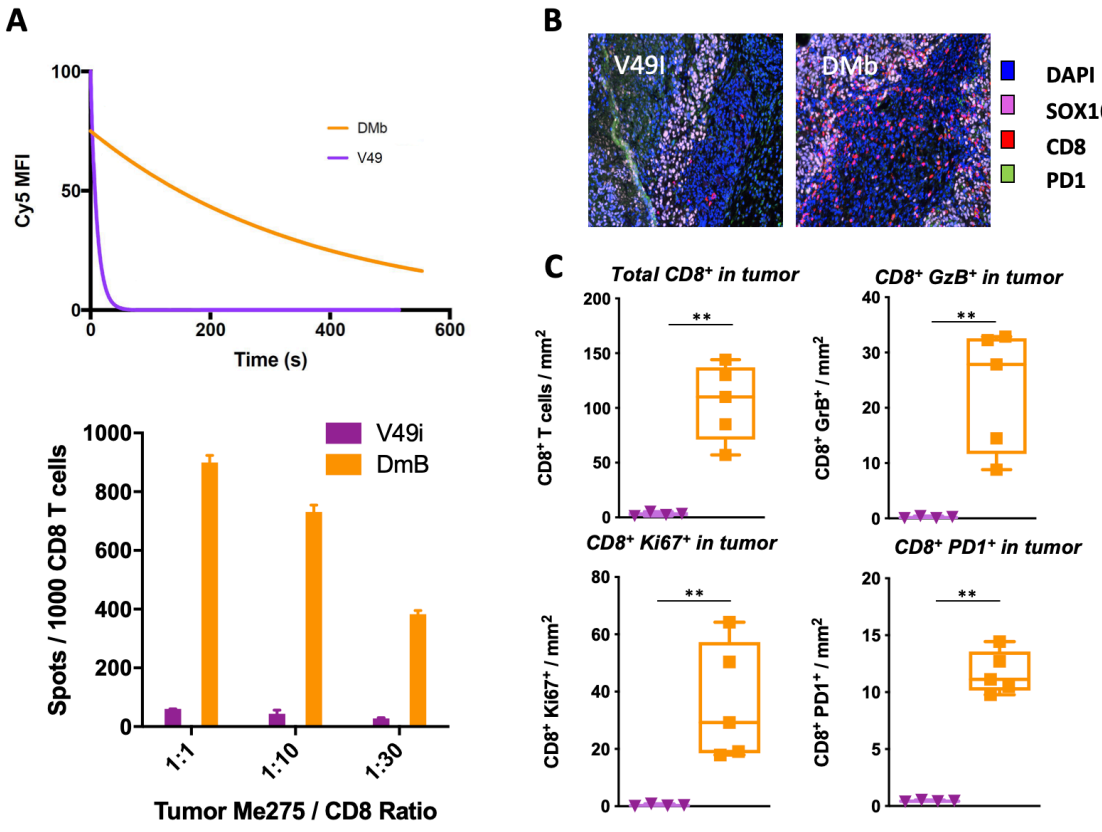

Figure 14: Adoptive cell transfer experiment in IL2 NOG mice bearing the autologous Me275 tumor with a pair of primary CD8 T cells clones transduced with NY-ESO-I-specific TCR of different avidities. A. Functional and structural analysis of primary CD8 T cells transduced with 2 different NYESO-I-specific TCRs. Monomeric pMHC-TCR off-rates are measured on NYESO-I-specific CD8 T cells using NTAmer technology. Monomeric dissociation of Cy5 labeled is plotted over time for each mutants (low affinity V49 in purple, high affinity DMB in orange (top)). IFN-γ release assay using NYESO-I positive melanoma tumor Me275 and NYESO-I-specific CD8 T cells at different ratios. B. Selected examples of tumor sections stained with fluorescent antibodies for SOX10 (violet), CD8 (red) and PD1 (green). DAPI (blue) was used to stained nuclei. Images were obtained with Inform software. C. Quantification and phenotype analyses of tumor infiltrated CD8 T cells (V49I in purple, DMB in orange). Analyses were performed using Inform and represent individual mice. Density (number of cells / mm2) are plotted. Percentages of PD1-expressing CD8 T cells are plotted in the bottom right panel.

Optimal structural affinity neoantigen-specific CD8 T cells preferentially control human tumors

We have established that high- but not low-affinity adoptively-transferred T cells were endowed with the capacity to infiltrate tumors, consistently with the observation that NeoAg- and TAA-specific TILs were more functional than blood counterpart. We then asked whether the ability to infiltrate tumors was quantitatively associated to T-cell potency and, in that case, whether the best correlate of infiltration would be the structural affinity or the functional avidity. To this end, we analyzed the association between the two functional parameters and first focused on 18 HLA-A*0201-restricted Ag (Neo, TAA and virus)-specific T cells responses. Interestingly, a strong positive correlation was observed (**Figure 15 A**), indicating that within a defined range (EC_{50} up to 10^{-12} and $T_{1/2}$ up to 100s), both parameters were consistent and quantitatively correlated. Of interest, when all HLA class I restricted Ag-specific T-cell responses were considered, then, among all additional epitopes (n=25), two T-cell responses (against ZCCHC11 and hCMV pp65) clearly fell out of the correlation and had very low K_{off} ($T_{1/2}$>150s) but moderate EC_{50} (10^{-7} - 10^{-9}). Strikingly, ZCCHC11-specific T cells were the unique outlier discussed earlier where TILs were not functionally more avid that PBL (but were of higher structural affinity, **Figure 12 B and E**). The uniquely high structural affinity of ZCCHC11-specific TIL was confirmed by molecular modelling confirming the highest number of TCR-pMHC favorable interactions (π) among the 10 models analyzed (**Figure 15 B and S4**).

The functional profile of ZCCHC11-specific TIL is, to the best of our knowledge, the first evidence that neoAg-specific T cells with very high structural affinity but moderate (and somehow discordant) functionality can be found in nature. This observation, however, is consistent with previous studies showing that engineered TCR with very low off-rates are dysfunctional and these were called supraphysiologic (*297, 301*). Therefore, these observations raised to the questions whether a too high structural affinity (associated with limited functional avidity) would prevent tumor infiltration and tumor control.

To this end, we included NYESO-1 TCR wtc51 (previously described as supraphysiologic) and compared its performances to that of V49I and DMB described earlier (**Figure 14**). Consistently with previous studies (*296, 297*), wtc51-transducted T cells have a very low off-rate but limited functionality (**Figure 15 C**). A hierarchy of structural affinity was thus confirmed with wtc51>DMB>V49I while wtc51- were less functionally avid that DMB-transduced T cells (**Figure 15C**). Of interest, compared to DMB-, wtc51-transducted cells did

not efficiently express tumor homing molecules (**data not shown**). Consistently, adoptively-transferred DMB-specific T cells successfully infiltrated but also fully controlled tumors *in vivo* while neither V49I- (low affinity and low avidity) nor wtc51- (very high affinity but moderate avidity) specific T cells were able to control tumors (**Figure 15 D**). Still, a low number of wtc51-specific T cells was found in tumors, but those were expressing very high levels of PD-1 (**Figure 15 D**).

Taken together, these observations suggest that beyond a certain point, too high structural affinity T cells are dysfunctional and get exhausted in tumors and indicate that only optimal structural affinity neoAg-specific CD8 T cells preferentially control human tumors.

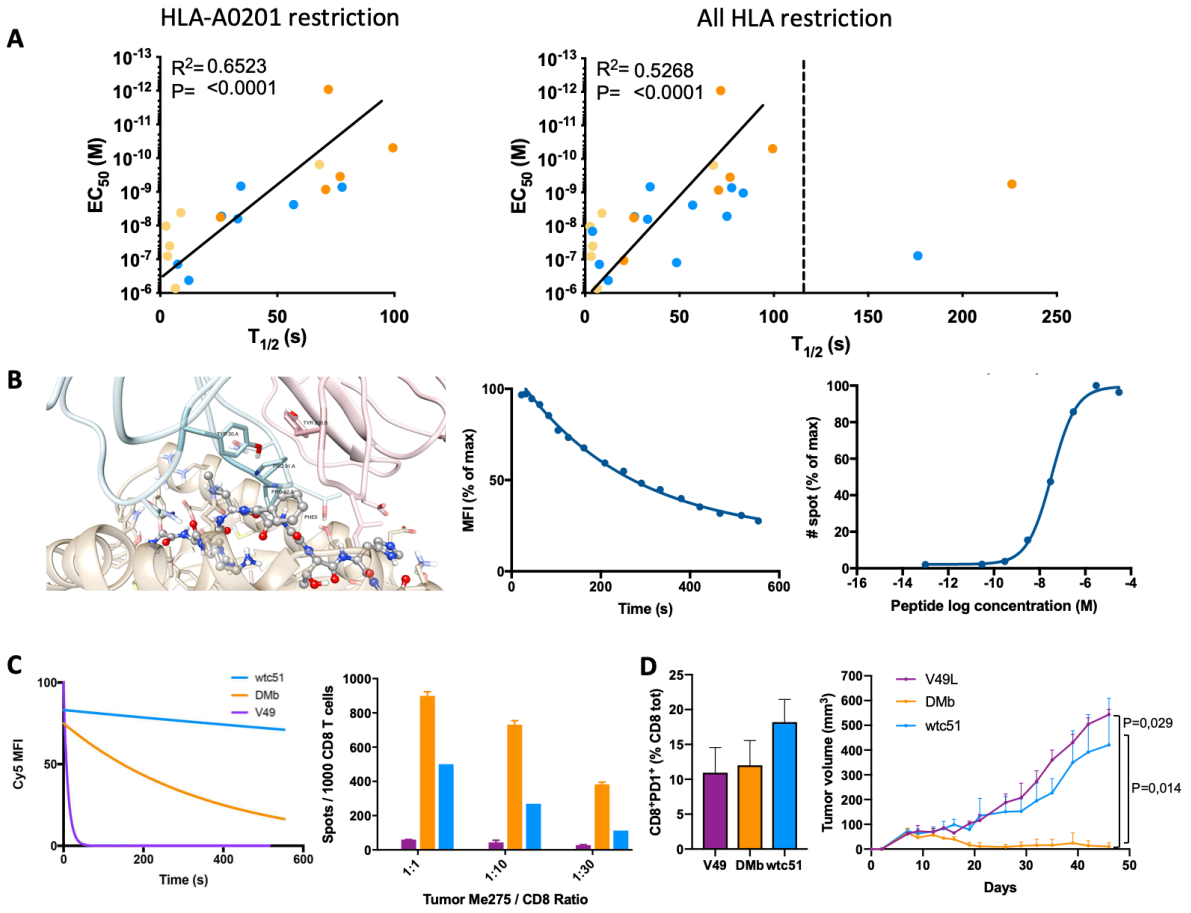

Figure 15: Analysis of the parameters influencing virus-, TAA- and neoAg-specific CD8 T cells functional heterogeneity. A. Correlation between the mean of functional (EC_{50} (M)) and structural affinity (pMHC-TCR $T_{1/2}$ (s)) obtained respectively by IFN-γ ELISpot assay and NTAmers on virus- (orange), TAA- (yellow) and neoAg-specific CD8 T cells clones (blue) restricted (right) or not (left) by HLA-A0201. The two parameters correlate until a (supraphysiological structural) threshold above which T cells functionality decreases. B. Structural and functional analysis of a supraphysiologic neoAg-specific primary CD8 T cell clone (ZCCHC11, HLA-B2705) derived from TILs. In silico analysis of the molecular interaction between TCR-p-MHCs for the ZCCHC11-specific TCR derived from TILs (left). TCRα ribbon is coloured in light blue, with residues displayed in sticks and coloured according to the atom types carbon coloured in light blue. TCRβ is coloured in pink, with residues displayed in sticks and coloured according to the atom types, with carbon coloured in pink. MHC is coloured in brown, with residues displayed in sticks and coloured according to the atom types, with carbon coloured in brown. The peptide is shown in grey ball and stick and coloured according to the atom types and carbon coloured in grey. Residues are labelled in black. The aromatic residues from CDRs alpha (TYR30.A, PRO91.A and PRO92.A) together with the TYR206 from CDR β and with the PHE in the position 5 of the peptide form several π-π interactions creating a π-network of interactions. The complex presents therefore a distinguished stability. A representative example of the monomeric pMHC-TCR dissociation kinetics of ZCCHC11-specific CD8 T cell clone derived from TILs assessed with NTAmers is in the middle. On the right, is a representative example of the functional avidity of the ZCCHC11-specific CD8 T cell clone. Cells were stimulated with serial dilutions of

cognate peptide and the functional response was assessed by IFN-γ ELISpot assay. C. Functional and structural analysis of primary CD8 T cells transduced with 3 different NY-ESO-I-specific TCRs. Monomeric pMHC-TCR off-rates are measured on live NY-ESO-I-specific CD8 T cells using NTAmer technology (low affinity V49I in purple, high affinity DMB in orange (middle), supraphysiologic affinity wtc51 in blue (top)). IFN-γ assay using NY-ESO-I positive melanoma tumor Me275 and NY-ESO-I-specific CD8 T cells at different ratios. D. ACT in IL2 NOG mice bearing the autologous Me275 tumor with primary CD8 T cells clones transduced with NY-ESO-I-specific TCR of different avidities. Mice received 2 millions of primary CD8 T cells transduced with low affinity (V49I, violet), high affinity (DMB, orange) and supraphysiological affinity (wtc51, blue) TCRs. Ratio of PD1+/CD8+ T cells in the tumor in mice injected with V49I, DMB or wtc51 mutants (left). Tumor growth over time (right).

E. Discussion

Next generation ACT requires new technologies and methodologies to improve identification and isolation of the most clinically relevant tumor-specific T cells. Many clinical successes have been associated with neoAg-specific T cells, resulting in a growing interest towards these particular Ags (*180-182*). However, deep characterization of NeoAg-specific CD8 T cells is still required to better understand their implication in superior clinical responses as opposed to TAA-specific CD8 T cells. Therefore, we comprehensively characterized the functional and structural avidities of numerous neoAg-specific CD8 T cells clones derived from TILs or PBLs extracted from patients with diverse cancers and compared their immune profile with the one of other classes of Ags such as TAA- and viral-specific CD8 T cells.

We first compared functional avidities of neoAg, TAA and viral Ag-specific CD8 T cells. By measuring the Ag sensitivity by IFN-γ release assay we found a broad range of functional avidities within each class of Ag but also among some single Ag-specificities. This observation highlights the diversity of TCRs targeting the same Ag. Despite a broad range of functional avidities (*31*), virus-specific CD8 T cells displayed significantly higher functionality than neoAg- and TAA-specific CD8 T cells. The superiority over TAA-specific T cells is in line with expectations, since virus-specific CD8 T cells express TCR of high affinity that have escaped central tolerance and recognizing non-self Ag (*302*). Initial virus-specific TCR repertoire is thus shaped during the course of the infection, in favor to the most effective T cells, becoming the dominant clonotypes (*335*). Of note, the HLA-A2 restricted viral specificity having the lowest functional avidity is EBV BMFL1, corresponding to an Ag presented in case of chronic infection with Epstein-Barr virus, often associated with a decrease of CD8 T cells effectiveness (*64*). On the other side, as TAA are self-Ag, TAA-specific CD8 T cells undergo negative thymic selection in order to prevent autoimmune reactions, leading to TCR repertoire of lower functional avidity, confirmed by our data and consistent with other studies (*219, 293*). Interestingly, no significant difference was observed between the functional avidities of neoAg- and TAA-specific CD8 T cells. These observations were not biased by the different HLA class I restrictions and were still valid when we considered exclusively HLA-A*0201-restricted T cells. Because neoAgs can be considered as non-self Ags, it has been hypothesized in the literature that neoAg-specific CD8 T cell clones would be of high functional avidity (*336, 337*). But, our data show that the functional avidity of neoAg-, virus- and TAA-specific CD8 T cells partially overlap with virus-specific CD8 T cells being composed in majority of highly functional cells while neoAg- and TAA-specific CD8 T cells mostly composed of average or low functionality T cells.

These data imply that neoAg-specific CD8 T cells might still be subjected to central tolerance. On the other side, it can also be due to cross-reactivity of TCR recognizing wild-type peptides from which neoAgs are derived. Many parameters should be considered when analyzing neoAgs, like the position of the mutation (i.e occurring at MHC anchor position or directed against the TCR) and its nature (i.e replacement of an amino acid by a more immunogenic residue). To be immunogenic a peptide should be presented by MHC with a

sufficient binding strength (*166, 325, 338*). If the mutation occurs in the MHC anchored residues, the neoAg might not be immunogenic since its TCR exposed residues remain identical, thus inducing central tolerance, but it can also generate a new peptide that can now be presented if the new residue favors MHC binding and stability (*12*). On the contrary, a mutation occurring in the TCR exposed residues might be seen as "non-self" Ag and induce immunogenicity. This "distance to self" parameter can explain the broad range of functionality observed for neoAg-specific CD8 T cells. However, even if all Ags from our library were experimentally confirmed to sufficiently bind to their cognate MHC (data not shown), we could not correlate the functional avidity with any distance to self-parameter but at least it confirmed that we can compare the different Ags without inducing any bias due to different Ag presentation (*339*). The lack of significant correlation between these parameters among different Ags is actually consistent with the fact that a wide range of functional avidity was also observed within some single Ag-specific CD8 T cell population, suggesting that peptide-MHC features may influence but do not strictly dictate T cell functionality. Currently, despite robust and reliable predictors of peptide-MHC binding affinities are available as well as advances in the field of mass spectrometry immunopeptidomic leading to better determination of MHC ligandome, the detection and prediction of immunogenic ligands remain poor and challenging. Of interest, in our case, the best predictor of functionality was the predictor of immunogenicity developed by Prof. David Gfeller (so called PRIME). Significant correlations were observed between the predicted PRIME score and the functional avidity of CD8 T cells clones (data not shown, Schmidt, Harari, Gfeller et. al, in preparation). However, the large range of avidity within one Ag-specificity highlights the limit of this new prediction tool.

In addition to central tolerance, peripheral tolerance can also occur on neoAg-specific CD8 T cells if a given neoAg is similar to self-Ag. Indeed, T cells encountering such a neoAg presented by non-activated APCs can receive incomplete priming signals, and either undergo apoptosis or exhibit a functionally tolerant phenotype. This state is often associated with limited ability to proliferate and expand in response to Ag stimulation, but is not systematically accompanied by a complete disrupt of the effector functions such as cytokine production or cytolytic activity (*340*). Furthermore, even if the NeoAg gives rise to an immunogenic peptide distinct from self-Ag, anergy can occur on neoAg-specific CD8 T cells, explaining their loss of function. Here, as the initial stimulation by neoAgs often occurs in an immunosuppressive environment or does not happen in an inflammatory context, priming can occur without co-stimulatory and/or inflammatory signals, which is associated with the dysfunctional state of T cells having reduced ability to proliferate in response to NeoAg (*340, 341*). Also, in the context of cancer, the chronic exposure to NeoAg might have induced an "exhausted" state of neoAg-specific CD8 T cells, associated with reduced antitumoral capacities, thus resulting in a selective depletion of too high avidity CD8 T cells. These explanations could support the lower functional avidity of neoAg-specific CD8 T cells, even in a context of immunogenic peptide

highly distinct from self-Ags. Finally, the moderate functional state of some neoAg-specific CD8 T cells can be explained by the fact that highly functional T cells may be either selectively eliminated *in vivo*, or selectively depleted by cell culture conditions, since stimulations and expansions were required to amplify the frequency of specific cells.

Another parameter to take into consideration is the cell shape and state when performing *in vitro* functional assays. The Rufer group showed high variability and volatility of different functional readouts and emphasized the need to characterize T cells by assessing stable biophysical parameters (*302*). To circumvent any potential functional bias, we then analyzed the structural affinity of our library of Ag-specific CD8 T cells using NTAmers (*330*). NTAmers were used in many studies (*302, 342, 343*), showing highly reproducible measurements, independent of the cell shape or state of activation. Structural affinities measured by NTAmers correlated well with CD8 T cell responsiveness (*302*). Here, wide ranges of structural affinities were observed within each class of Ag but also within some of the single specificities, supporting the TCR diversity discussed above. Virus-specific CD8 T cells presented again higher structural affinity than TAA-specific CD8 T cells which was in line with our expectations and data obtained in other studies (*293, 302, 303*). Interestingly, unlike functional avidity, neoAg-specific CD8 T cells exhibited superior structural affinity than TAA-specific CD8 T cells and were not significantly different from virus-specific CD8 T cells when all the HLA restrictions were considered. However, when only HLA-A*0201-restricted CD8 T cells were analyzed, neoAg-specific T cells were still superior to TAA-specific T cells but were slightly lower than virus-specific T cells. Besides these global differences, our data also demonstrated that virus-specific CD8 T cells only comprised high and intermediate affinity cells in contrast to TAA-specific T cells which mostly contained low affinity cells. NeoAg-specific CD8 T cells had an intermediate profile with high, intermediate and low affinity T cells. It is noticeable that MAGE-A3-specific CD8 T cells presented high structural affinity TCR. This observation can be justified by the tumor-specific nature of the MAGE-A3 Ag. It is indeed a cancer germline Ag normally not expressed in healthy tissue, and protein expression is only restricted to germline cells of the testis which are devoid of MHC. However, this Ag is frequently shared and overexpressed in many cancer types such as melanoma and lung cancer, making this TSA a good target for immunotherapy (*153, 344*). Concerning neoAg-specific CD8 T cells, our study suggests a trend for covering a large range of structural affinity overlapping with the one of virus- and TAA specific CD8 T cells, probably induced by the distance or similarity to self-Ag resulting in varying degrees of peripheral and central tolerance. This is contrasted with their functional behavior, being potentially impacted by the different parameters discussed above. To circumvent the discrepancy between structural and functional avidities of some Ag-specific CD8 T cells under study, we started cloning pairs of TCRs (high and low structural affinities) in naïve primary CD8 T cells. Preliminary results show that the structural affinity between primary and transduced CD8 T cells remains unchanged, as opposed to the functional avidity which is improved in transduced cells while keeping the same functional hierarchy between

clones (data not shown). Some studies highlighted a phenomenon of imprinted "epigenetic memory" of T cell dysfunction (*65, 340, 345*). Self-tolerant or anergic T cells can "memorize" the tolerance/anergic program triggered during T cell priming in the periphery and heritable epigenetic marks-related function is independent of environmental signals (*346*). Cell exhaustion can also induce this dysfunctional imprinting. An elegant experiment which remains to be done is the transduction of TAA-specific TCR into TAA- and virus-specific CD8 T cells. The functional characterization of TAA TCR-transduced EBV-specific T cells would be a relevant assay to highlight the imprinted dysfunctional state inherent to the ag-specific T cell.

Our group previously reported in ovarian cancer patients that neoAg-specific CD8 TILs are of higher functional avidity than PBLs targeting the same neoAg (*324*). We confirmed and extended this observation to melanoma, lung and colorectal cancer, but also to TAA- and virus-specific CD8 TILs. Only one outlier was reported to have superior functionally in clones derived from PBLs. We confirmed that these functional differences were not biased by the different cell culture protocols used to generate CD8 T cells clones extracted from TILs and PBLs, since EBV-specific CD8 T cells extracted from PBLs and grown with both protocols did not exhibit functional differences (data not shown). We also confirmed that virus-specific T cells, either coming from TILs or PBLs, are more functional than both neoAg- and TAA-specific CD8 T-cells. Interestingly, virus-specific CD8 TILs and PBLs have comparable functionality, as opposed to TAA- and neoAg-specific CD8 T cells that exhibit higher functionality in TILs. These observations were also transposable to structural affinity, where the average structural affinity of TILs is consistently higher than the one of related PBLs, whatever the class of Ag, including the aforementioned outlier exhibiting here the highest difference between PBLs and TILs. As opposed to the functional avidity, our data highlight the superior structural affinity of neoAg-specific CD8 T cells in TILs, which are comparable to virus-specific TILs but also to some of the TAA-specific TILs. Interestingly, the whole range of structural and functional avidity of CD8 T cells extracted from PBLs is considerably broader than the one extracted from TILs, suggesting defined CD8 T cells functional prerequisite for tumor infiltration and persistency. Altogether, the absolute comparison between the different classes of Ag specificities might have been biased by the number of CD8 T cells clones characterized within each population and the compartment they were extracted from (indeed only a few viral and TAA-specific T cells were identifiable in TILs, despite systematic screening). This suggests that, despite similar characteristic to neoAg-specific CD8 T cells when extracted from the same compartment, TAAs were mostly not able to generate CD8 T cells able to infiltrate and/or persist in the tumor.

To understand the balance between PBL and TIL at the clonotypic level, neoAg-specific CD8 T cells bulks sorted from the same patient's PBL and TIL were sequenced for their TCR and compared between both populations. For the 3 neoAgs studies, results showed that neoAg-specific PBL and TIL were oligoclonal, and that some TCRs were shared between CD8 T cells isolated from both compartments, but with an inverted clonal dominance. In the three examples, NeoAg-specific TILs contain mostly "shared" TCR which are also identified in PBL,

while neoAg-specific PBL contain high proportion of unique and shared TCRs. Interestingly, we confirmed by analyzing the structural affinity of 3 neoAg-specific CD8 T cells clones bearing "shared" TCR specific for the same epitope, that there is a direct correlation between structural affinity and relative clonal frequency in TIL as opposed to PBL where these parameters negatively correlate. This observation suggests that T cells with low affinity TCR do accumulate in PBL, while the one bearing high affinity TCR mostly migrate and persist in the tumor compartment. The presence of higher proportion of unique TCRs in PBL suggests that TILs originate from the large PBL repertoire, which is depleted from highly functional clones able to migrate and persist in tumors. Therefore, analysis of PBLs and TILs repertoires would predict which clonotype could be the most relevant based on its frequency. Also, for the rare shared TCRs in TILs, we cannot exclude that clonal contamination of the TILs by blood (PBLs) occurred during the tumor extraction and processing, that could explain such low frequencies. TCR repertoire analysis might as well be biased by contaminations (index hoping) induced by Illumina sequencing, despite the absence of common sequence between TCR repertoires originating from distinct Ag-specific T cells bulks, which strengthen our hypotheses, indicating that high- and low-affinity neoAg-specific CD8 T cells are preferentially found in tumors and in peripheral blood, respectively.

We then hypothesized that the selective enrichment of high avidity CD8 T cells in TILs was due to a pMHC-TCR affinity-related expression of tissue homing receptors. Several studies reported that specific chemokine receptors and integrins are associated with tumor infiltration and eradication In order to confirm that expression of these markers was mediated by T cell priming and linked to TCR-pMHC affinity, we analyzed the expression of a panel of chemokine receptors and integrins on Ag-specific CD8 T cell clones of low and high structural affinity targeting the same Ag, either directly or after short-term TCR-dependent stimulations. We confirmed that high-avidity CD8 T cell clones express higher level of CXCR3 and CCR5 but also VLA-1 and VLA-2 than lower avidity counterparts at baseline. No difference was observed, in contrast, for chemokine receptors that are not known to be involved in tumor infiltration (e.g. CCR6 or CCR4). However, neither CD103 nor CX3CR1 presented differences at the baseline level. Interestingly, after TCR-mediated stimulation, high avidity CD8 T cell clones more strongly upregulated CXCR3 and CD103 compared to low avidity cells. This observation was not transposable to other chemokine receptors and integrins. Surprisingly, CCR5 which had high baseline level of expression was downregulated or internalized in most of the experiments (which need to be further investigated). Taken together, these observations suggest that high affinity T cells preferentially express important tumor-homing chemokine receptors and integrins mediating CD8 T cells retention in the tumor bed, promoting antitumor activity. These observations are consistent with other studies showing the association of some chemokine receptors with TCR signaling pathway. One of them showed that pMHC-TCR affinity had an impact on CXCR3 chemokine receptor expression in lymph node (LN) (*295*). Prolonged interactions in the LN of high affinity TCR-pMHC allowed superior

function and proliferation, but also upregulation of CXCR3. They concluded that low affinity T cells leave earlier the LN with a suboptimal priming, function, and low CXCR3 (and potentially other integrin and selectins) expression, whereas high affinity T cells remain longer in LN to undergo successive stimulation by DC, proliferation, and upregulation of CXCR3 and many other integrins and selectins. Others reports further supported this conclusion showing that ligand-mediated activation of CXCR3 induces phosphorylation of ZAP-70, a key element of TCR signal cascade (*347*). This supports the close relationship between TCR-pMHC affinity and CXCR3 expression through the TCR signaling pathway, CXCR3 also acting as a costimulatory molecule for subsequent T cell activation. Additionally, specific pMHC-TCR interaction in the presence of TGF-β induces CD103 integrin expression, whose engagement with its ligand E-cadherin has shown to trigger the phosphorylation of ERK1/2, two important kinases of the signaling pathway supporting the association between CD103 and the TCR signaling pathway (*348*).

Altogether, our findings are consistent with these studies, higher structural affinity T cells are found at the tumor site, confirming better tumor infiltration than lower affinity counterparts remaining in periphery. This strengthen the link between TCR affinity and tumor infiltration and the importance of structural affinity as a parameter potentially associated to or predictive of clinically relevant CD8 T cells.

However, further experiments are needed (and currently ongoing) since, despite the fact we saw clear trends, we did not reach statistical significance in the associations between functionality and markers of tumor tropism yet. CD8 T cells clones should be experienced after minimal stimulation and *in vitro* manipulation, reducing as much as possible the potential bias induced by cell culture conditions. Pairs of high and low affinities TAA and NeoAg-specific CD8 T cells might be analyzed to extend these conclusions to tumor-specific CD8 T cells implying Ags expressed in different types of tissues. Also, other tumor-homing receptors could have been interrogated to extend our conclusions, such as CXCR4, CXCR6, LFA-1 or VLA-4 (*349, 350*). A major defense mechanism by the tumor is the local alteration of chemokine secretion to inhibit the attraction of tumor-specific CD8 T cells but promoting homing of inhibitory immune cells (*333*). Immunotherapeutic approaches must also focus on this major issue and propose combinatorial therapies also countering the hostile TME.

Other reports proposed explanations regarding the tumor infiltration differences observed for high and low affinity tumor-specific CD8 T cells. An interesting *in vivo* study claimed that high avidity CD8 T cells are more prone to proliferate, persist in the tumor environment, and eradicate the tumor (*305*). Also, high-affinity T cells exhibited lower expression of inhibitory molecules (PD-1, LAG-3 and NKG2A), therefore associated with a decreased susceptibility to immune suppressive mechanisms. Other ongoing investigations in the Coukos group (Vuillefroy de Silly et. al, in preparation) are currently showing the superior capacity of high avidity CD8 T cells to tolerate hypoxia or abnormally low pH of the TME. In

such hostile conditions, they seem to be more adapted than low avidity T cells to keep their functional capacity and persist over time.

In order to validate the relevance of pMHC-TCR affinity as predictors but also mediators of tumor homing, we used our model of primary CD8 T cells transduced with NYESO-1 TCRs of incremental structural affinity (*297, 310, 334*). We performed ACT of primary T cells transduced with either DMB or V49I mutant (high vs low avidity, respectively) into IL2 NOG mice bearing the autologous Me275 melanoma tumor. Interestingly, only DMB-, but not V49I-transduced T cells successfully infiltrated tumors. These data support that adoptively transferred low-affinity T cells do not infiltrate or persist in tumors.

Based on the previous conclusions regarding the differences between CD8 TILs and PBL, we then examined whether we could associate the ability to infiltrate tumors to T-cell potency and, in that case, to structural affinity or to functional avidity. First, the association between the two functional parameters on HLA-A*0201-restricted Ag-specific CD8 T cells displayed a strong positive correlation within a defined range of functional and structural avidity (i.e. $EC_{50} \leq 10^{-12}$ and $T_{1/2} \leq 100$ s). Interestingly, outliers appeared in the very high $T_{1/2}$ range but with moderate EC_{50} when all HLA class I restricted Ag-specific CD8 T cell were considered. Of interest, the ZCCHC11-specific TIL was one of the two outliers and this explained why these had a lower functional avidity than ZCCHC11-specific PBL. These unique structural outliers (ZCCHC11 and hCMV pp65) appear to be the first evidence that Ag-specific T cells with very high structural affinity but moderate functionality can be identified in nature, although this observation is coherent with previous studies discussed above showing on models of engineered TCR that very high affinity CD8 T cells (called supraphysiologic) are functionally impaired (*291, 296, 297*). We then interrogated such supraphysiologic CD8 T cells *in vivo* to examine their tumor infiltration and tumor control capacity, by repeating *in vivo* ACT including wtc51 mutant TCR transduced CD8 T cell clone (very high off-rate but limited functionality). Here, adoptively-transferred DMB-specific CD8 T cells infiltrated and fully controlled tumors growth *in vivo* while neither V49I- nor wtc51-specific CD8 T cells were able to control tumors. Interestingly, a few wtc51-specific T cells infiltrated the tumors, but expressed very high levels of PD-1. Consistently with the above comments, this observation suggests that over a certain threshold of structural affinity, T cells are functionally impaired and get exhausted in tumors as a consequence of negative feedback loops in the TCR signaling pathway and an increased expression of inhibitory receptors, thus preventing tumor control (*296*). Characterization of "supraphysiological" TCR *in vitro* and *in vivo* is still under investigation and it will be valuable to understand the clinical potential of these rare T cells. Kinetic models of pMHC-TCR interactions have been proposed to decipher this phenomenon. Initially, kinetic models of pMHC-TCR interaction suggested that functional capacity is mostly determined by the time of interaction since long off rates might be needed for

accomplishment of signaling cascades inducing T cell activation (*351*). However, the serial triggering model (*352*) suggests that off rate should not exceed a certain threshold to permit an optimal dwell time of pMHC-TCR interaction so that several TCRs can engage a pMHC complex for effective T cell activation. It is suggested that too slow off-rate induce longer pMHC time of confinement precluding serial triggering required for optimal T cell activation (*353, 354*) and that supraphysiologic affinity of CD8 T cells is linked with several down regulation mechanisms (*296*). By studying the TCR signaling and the regulatory mechanisms, Rufer et al. showed that high affinity T cells have fast, strong, but only temporary proximal signaling and reduced distal signaling capacity. The reduction of TCR-mediated signaling molecules was also associated to higher PD-1 expression. TCR-pMHC affinity-associated regulatory mechanisms were hypothesized to act at various degrees of the TCR signaling cascade, particularly at the MAPK amplification node which may quickly reduce downstream propagation and amplification signals. These negative feedback loop might certainly be use as a way to avoid to strong immune response and preclude autoimmunity.

Even if our NTAmer technology provides a rapid way to screen and identify personalized T cells with optimal potency in most cases, limitations occur when rare "supraphysiological" affinity T cells are found. It calls for the development of new methods or strategies to efficiently and quickly identify tumor-specific cells of interest. One possibility, called "TCR subtraction assay" has been proposed and is discussed in Appendix B. In the literature, others methods assessing pMHC-TCR interaction have been proposed to predict the functional capacity of T cells. They are mostly based on the mechanosensing of CD8 T cells and the forces induced by TCR engagement following encounter with their cognate pMHC, inducing mechanical and molecular changes, cytoskeletal structures rearrangement related to positive or negative feedback activation loop (*355-358*). Developed by Drs C. Zhu and B. Evavold, 2D binding affinity measurements exploit pMHC presented by a surrogate APC and viable T cells attached on pipets than can move along an axis to provoke successive TCR-pMHC encounter to measure the adhesion frequency or apply force to provoke "catch" or "slip" bond (*359-361*). Interestingly they reported that 2D binding affinities measured under force are better correlates of T cell functions than off-rate measured by NTAmer technology. Of note, preliminary results obtained in collaboration with the group of Dr. Evavold tend to confirm these observations and are currently under study (Schmidt et al, in preparation). An interesting study has described the important role of mechanical forces creating catch bond, independently of pMHC-TCR affinity, to trigger the TCR signaling cascade (*362*). They showed that subtle modifications of the TCR-pMHC complex can induce huge differences in signaling outcomes. Perturbations such as peptide mutations, changes in docking geometry or TCR point mutations can drastically affect the potential formation of catch or slip bonds and subsequent signaling triggering. Catch bonds represent a reorganization of molecular interactions, able to form ''rescue'' salt bridges or hydrogen bonds with other molecules when

an initial bond breaks, thus prolonging the bond lifetime. Slip bonds have a reduced capacity to form ‘‘rescue’’ bonds and are associated to shorter bond lifetime, independently of the initial TCR-pMHC affinity. This study further reinforced the legitimacy of the 2D binding assays. However, these specialized technologies do not allow high throughput measurements, and could not be used yet in a clinical context. Ideally, these instruments will have to be engineered in the future to allow efficient high throughput screening of clinically relevant tumor-specific T cells.

General conclusion

During my PhD, I have confirmed and extended the evidence that the repertoire of neoAg-specific T cells is discordant between PBLs and TILs, not only in ovarian cancers as initially highlighted in our group (*324*), but also in melanoma, lung and colorectal cancers. This observation was also verified for TAA- and virus-specific T cells. By taking advantage of the great expertise of the team and proprietary technologies, I comprehensively profiled CD8 T cells targeting various classes of Ag. An important finding of this research is that tumor-specific CD8 T cells originating from TILs, almost systematically exhibited, not only higher functional avidities, but also higher structural affinities than their PBLs counterparts targeting the same antigen, rendering TILs a favored source for isolation of attractive candidates for ACT. In addition to display distinct TCR repertoires between PBLs and TILs, I revealed a clear correlation between the structural affinity and the clonotype frequency in tumors. Importantly, when looking more globally at different classes of antigens, I showed that if viral antigen-specific CD8 T cells have generally higher functional and structural affinities than TAA-specific CD8 T cells, neoAg-specific ones cover broad ranges of functional and structural avidities. Surprisingly, their T cell responsiveness is similar but not superior to the one of TAA-specific T cells whereas their structural affinities can be as high as the one of viral- specific T cells. This heterogeneity is directly related to the nature of neoAg themselves. Somatic mutations can lead to neoAg which are similar or completely different from their wild-type antigen counterpart, known as the distance to self, leading to more or less immunogenic mutated peptide. I was also able to demonstrate a correlation between TCR affinity and tumor infiltration and persistence *in vivo*. Finally, exhibiting a clear correlation between TCR affinity and T cell function within a defined range of affinity, my results confirmed the existence of a TCR affinity window associated with optimal CD8 T cell potency and stated the structural affinity as robust marker of T cell potency.

Altogether, my findings highlight the heterogeneity of neoAg-specific CD8 T cells and the importance of additional filters to refine and prioritize selection of clinically relevant candidate for improved ACT. Unique tools, like the NTAmer technology, allowed a better understanding of neoAg-specific CD8 T cells showing that a selection of highly functional clones, even rare, from TILs remains feasible but call for new developments to speed-up their personalized identification and isolation for better clinical outcomes.

Perspectives

My work exposed the limitations of several steps within the overall antigen discovery pipeline. The main one is inherent to the *in vitro* stimulations required to increase antigen-specific CD8 T cell frequencies for further detection, isolation and characterization. Future

perspectives aim at improving sensitivity of our various assays and reduce the number of cells required for their identification and characterization. In line with this problematic, we have initiated different projects such as the TCR affinity measurement and TCR sequencing at the single cell level or the DNA barcoded reversible-pMHC multimers allowing multiplexed CD8 T cells screening. Combining an optimized high-throughput antigen discovery strategy with rapid and comprehensive analysis of antigen-specific CD8 T cells will increase success rates of personalized ACT. Importantly, all these new technologies will be possibly applied for the analysis of antigen-specific CD4 T cells known to play an important role in tumor control. Also, accumulation of comprehensive data (neoAgs, TCR affinity, peptide-MHC binding strength, TCR sequences…) will contribute to the development of new *in silico* models of pMHC-TCR interactions that in a long-term view will help to rapidly select the most relevant personalized TCR.

Appendix

A. Supplementary figures.

Patient	Age	Gender	Cancer
LAU 969	66	M	Melanoma
LAU 147	62	F	Melanoma
TIL004	55	M	Melanoma
ITA02 1043	55	F	Melanoma
Mel11	44	M	Melanoma
LAU 155	56	M	Melanoma
DEG 1187	NA	NA	Melanoma
CRCp5	73	M	Colorectal
CRCp7	81	F	Colorectal
19809-302	49	F	OvCa
19809-304	47	F	OvCa
19809-06	63	F	OvCa
19809-207	63	F	OvCa
JM	NA	F	Breast
SCC001	75	M	NSCLC
SCC003	69	M	NSCLC
ADK-008	69	M	NSCLC
SCC010	68	F	NSCLC

Table 1 : Summary of the different epitopes under study.

Protein		HLA restriction	Native sequence (WT)	Mutated sequence (Neo)
Viral	Influenza A MP	A0201	GILGFVFTL	/
	EBV BMLF1	A0201	GLCTLVAML	/
	hCMV pp65	A0201	NLVPMVATV	/
	Influenza A PB1	A0101	VSDGGPNLY	/
	hCMV pp65	B3501	IPSINVHHY	/
TAA	MelanA	A0201	EAAGIGILTV	/
	GP100	A0201	ITDQVPFSV	/
	NYESO1	A0201	SLLMWITQC	/
	MAGE A3	A0101	EVDPIGHLY	/
	MAGE A10	A0201	GLYDGMEHL	/
	MUC1	A0201	VLVCVLVAL	/
Neo	UTP20	A0201	AMDLGIDKV	AMDLGIHKV
	MMP9	A0201	NIFDAIAEI	NILDAIAEI
	HHAT	A0201	KQWLVWLLL	KQWLVWLFL
	ZCCHC11	B2705	GRKLFGTPF	GRKLFGTHF
	NBEA	B0702	LPQARRISL	LPQARRILL
	PHLPP2	A0101	GLQAILVHE	GLQAILVHV
	NUP210	A0201	QSDNGLDSDD	QSDNGLDSDY
	SLC25A48	A2402	PYVFLSEWI	PYMFLSEWI
	HS6ST1	B4001	TEDYMSHII	TEDYMIHII
	NUP205	B3503	EPLQTPTIM	EPLHTPTIM
	KIT	B3503	IPDPKAGIM	IPNPKAGIM

Table 2: Summary of the TCR sequences identified in CD8 T cells clones derived from PBLs and TILs

	ID	TCRa	TCRb	pMHC
Viral	EBV BMLF1 (A0201) PBLs	hTRAV30_CGTEGQMNTGFQKLVFG_hTRAJ08	hTRBV06-8_CASSENVGIGANVLTFG_hTRBJ02-6	HLA-A:02:01/GLCTLVAML
		hTRAV05_CAEDSNARLMFG_hTRAJ31	hTRBV20_CSARDRGLGNTIYFG_hTRBJ01-3	HLA-A:02:01/GLCTLVAML
	hCMV pp65 (B3501) PBLs	hTRAV24_CAFLTGTYKYIFG_hTRAJ40	hTRBV05-4_CASSSLATSTDTQYFG_hTRBJ02-3	HLA-B:35:01/IPSINVHHY
		hTRAV12-2_CAGYSGTYKYIFG_hTRAJ40	hTRBV02_CASMGGAYNEQFFG_hTRBJ02-1	HLA-B:35:01/IPSINVHHY
		hTRAV16_FNKFYFG_hTRAJ21	hTRBV02_CASSEEETGGSPLHFG_hTRBJ01-6	HLA-B:35:01/IPSINVHHY
		hTRAV22_CAGREVTGGGNKLTFG_hTRAJ10	hTRBV04-1_CASSQDGTNYGYTFG_hTRBJ01-2	HLA-B:35:01/IPSINVHHY
	hCMV pp65 (A0201) PBLs	hTRAV26-2_CILDNNNDMRFG_hTRAJ43	hTRBV07-6_CASSLAPGATNEKLFFG_hTRBJ01-4	HLA-A:02:01/NLVPYVATV
	Influenza A PB1 (A0101) PBLs	hTRAV21_CAVINAGNNRKLIWG_hTRAJ38	hTRBV11-2_CASSLDGQGPLYGYTFG_hTRBJ01-2	HLA-A:01:01/VSDGGPNLY
TAA	GP100 (A0201) PBLs	hTRAV08-1_CAGGGDRDDKIIFG_hTRAJ30	hTRBV10-2_CASSYRGNSPLHFG_hTRBJ01-6	HLA-A:02:01/ITDQVPFSV
		hTRAV01-2_CAVPSYGQNFVFG_hTRAJ26	hTRBV19_CASSLRLAATIYNEQFFG_hTRBJ02-1	HLA-A:02:01/ITDQVPFSV
		hTRAV41_CASTNVGGSGNTPLVFG_hTRAJ29	hTRBV19_CASSARGYASPLHFG_hTRBJ01-6	HLA-A:02:01/ITDQVPFSV
	GP100 (A0201) TILs	hTRAV24_CAFAELWGGSQGNLIFG_hTRAJ42	hTRBV19_CASSITTSGGYEQYFG_hTRBJ02-7	HLA-A:02:01/ITDQVPFSV
	Melan-A (A0201) TILs	hTRAV12-2_CAGGGSNYQLIWGAG_hTRAJ33	hTRBV20_CSASPGLAEQFFG_hTRBJ02-1	HLA-A:02:01/EAAGIGILTV
		hTRAV12-2_CAVDVGARLMFG_hTRAJ31	hTRBV14_CASSQDTGLSSYNEQFFG_hTRBJ02-1	HLA-A:02:01/EAAGIGILTV
		hTRAV12-2_CAYQAGTALIFG_hTRAJ15	hTRBV06-1_CASSELGLAGNEQFFG_hTRBJ02-1	HLA-A:02:01/EAAGIGILTV
		hTRAV12-2_CAVNTGNQFYFG_hTRAJ49	hTRBV20_CSAERGLGQPQHFG_hTRBJ01-5	HLA-A:02:01/EAAGIGILTV
		hTRAV12-2_CAPGGGYQKVTFG_hTRAJ13	hTRBV19_CASTSGELGQPQHFG_hTRBJ01-5	HLA-A:02:01/EAAGIGILTV
		hTRAV12-2_CAVIHAGKSTFG_hTRAJ27	hTRBV27_CASSLSGLAGVEQYFG_hTRBJ02-7	HLA-A:02:01/EAAGIGILTV
		hTRAV35_CAGVLGSARQLTFG_hTRAJ22	hTRBV19_CASKWGALMNTEAFFG_hTRBJ01-1	HLA-A:02:01/EAAGIGILTV
		hTRAV12-2_CAASIGFGNVLHCGSG_hTRAJ35	hTRBV27_CASSSLGATYEQYFG_hTRBJ02-7	HLA-A:02:01/EAAGIGILTV
		hTRAV12-2_CAASIGFGNVLHCGSG_hTRAJ35	hTRBV27_CASSWTSGSPSEQFFG_hTRBJ02-1	HLA-A:02:01/EAAGIGILTV
		hTRAV12-2_CAVTIGFGNVLHCGSG_hTRAJ35	hTRBV27_CASSLFSGSSGELFFG_hTRBJ02-2	HLA-A:02:01/EAAGIGILTV
		hTRAV12-2_CAVGGGADGLTFG_hTRAJ45	hTRBV03-1_CASSQGSLAGSEQYFG_hTRBJ02-7	HLA-A:02:01/EAAGIGILTV
		hTRAV12-2_CAVGGAAGNKLTFG_hTRAJ17	hTRBV28_CASRVQGLGQPQHFG_hTRBJ01-5	HLA-A:02:01/EAAGIGILTV
	Melan-A (A0201) PBLs	hTRAV12-2_CAVSSGFQKLVFG_hTRAJ08 hTRAV27_CAGGRGRRALTFG_hTRAJ05	hTRBV13_CASSLDPSGSPNEQFFG_hTRBJ02-1	HLA-A:02:01/EAAGIGILTV
		hTRAV12-2_CAVNDAGKSTFG_hTRAJ27 hTRAV26-1_CIGSSASKIIFG_hTRAJ03	hTRBV03-1_CASSQGDLAWIPTEAFFG_hTRBJ01-1	HLA-A:02:01/EAAGIGILTV
		hTRAV14_CAMRGPYNTDKLIFG_hTRAJ34	hTRBV20_CSARDVGLGIYEQYFG_hTRBJ02-7	HLA-A:02:01/EAAGIGILTV
	MAGE-A3 (A0101) PBLs	hTRAV12-1_CVVNRDNDMRFG_hTRAJ43	hTRBV24-1_CATSEGGPPYEQYFG_hTRBJ02-7	HLA-A:01:01/EVDPIGHLY
	MAGE-A10 (A0201) PBLs	hTRAV06_WNNFNKFYFG_hTRAJ21	hTRBV07-8_CASSWDSGYEQYFG_hTRBJ02-7	HLA-A:02:01/GLYDGMEHL
NeoAg	NUP210 (A0201) TILs	hTRAV29_CAPVDNQGGKLIFG_hTRAJ23	hTRBV28_CASSFSAGLLYGYTFG_hTRBJ01-2	HLA-A:02:01/GLQAILVHV
	PHLPP2 (A0101) TILs	hTRAV23_CAAPMPMDTGRRALTFG_hTRAJ05	hTRBV10-3_CAISGGSVGEQYFG_hTRBJ02-7	HLA-A:01:01/QSDNGLDSDY
	PHLPP2 (A0101) PBLs	hTRAV21_CAVSSGSARQLTFG_hTRAJ22	hTRBV5-4_CASTLSTGQGIYGYTFG_hTRBJ01-2	HLA-A:01:01/QSDNGLDSDY
	ZCCHC11 (B2705) TILs	hTRAV04_CLVGGPPTGNQFYFG_hTRAJ49	hTRBV07-8_CASSLDIGTYEQFFG_hTRBJ02-1	HLA-B:27:05/GRKLFGTHF
		hTRAV21_CAVRLTGQGAQKLVFG_hTRAJ54	hTRBV28_CASSLAGLNTEAFFG_hTRBJ01-1	HLA-B:27:05/GRKLFGTHF
	ZCCHC11 (B2705) PBLs	hTRAV8-6_CAANNNNDMRFG_hTRAJ43 hTRAV13-1_CAVIQGGKLIFG_hTRAJ23	hTRBV7-8_CASSWDSGYEQYFG_hTRBJ02-7	HLA-B:27:05/GRKLFGTHF
	NBEA (B0702) TILs	hTRAV08-4_CANAGNNRKLIWG_hTRAJ38	hTRBV04-1_CASSQDWAGGSTDTQYFG_hTRBJ02-3	HLA-B:07:02/LPQARRILL
	HHAT (A0201) PBLs	hTRAV12-2_CAVNYNNARLMFG_hTRAJ31	hTRBV4.2_CASSQDAETQYFG_hTRBJ2.5	HLA-A:02:01/KQWLVWLFL
	HHAT (A0201) TILs	hTRAV38-2_CAFMDSNYQLIWGAG_hTRAJ33	hTRBV12-3_CASSRTSPTDTQYFG_hTRBJ02-3	HLA-A:02:01/KQWLVWLFL
	UTP20 (A0201) TILs	hTRAV25_CAGMDSSYKLIFG_hTRAJ12	hTRBV11-1_CASSFQTGWNEQFFG_hTRBJ02-1	HLA-A:02:01/AMDLGIHKV
	UTP20 (A0201) PBLs	hTRAV12-2_CAGGVDSNYQLIWGAG_hTRAJ33	hTRBV05-6_CASSLGGGRDEQYFG_hTRBJ02-7	HLA-A:02:01/AMDLGIHKV
		hTRAV24_CAFINSGNTPLVFG_hTRAJ29	hTRBV10-1_CASSDSTAKETQYFG_hTRBJ02-5	HLA-A:02:01/AMDLGIHKV
		hTRAV20_CAVSGGSYIPTFG_hTRAJ06	hTRBV04-3_CASSQEESYEQYFG_hTRBJ02-7	HLA-A:02:01/AMDLGIHKV
		hTRAV19_CALIFNQAGTALIFG_hTRAJ15	hTRBV05-6_CASSLGGGRDTQYFG_hTRBJ02-3	HLA-A:02:01/AMDLGIHKV
	MMP9 (A0201) TILs	hTRAV24_CAPNRDDKIIFG_hTRAJ30	hTRBV12-3_CASATGVKLAKNIQYFG_hTRBJ02-4	HLA-A:02:01/NILDAIAEI
		hTRAV12-312-4_CAMRSIGGSNYKLTFG_hTRAJ53	hTRBV07-9_CASSPIAGGTDTQYFG_hTRBJ02-3	HLA-A:02:01/NILDAIAEI
	MMP9 (A0201) PBLs	hTRAV35_CAGHGNTGKLIFG_hTRAJ37	hTRBV05-4_CASFFSGGGTDTQYFG_hTRBJ02-3	HLA-A:02:01/NILDAIAEI
		hTRAV12-2_CAVRGNEKLTFG_hTRAJ48	hTRBV20_CSASRADTYEQYFG_hTRBJ02-7	HLA-A:02:01/NILDAIAEI
		hTRAV13-1_CAASSMNRDDKIIFG_CAASSMNRDDKIIFG	hTRBV07-2_CASTDTDTQYFG_hTRBJ02-3 hTRBV07-9_CASSPIAGGTDTQYFG_hTRBJ02-3	HLA-A:02:01/NILDAIAEI
		hTRAV13-1_CAASINTDKLIFG_hTRAJ34	hTRBV05-4_CASFFSGGGTDTQYFG_hTRBJ02-3	HLA-A:02:01/NILDAIAEI
		hTRAV35_CAGHGNTGKLIFG_hTRAJ37	hTRBV09_CASSLQGASTGELFFG_hTRBJ02-2	
		hTRAV12-2_CAVGGTSYGKLTFG_hTRAJ52	hTRBV10-2_CASSLGQETQYFG_hTRBJ02-5	HLA-A:02:01/NILDAIAEI
		hTRAV27_CAGGNSGGYQKVTFG_CAGGNSGGYQKVTFG	hTRBV05-4_CASFFSGGGTDTQYFG_hTRBJ02-3	HLA-A:02:01/NILDAIAEI
	SLC25A48 (A2402) PBLs	hTRAV21_CAVPSTSGTYKYIFG_hTRAJ40	hTRBV19_CASSIGKTGKLFFG_hTRBJ01.4	HLA-A:24:02/PYMFLSEWI
		hTRAV17_CATGGALGYGGSQGNLIFG_hTRAJ42	hTRBV19_CASSIARVTEAFFG_hTRBJ01-1	HLA-A:24:02/PYMFLSEWI
		hTRAV21_CAVPSTSGTYKYIFG_hTRAJ40	hTRBV19_CASSIGKTGKLFFG_hTRBJ01-4	HLA-A:24:02/PYMFLSEWI

Table 3: Summary of the TCR sequences identified in CD8 T cells clones derived from PBLs and TILs

PEPTIDE	MHC
1)ALA483(bb)	hb-TYR224(sc) hb-TYR388(sc) np-TRP384(sc)
2)MET484(bb)	hb-GLU280(sc) hb-LYS283(sc) np-LYS283(sc)
3)ASP485(bb)	hb-TYR316(sc)
4)LEU486	-
5)GLY487	-
6)ILE488	np-HIS287
7)HIS489(bb)	hb-ARG314(sc) np-ALA387
8)LYS490(bb)	hb-TRP364(sc)
9)VAL491(sc)	hb-ASP294(sc) hb-LYS363(sc)

*Table 4: Molecular interactions between the peptide epitope (AMDLGIHKV) and HLA-A*0201 in UTP20 (A0201) TILs hTRAV25_CAGMDSSYKLIFG_hTRAJ12 hTRBV11-1_CASSFQTGWNEQFFG_hTRBJ02-1 HLA-A:02:01/AMDLGIHKV, UTP20-TIL, as predicted by homology modeling. bb: backbone, sc: side chain; hb: hydrogen bond, io: ionic interaction; np: non-polar interaction, π: π-π interaction, cπ: cation-π interaction. Unless indicated, interactions are taking place between side chains. In the structure TCRα is chain A, TCRβ is chain B, MHC is chain C and the peptide is chain D and the residue numbers are sequential.*

TCR	PEPTIDE	MHC
CDR1α-THR24.A(sc)	-	hb-GLU275(sc)
CDR1α-VAL47.A(sc)	-	np-ALA375(sc)
CDR3α-SER91.A(sc)	-	hb-GLU275(bb)
CDR3α-SER92.A(sc)	-	hb-ARG282(sc)
CDR3α-TYR93.A(sc)	np-LEU486|MET484(sc)	cπ-LYS283(sc)
CDR2β-ASP15.B(sc)	io-LYS490(sc)	-
CDR3β-GLN200.B(sc)	np-LEU486(sc)	-
CDR3β-TRP203.B(sc)	np-LEU486(sc)	

Table 5: Molecular interactions between TCRs and pMHC in UTP20-TIL as predicted by homology modeling. bb: backbone, sc: side chain; hb: hydrogen bond, io: ionic interaction; np: non-polar interaction; π: π-π interaction, cπ: cation-π interaction. In the structure TCRα is chain A, TCRβ is chain B, MHC is chain C and the peptide is chain D and the residue numbers are sequential

PEPTIDE	MHC
1)ALA484(bb)	hb-TYR377(sc) hb-TYR225(sc) hb-TYR389(sc)

2)MET485(bb)		hb-LYS284(sc) hb-GLU281(sc)
3)ASP486(bb)		hb-TYR317(sc)
4)LEU487		np-ALA368(sc)
5)GLY488		
6)ILE499		
7)HIS490(sc)		hb-LYS491(bb) np-ALA368(sc)
8)LYS491(bb)		hb-TRP365(sc)
9)VAL492(bb)		hb-LYS364(sc) hb-ASP295(sc)

*Table 6: Molecular interactions between the peptide epitope (AMDLGIHKV) and HLA-A*0201 in UTP20 (A0201) PBLs hTRAV24_CAFINSGNTPLVFG_hTRAJ29 hTRBV10-1_CASSDSTAKETQYFG_hTRBJ02-5 HLA-A:02:01/AMDLGIHKV, UTP20-PBL, as predicted by homology modeling. bb: backbone, sc: side chain; hb: hydrogen bond, io: ionic interaction; np: non-polar interaction, π: π-π interaction, cπ: cation-π interaction. In the structure TCRα is chain A, TCRβ is chain B, MHC is chain C and the peptide is chain D and the residue numbers are sequential*

TCR	PEPTIDE	MHC
CDR1α -SER25.A(sc)	-	hb-GLU276(sc)
CDR1α -TYR28.A(sc)	-	hb-GLN373(sc)
CDR2α -THR48.A(sc)	np-LEU487(sc)	
CDR2α- LYS66.A(sc)	-	hb-GLU384(sc)

Table 7: Molecular interactions between TCRs and pMHC in UTP20-PBL, as predicted by homology modeling. bb: backbone, sc: side chain; hb: hydrogen bond, io: ionic interaction; np: non-polar interaction, π: π-π interaction, cπ: cation-π interaction. In the structure TCRα is chain A, TCRβ is chain B, MHC is chain C and the peptide is chain D and the residue numbers are sequential.

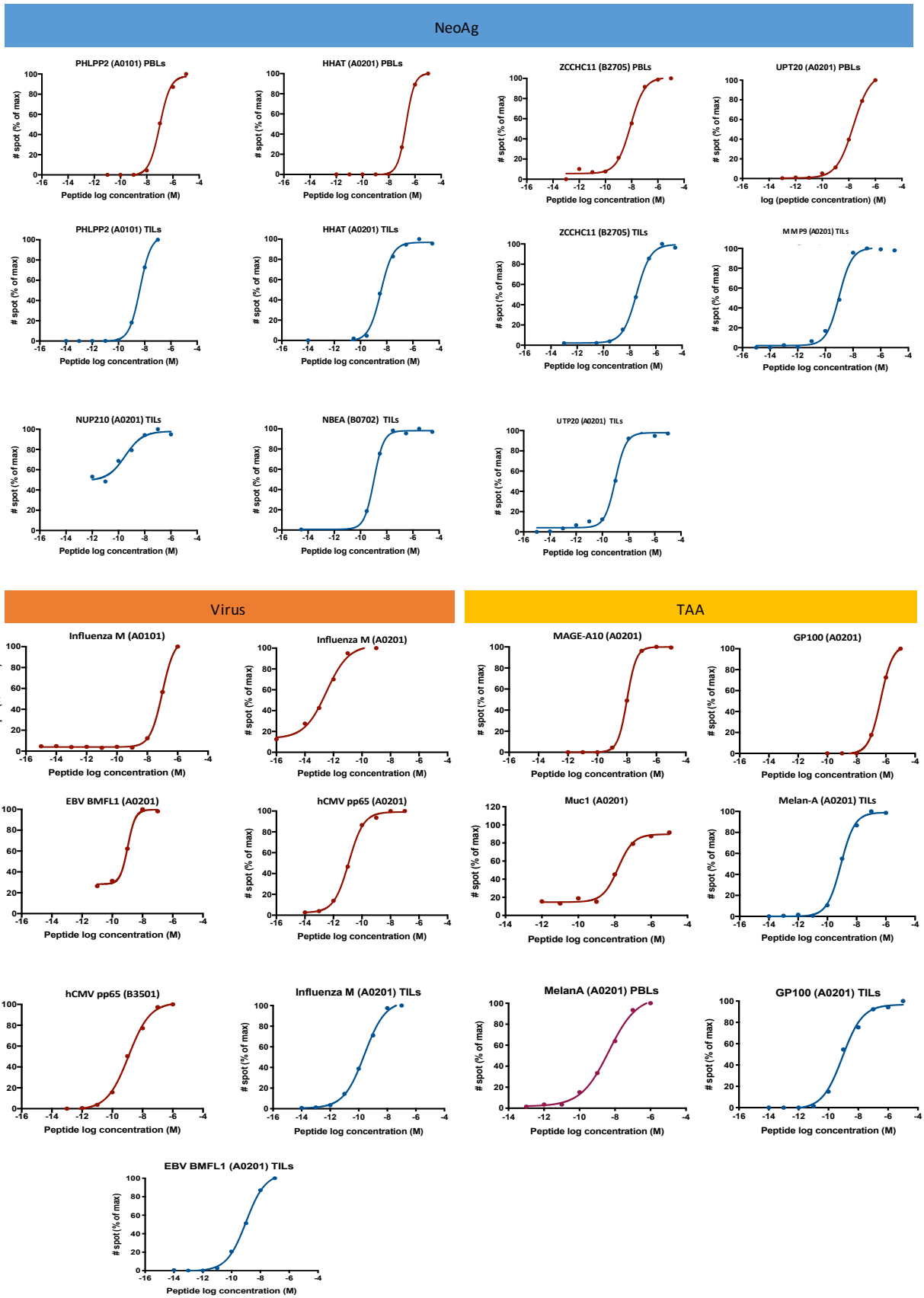

Figure S1: Representative examples of the functional avidity of virus-, TAA- or neoAg-specific primary CD8 T-cells derived from TILs or PBLs. Cells were stimulated with serial dilutions of cognate peptides and functional responses were assessed by IFN-γ ELISpot assay.

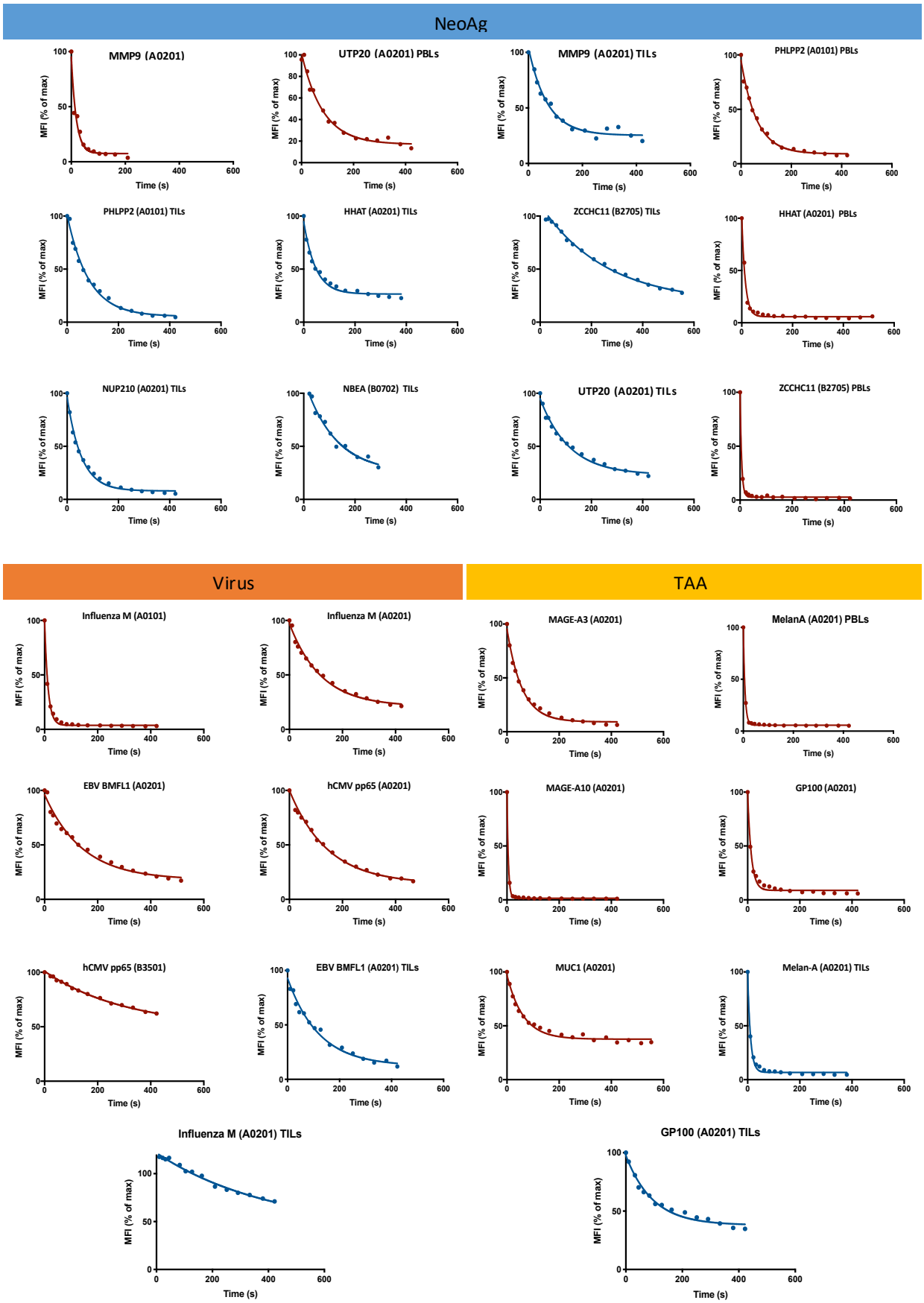

Figure S2: Representative examples of the structural affinity of virus-, TAA- or neoAg-specific primary CD8 T-cells derived from TILs or PBLs. NTAmers were used to measure monomeric pMHC-TCR $T_{1/2}$ (s).

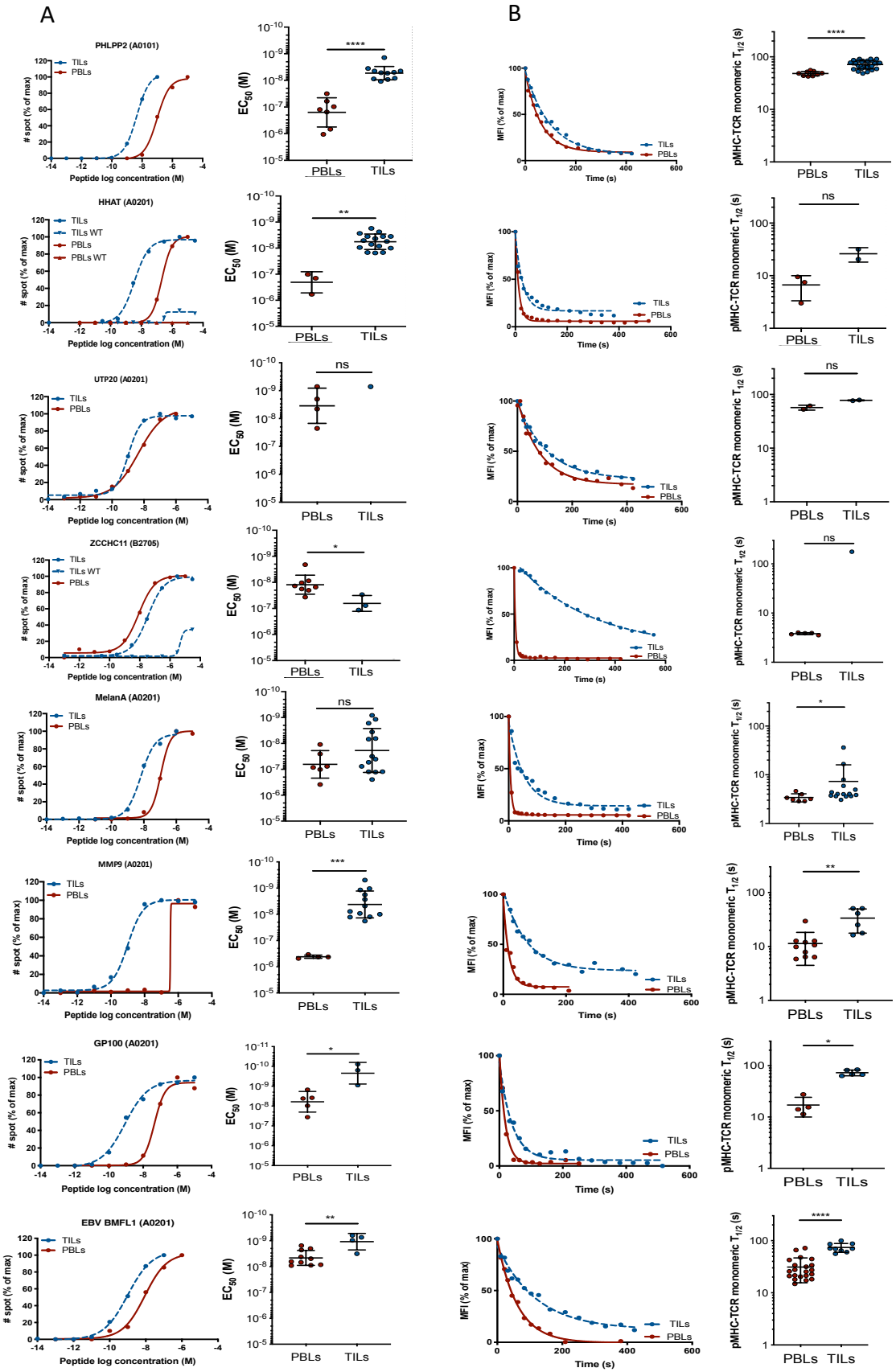

Figure S3: Functional and structural avidity of neoAg-specific PBLs and TILs. A. Representative examples (left) and cumulative analyses (mean ± SD) (right) of the functional avidity of neoAg-specific PBLs (red lines) and TILs (blue dotted lines) assessed by IFN-γ ELISpot assay D. Representative examples (left) and cumulative analyses (right) of the monomeric pMHC-TCR dissociation kinetics of neoAg-specific PBLs (red lines) and TILs (blue dotted lines) assessed with NTAmers.

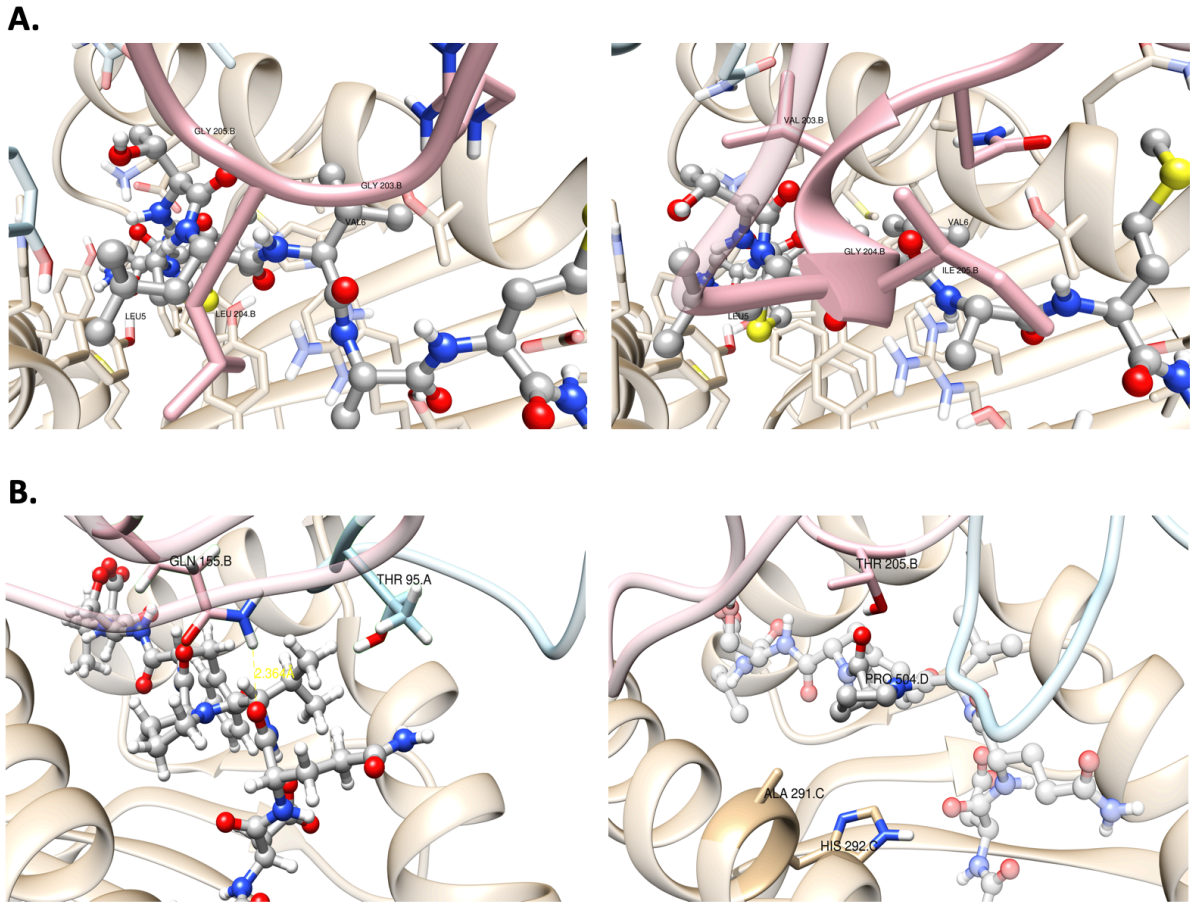

Figure S4: TCR-pMHC structure modeling. A. Calculated TCR-p-MHCs for EBV A ($T_{1/2}$=16 s) on the left, and EBV B ($T_{1/2}$= 77 s) , on the right. TCRα ribbon is coloured in light blue, with residues displayed in sticks and coloured according to the atom types, except for carbon which are coloured in light blue. TCRβ is coloured in pink, with residues displayed in sticks and coloured according to the atom types, with carbon coloured in pink. MHC is coloured in brown, with residues displayed in sticks and coloured according to the atom types, with carbon coloured in brown. The peptide is shown in grey ball and stick and coloured according to the atom types and carbon coloured in grey. Residues are labelled in black. For EBV B, hydrophobic residues of TCRβ CDR3, namely VAL203.B, GLY204.B and ILE205.B, engage in hydrophobic interactions with the middle residues of the peptide LEU on position 5 and VAL on position 6. The stronger hydrophobic interactions observed between TCR and the peptide for EBV B, when compared to EBV A, could justify a higher mean half-life for EBV B. More numerous favorable interactions can be found between TCRs and pMHC in both. Calculated TCR-p-MHCs for the PBL GP100 ($T_{1/2}$= 9 s) on the left, and for the TIL GP100 ($T_{1/2}$= 70 s), on the right. TCRα ribbon is coloured in light blue, with residues displayed in sticks and coloured according to the atom types carbon coloured in light blue. TCRβ is coloured in pink, with residues displayed in sticks and coloured according to the atom types, with carbon coloured in pink. MHC is coloured in brown, with residues displayed in sticks and coloured according to the atom types, with carbon coloured in brown. The peptide is shown in grey ball and stick and coloured according to the atom types and carbon coloured in grey. Residues are labelled in black. For TIL GP100, we present an interesting chain of interactions that extends from MHC up to TCR, i.e., the aromatic residue HIS292 from MHC interacts via π-π with PRO on position 6 of the peptide, (PRO504.D in the left figure), that has non-polar and polar interactions with THR205.B. PBL has less contacts. More numerous favorable interactions can be found between TCRs and pMHC in both cases. These interactions were based on an analysis of the best 5 ranked homology models for each complex.

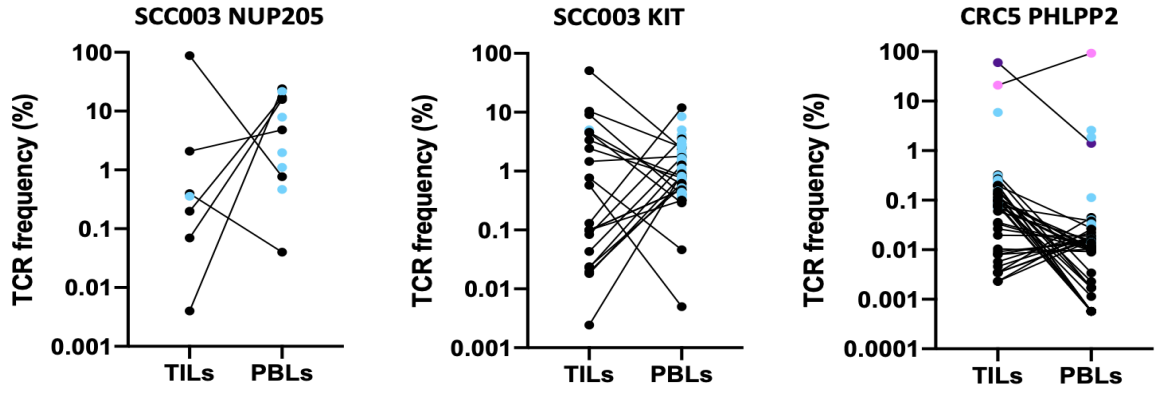

Figure S5: H. TILs and PBLs TCR repertoires comparison: frequency of shared (black and purple) and unique (blue) TCRs found in Ag-specific PBLs and TILs of patients SCC003 and CRC5. The two dominant clones identified in clones derived from PBLs and TILs from CRC5 are identified in purple ($T_{1/2}$=69 s) and pink ($T_{1/2}$=48 s))

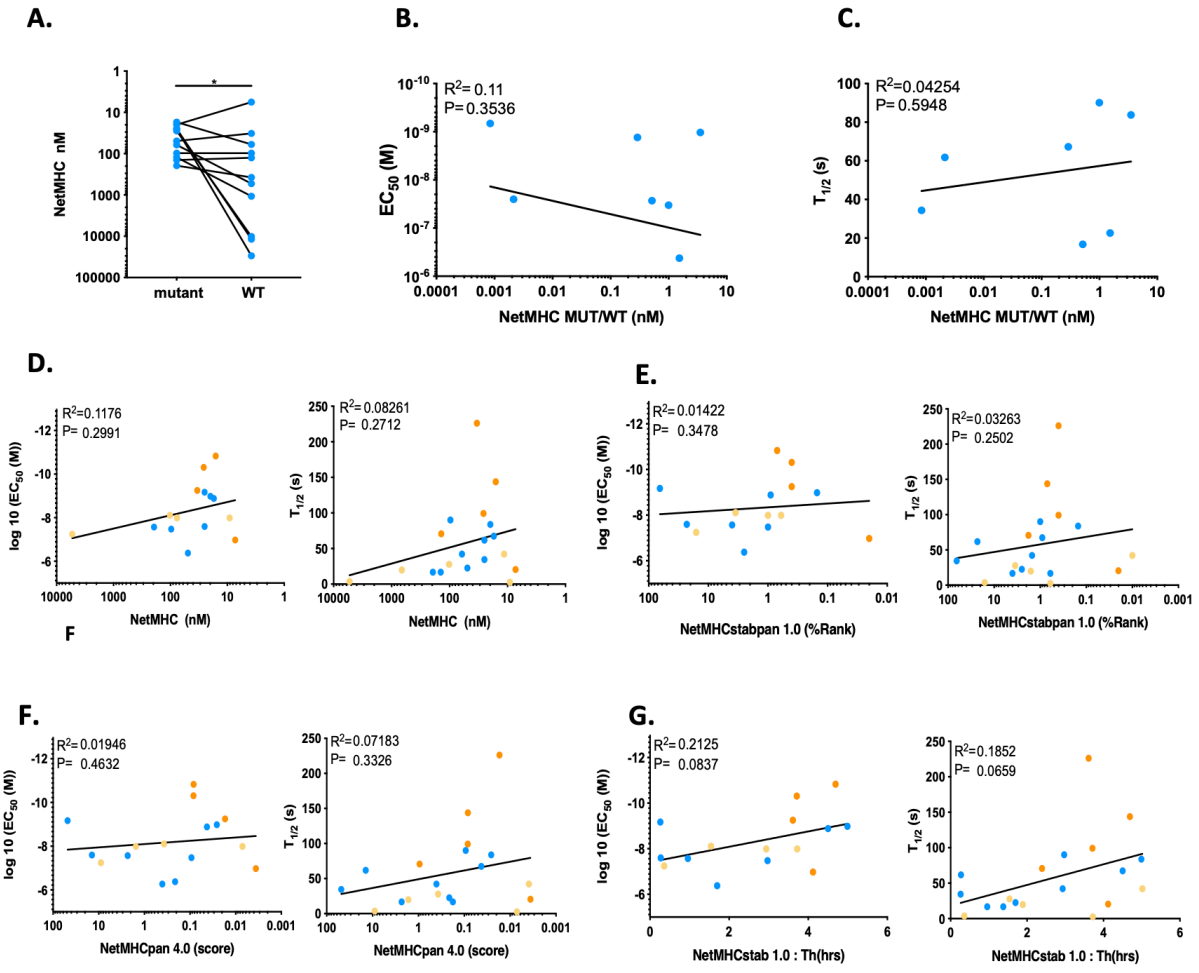

Figure S6: Meta-analysis of the parameters influencing virus-, TAA- and neoAg-specific CD8 T cells functional heterogeneity. A. B. C. Analysis of the neoAg distance to self and its impact on the median of structural and functional avidity of neoAg-specific CD8 T cells: A. NetMHC 4.0 peptide-MHC binding predictions of mutated or native (WT) neoAgs. B.C. Correlations between the median of functional (EC_{50} (M)) or structural affinity (pMHC-TCR $T_{1/2}$ (s)) of neoAg-specific CD8 T cells and the neoAg distance to self represented by NetMHC MUT/ NetMHC WT. D.E.F.G. Correlation between the mean of functional (EC_{50} (M)) or structural avidity (pMHC-TCR $T_{1/2}$ (s)) obtained respectively by IFN-γ ELISpot and NTAmers on virus- (orange), TAA- (yellow) and neoAg-specific CD8 T cells clones (blue) and their cognate Ag p-MHC binding predictions obtained using D. NetMHC 4.0 E. NetMHCstabpan 1.0 F. NetMHCpan 4.0 G. NetMHCstab 1.0. predictor algorithms.

B. Side project: TCR repertoire subtraction assay: a new method for rapid identification of highly potent tumor-specific TCRs

1. Aim

As TAA- and neoAg-specific CD8 T cells are unequally functional and because highly functional tumor-specific CD8 T cells are present at really low frequency, next generation ACT will require rapid identification and isolation of highly functional CD8 T cells or their TCR. We previously reported that NTAmer are limited in the upper range of affinity to predict T cell functionality and that cytokine release assays are too variable to reliably predict antitumor efficacy. Here, we propose a new strategy for the rapid identification of highly potent tumor-specific TCRs based on the cell's susceptibility to apoptosis upon TCR triggering. Based on previous studies highlighting the pMHC multimer-induced cell death of highly Ag-sensitive clones when staining is performed under physiological conditions (*363*), the main aim is to validate the use of this phenomenom after overstimulation as a robust parameter to identify the most functional CD8 T cells. By staining and sorting CD8 T cell populations with conventional and reversible multimers, we aim at the identification of highly functional TCR by comparison of the scTCR-Seq repertoires.

2. Results

TCR induced apoptosis correlates with TCR binding strength.

To compare the TCR-induced cell death upon incubation with pMHC multimers (*364, 365*), conventional multimers or reversible NTAmers were used to sort TAA-, virus- and neoAg-specific CD8 T cells covering a broad range of structural and functional avidity (**Table 8**). After isolation and cloning of CD8 T cells by limiting dilution, the cloning efficiency (*i.e.* number of specific clones obtained out of 300 single cells plated) was evaluated (**Figure 16)**. Using reversible multimers, we observed that, as expected, the cloning efficiency was improved for viral-specific CD8 T cells but not for TAA-specific CD8 T cells (2.7-fold against 1.2-fold). Of interest, the cloning efficiency of neoAgs-specific CD8 T cells was heterogeneous. Indeed, slight increase in cloning efficiency was observed for NUP210- and SLC25A48-specific CD8 T cells (1.5-fold) while it was improved by 1.8-fold for PHLPP2-specific CD8 T cells (1.8-fold).

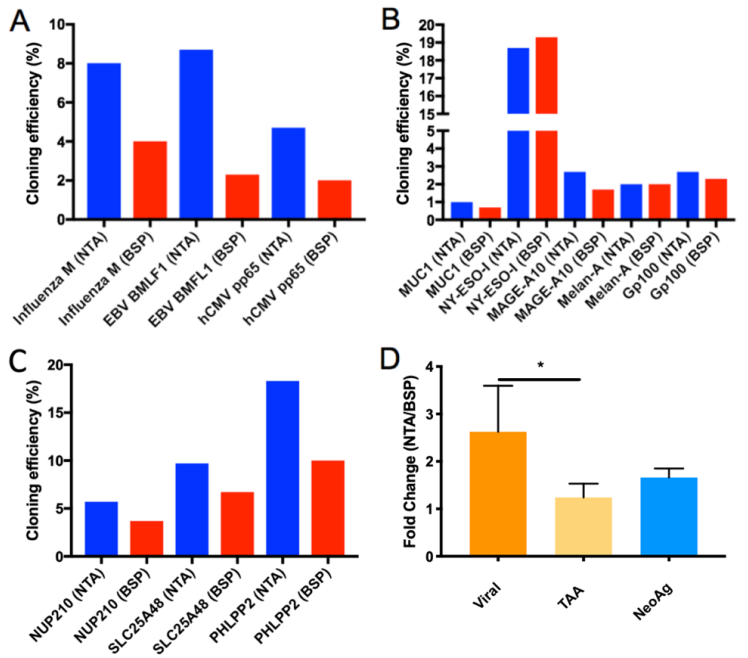

Figure 16: Cloning efficiency after sorting with conventional or reversible pMHC multimers. Cloning efficiency of viral-specific (A), TAA-specific (B) or neoAgs-specific CD8 T cells (C) clones sorted with conventional (red) or reversible (blue) pMHC multimers. D. Fold change between cloning efficiency using NTA vs conventional multimers for viral- (orange), TAA (yellow) or neoAg-specific CD8 T cells (blue).

Altogether, these observations raised the question whether additional clones obtained with NTAmers are different and of higher structural affinity from those obtained with conventional pMHC multimers. TCR β chain was sequenced on each individual clone using a proprietary method developed by Dr. Raphaël Genolet. As TCR sequencing was concomitantly developed in our laboratory, we were only able to complete sequencing of TCR β chains for 9 of the viral-, TAA and neoAg-specific CD8 T cell clones (**Figure 17**). NTAmer sorting increased TCR diversity. For EBV BMLF1 and CMV pp65, respectively, 2 and 3 unique TCRs were identified in clones sorted with reversible multimers whereas no unique TCR was found in clones sorted with conventional multimers. For Influenza MA, 3 additional unique TCRs were identified in clones reversibly sorted, but 1 for the cells sorted with conventional multimer. Nonetheless, in each specificity, a predominant TCR was consistently identified, both in clones sorted with

NTAmers or with conventional multimers. This TCR over-representation may have been induced by cell culture conditions. Still, even if the dominant TCR is found in both reversible and conventional sorted populations, the number of clones obtained with this TCR is higher when sorted with NTAmers. For TAA specificities, reversible sorting increased the TCR diversity only for MUC1 (1 unique additional TCR). For MAGE-A10, no unique TCR was found in the two subsets, as opposed to Melan-A-specific CD8 T cell clones, comprising 1 shared and 1 unique TCR in the populations sorted either with reversible or conventional pMHC multimer. Finally, for neoAgs specificities, NTAmer sorting enriched the TCR diversity for SLC25A48, with 4 unique TCRs against 2 when using conventional pMHC multimer sorting. A dominant TCR was also found in both reversible and conventional sorted populations, but with a higher number of clones obtained when sorted with NTAmers. It is worth noting that the 2 last neoAgs, NUP210 and PHLPP2-specific CD8 T cell clones only contained one shared TCR among reversible and conventional sorted populations. However, the higher cloning efficiency for NTAmer sorted populations highlighted the potential susceptibility to apoptosis described above. Finally, data of TCR sequencing were grouped per classes of Ag. This highlighted that reversible sorting enriched the TCR diversity of virus-specificity as opposed to TAA-specificity. For neoAgs, increased TCR diversity following NTAmer sorting was heterogeneous, emphasizing the functional overlap between TAA- and virus-specific CD8 T cells. Despite the low number of clones (and TCR) obtained with this method and precluding a robust analysis, these observations confirmed that reversible sorting preserves the TCR diversity and improves cloning efficiency of virus- and some neoAg-specific CD8 T cells. It is also in line with the disparities regarding the functional and structural avidity previously observed between the different classes of Ags.

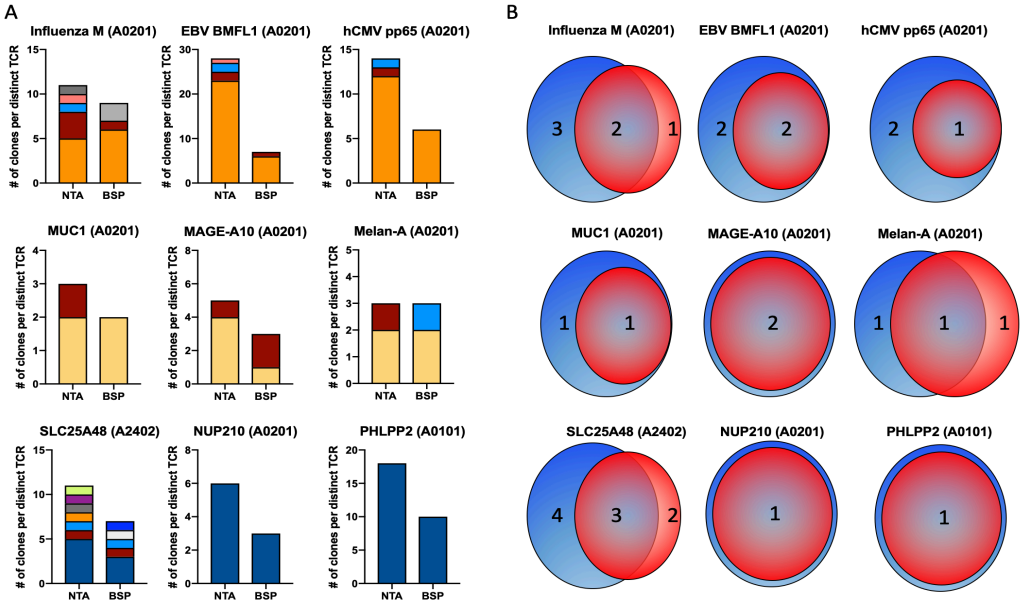

Figure 17: TCR diversity of viral Ag- TAA-, and neoAg-specific CD8 T cells after sorting with conventional (BSP) or reversible pMHC multimers (NTA). A. Left panel. Number of distinct TCR beta chains identified for viral-, TAA- or neoAgs-specific CD8 T cells after sorting with conventional or reversible pMHC multimers (each color is a unique sequence). B. Venn diagram representing unique TCRs identified after sorting with BSP (Red), NTA (Blue), or shared sequences (purple) between the two subsets for the individual specificities.

As TCR-induced cell apoptosis was only partial for the dominant TCRs, we aimed to validate previous studies demonstrating that cell apoptosis is directly related to T cell structural and functional avidity. We then looked at TCR-induced cell death after activation with unlabeled pMHC tetramers. Stimulation was performed with both irrelevant and cognate unlabeled pMHC tetramers on CD8 T cell clones derived from TILs or PBLs (**Table 8**) and TCR-induced cell death assessed by FACS analysis (**Figure 18**). We showed that viral-specific CD8 T cells are highly prone to cell death (between 20 and 78 % of apoptosis, median at 43 %). Minor apoptosis was detected in TAA-specific CD8 T cells (between 0 and 35 % of apoptosis, median at 6,8 %). Finally, the level of pMHC tetramer-induced cell death was moderate in neoAg-specific CD8 T cells and overlapped with that of virus and TAA (between 12 and 41 % of apoptosis, median at 35,8%). These data confirm that susceptibility to apoptosis is Ag-dependent and none of the clone underwent a total deletion under these conditions. Viral Ag-specific CD8 T cells are more prone to cell death than TAA-specific ones, reflecting their higher Ag-sensitivity. For neoAgs, the heterogeneous profile highlights their functional overlap with TAA- and virus- specific CD8 T cells, consistently with the observation of the clonal efficiency.

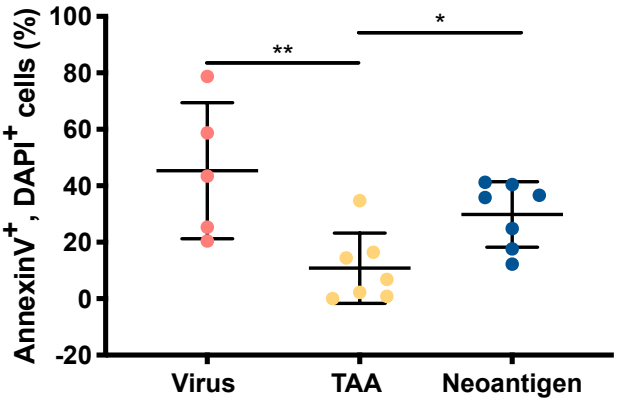

Figure 18: pMHC-induced apoptosis of viral-, TAA- or neoAg-specific CD8 T cells. Relative cell death after 4h stimulation with specific or irrelevant pMHC tetramers (1 µg/ml) at 37°C. Apoptotic cells are represented by DAPI and Annexin V positive staining. The relative % of apoptotic cells has been calculated by subtracting the cell death induced by irrelevant pMHC tetramers

We then investigated the correlation between structural and functional avidities (**Table 8**) and the susceptibility to apoptosis (**Figure 19**). We observed significant correlations between pMHC multimer-induced cell death and both EC_{50} and monomeric pMHC-TCR dissociation kinetics. However, this correlation was stronger for EC_{50} (R^2=0.66 P=0.0003) as compared to off rate (R^2=0.40 P=0.0047). These observations confirm that T cells bearing TCR of high affinity are more prone to cell death following TCR-mediated activation. Therefore, TCR-induced cell death can be used to identify functionally relevant CD8 T cells. However, we have to consider that only a fraction of each clonotype undergoes TCR-induced apoptosis, the degree of apoptosis being dependent on their pMHC-TCR affinity.

Antigen/Gene	Sample	HLA-restriction	Peptide sequence	$T_{1/2}$ (s)	EC_{50} (M)
Influenza A PB1	PBLs	A0101	VSDGGPNLY	20,44	1,06E-07
Influenza MA MP	PBLs	A0201	GILGFVFTL	71,8	9,1E-13
EBV BMLF1	PBLs	A0201	GLCTLVAML	76,8	3,52E-10
hCMV pp65	PBLs	A0201	NLVPMVATV	99,35	4,9E-11
hCMV pp65	PBLs	B3501	IPSINVHHY	226,2	5,604E-10
MAGE-A10	PBLs	A0201	GLYDGMEHL	2,5	1,027E-08
GP100	PBLs	A0201	ITDQVPFSV	6,43	7,328E-07
MelanA	PBLs	A0201	EAAGIGILTV	3,17	8,051E-08
MelanA	TILs	A0201	EAAGIGILTV	4,03	4,031E-08
MUC1	PBLs	A0201	VLVCVLVAL	/	1,2E-08
NY-ESO-I	PBLs	A0201	SLLMWITQC	19,88	/
MelanA	PBLs (post vaccine)	A0201	EAAGIGILTV	23,45	7,081E-10
MAGE-A3	PBLs	A0101	EVDPIGHLY	42,1	/
ZCCHC11	PBLs	B2705	GRKLFGTHF	3,89	1,439E-08
HS6ST1	PBLs (post ACT)	B4001	TEDYMIHII	16,7	9,65E-08
NUP210	TILs	A0201	QSDNGLDSDY	34,4	5,909E-10
SLC25A48	PBLs (post ACT)	A2402	PYMFLSEWI	42,2	5,4E-07
PHLPP2	PBLs	A0101	GLQAILVHV	48,46	1,245E-07
FPR2	PBLs	A2402	VFSFTATLPF	72,2	4,358E-11
PHLPP2	TILs	A0101	GLQAILVHV	75,15	5,118E-09

Table 8: Summary of the different CD8 T cells specificities extracted from PBLs or TILs and their corresponding structural and functional avidity. NTAmers were used to measure monomeric pMHC-TCR $T_{1/2}$ (s) of viral-specific (orange), TAA-specific (yellow) or neoAgs-specific CD8 T cells (blue) clones. Functional avidity measured by IFN-γ ELISPOT and reflected through the EC_{50} (M). Data include neoAgs-specific CD8 T cells identified after ACT and MelanA-specific CD8 T cells identified post vaccination with the analogue peptide (ELAGIGILTV).

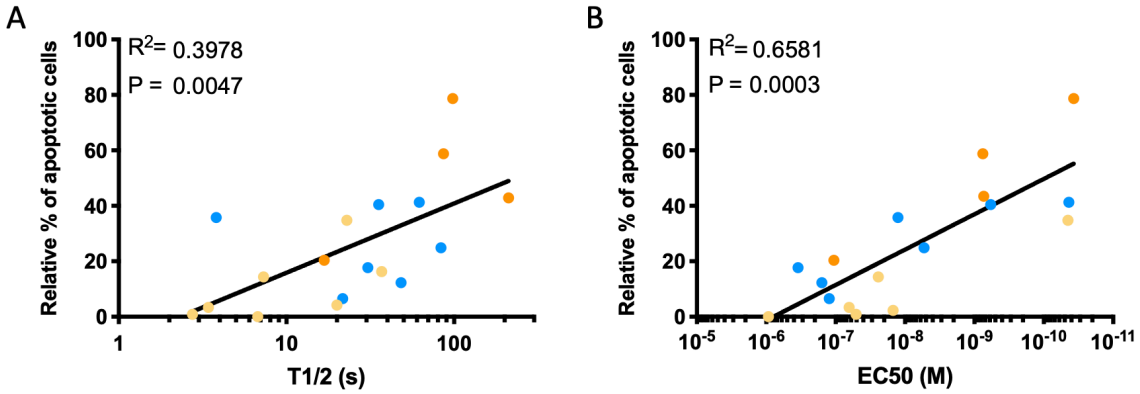

Figure 19: Correlations between structural and functional parameters. A. Correlation between monomeric pMHC-TCR dissociation kinetics and susceptibility to apoptosis following pMHC tetramer stimulation. B. Correlation between EC_{50} and susceptibility to apoptosis.

TCR-induced cell death correlates with structural affinity of CD8 T cells. As proof of concept for the TCR subtraction assay, we followed over time by flow cytometry the proportion of live CD8 T cells clones FPR2 (A2402) and Influenza MA (A0201)) spiked in PBMCs, following stimulation with specific/irrelevant pMHC multimers (**Figure 20**). A decrease of cell viability was observed for the 2 Ag-specificities in the first 2 hours (from 100% to 58% and

from 100% to 67% for FPR2 and Influenza MA, respectively). After 2 hours, cell viability decreased more slowly to reach 35% and 58% for FPR2 and Influenza MA, respectively. FPR2-specific CD8 T cell clones have higher structural affinity ($T_{1/2}$= 62 s) than Influenza MA-specific CD8 T cell clones ($T_{1/2}$= 40 s). The faster cell death of FPR2 confirms that the higher is the TCR affinity, the higher is the TCR-induced cell death. This observation was also true when clones were mixed (**Figure 20 C**), resulting in 51% of relative viability after 5h of stimulation for FPR2, against 60% for Influenza MA-specific CD8 T cells. However, this experiment needed to be validated with cells bearing TCRs with a larger range of structural affinity in order to observe significant differences between clones.

In order to validate the strategy of the TCR subtraction assay based on the subtraction of two TCR repertoires of Ag-specific CD8 T cells following sorting and incubation with conventional or reversible pMHC multimers, we mixed clonal populations bearing TCRs of different specificities and affinities (hCMV $pp65_{495\text{-}503}$ $T_{1/2}$=99 s, $EBV_{259\text{-}267}$ $T_{1/2}$=90 s, and $MAGE\text{-}A10_{254\text{-}262}$ $T_{1/2}$=3 s) (**Figure 21**). Cells were stimulated with specific/irrelevant pMHC multimers before sorting live cells by flow cytometry. Cells were then lysed and TCR repertoires sequenced. TCR repertoires revealed the complete loss of the EBV BMFL1 CD8 T cell clone of high structural affinity and a slight reduction of the frequency for the other ones. Despite their moderate reliability, these experiments validate the possibility to compare the two TCR repertoires to identify clones of high avidity.

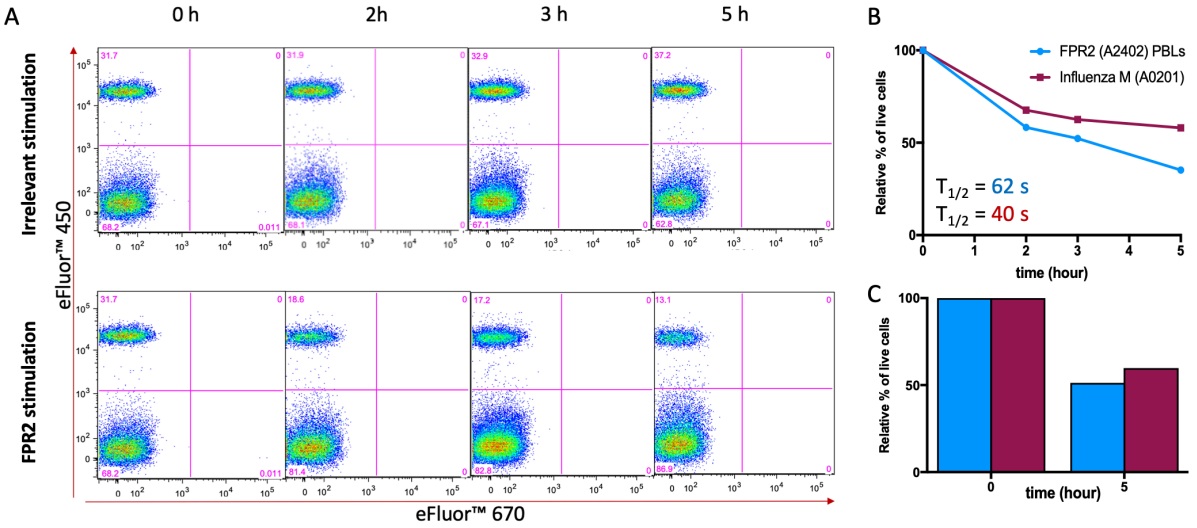

Figure 20: TCR-induced cell death over time of CD8 T cells clones. A. Dot plot representation of the live CD8 T cell population after specific or unspecific stimulation with pMHC tetramer (T=0, 2, 3 ,5h). eFluorTM 450^{neg}, eFluorTM 670^{neg} population represents irrelevant CD8 T cells and eFluorTM 450^{pos}, eFluorTM 670^{neg} population represents FPR2-specific CD8 T cell clones. B. Relative frequency of live individual CD8 T cell clones over time following stimulation with cognate pMHC tetramers (FPR2 (A2402) or Influenza M (A0201)). C. Relative frequency of live mixed CD8 T cell clones over time following stimulation with cognate pMHC tetramers (FPR2 (A2402) and Influenza M (A0201)).

Nevertheless, it emphasizes the importance to quantify TCR-induced cell apoptosis for each clonotype in order to predict T cell responsiveness. Thus, single cell TCR sequencing (scTCR-Seq, allowing full α and β chain sequencing of hundreds single cells) would be the most

relevant solution to compare two TCR repertoires following activation or not with pMHC multimer, allowing the identification of clinically relevant TCRs.

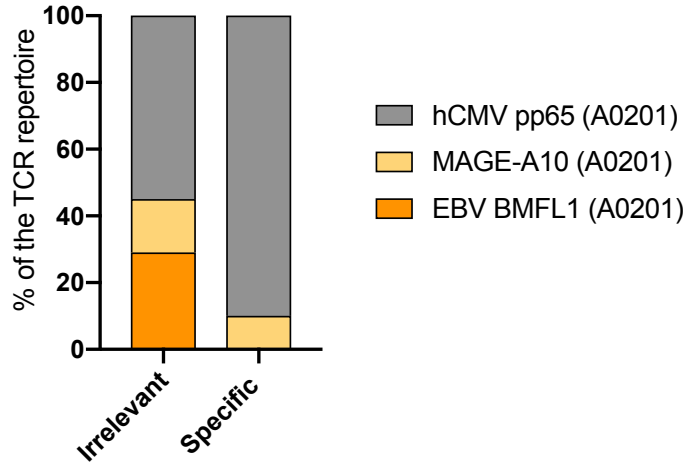

Figure 21: TCR repertoire of mixed CD8 T cells clones following 4 hours of incubation with cognate or irrelevant pMHC and sorting of live T cells by flow cytometry.

3. Discussion

High functional heterogeneity of TAA- or neoAg-specific CD8 T cells calls for novel strategies to quickly identify and isolate highly potent tumor-specific CD8 T cells or their TCR for next-generation ACT. In the main project of my PhD we showed that monomeric pMHC-TCR dissociation kinetics correlates with CD8 T cell function only in a defined range of affinity, preventing its use to predict the clinical relevance of CD8 T cells bearing TCR of really high affinity. Also, the different functional assays depend on the cell's state of activation and have low reproducibility to be used as conventional assay to assess CD8 T cell potency. Previous studies revealed that pMHC-TCR avidity is associated with cell apoptosis after TCR-dependent overstimulation (*363*). Here, we interrogated the possibility to exploit the susceptibility to apoptosis following stimulation with pMHC complexes to rapidly identify TCRs of highly potent CD8 T cells.

Our results showed that sorting with NTAmer highly enriched the cloning efficiency of virus-specific CD8 T cells, moderately increased the one of NeoAg-specific CD8 T cells and did not improve for TAA-specific CD8 T cells. These results support the previous study showing that neoAgs are functionally heterogeneous and are overlapping with TAA- and virus-specific CD8 T cells. Also, this confirms that susceptibility to apoptosis is related to the nature of targeted Ags, each class of Ags having its range of functional and structural avidities. These experiments raised the question whether additional clones obtained with reversible pMHC multimer are different from those obtained with conventional multimers. To interrogate this, TCR β chain was sequenced on each clone using a proprietary method. All the virus-specific CD8 T cells exhibited a superior TCR diversity in the NTAmer sorted clonal subset. For neoAg-specific CD8 T cells, only one specificity showed an enrichment in the TCR diversity for the clonal subset previously sorted with reversible multimer. The two other neoAg specificities had a unique TCR. As expected, sorting with NTAmer did not improved the TCR diversity of TAA-specific CD8 T cells clones. Despite a substantial TCR diversity for certain classes of Ags, a predominant TCR was systematically identified, both in clones sorted with NTAmers or with conventional multimers. This TCR over-representation might have been induced by cell culture conditions. For example, the concentration of peptide used for IVS may impact the expansion of Ag-specific cells. Also, the consecutive IVS and/or REP used to expand TAA or neoAg-specific CD8 T cells are known to bias the TCR repertoire by favoring the growth of a particular clonal population. Taken together, results support the use of NTAmer to get an unbiased TCR repertoire and increase the cloning efficiency of virus- and neoAg-specific CD8 T cells. Thus, this underlines the disparities between the different classes of Ags and their susceptibility to apoptosis. This implies that some TCRs of high avidity induce higher CD8 T cell activation than other after binding to pMHC multimer, ultimately leading to apoptosis. This is concordant with previous studies showing that reversible pMHC multimers or drugs like

Dasatinib prevent T cell activation of high avidity CD8 T cells during pMHC multimer staining and sorting.

In order to exploit susceptibility to apoptosis for the assessment of CD8 T cell function, we evaluated the TCR-induced apoptosis of the different classes of Ags. Here, virus-specific CD8 T cells clones exhibited higher susceptibility to death than neoAg-, being higher than TAA-specific CD8 T cells. For neoAg, the heterogeneous profile is in line with their functional overlap with TAA- and virus-specific CD8 T cells previously determined, and is consistent with the observation made for the clonal efficiency. As this preliminary experiment confirmed that susceptibility to death is closely related to Ag-specificity and thus to TCR-pMHC structural affinity, we measured the direct correlation between structural/functional avidity and TCR-induced apoptosis. Correlations between multimer-induced cell death and both EC_{50} and monomeric pMHC-TCR dissociation kinetics were observed, with a greater correlation for the functional avidity. Susceptibility to apoptosis may reflect Ag sensitivity of a cell, and thus is closely related to its functionality revealed by IFN-γ release. Therefore, additional assays might be required to validate the reproducibility of this parameter as it might also depend on the cell's state of activation. Together, this study confirms that T cells with high affinity TCR are more prone to apoptosis following TCR dependent activation. This also implies that susceptibility to death is a parameter that can be exploited to predict functional avidity of cells and identify highly relevant CD8 T cells.

The TCR subtraction assay consists in the subtraction of two TCR repertoires of CD8 T cells after sorting and incubation with conventional or reversible pMHC multimer. It exploits the higher susceptibility to death of high avidity CD8 T cells, allowing their identification by detecting higher TCRs proportion in the population sorted with reversible multimer. As proof of concept, we followed the frequency over time of fluorescently labelled live CD8 T cells clones among unlabeled irrelevant cellular population after stimulation with pMHC tetramers. Using clonal populations bearing TCRs of different specificities and affinities, we showed that high avidity T cell clones are more prone to cell death than their lower avidity counterparts. A comparable assay has been carried out on a mix of clones. TCR repertoires were determined after stimulation with specific/irrelevant pMHC multimers. After stimulation, high avidity T cell clones were lost from the repertoire, as opposed to the ones of low avidity, highlighting the great potency of this assay. By extension, staining and sorting CD8 T cell populations with conventional and reversible multimers may allow the isolation of high avidity clones by comparison of the resulting TCR repertoires. However, additional experiments need to be performed in order to validate the reproducibility of the TCR repertoire sequencing after sorting with NTAmer and conventional pMHC multimer, by exploiting cells which are not susceptible to TCR-induced cell death. Also, this study emphasized the need to quantify apoptosis for every clonal population after pMHC multimer stimulation to better predict T cell responsiveness. Strict TCR subtraction might not be able to identify high avidity TCRs, considering the partial TCR-induced apoptosis. The subtraction assay should indeed reflect

the cloning efficiency results described above, meaning that the TCR frequencies and diversities should be different only for highly functional Ag-specific CD8 T cells, being of great interest when included in the pipeline of next generation ACT.

In order to practically design this assay, we are currently optimizing single cell TCR sequencing. This technology will allow a clear assessment of each clonotypes frequency in the CD8 T cell groups previously sorted with NTAmer or conventional multimer. From the clonotype frequency variation could be deduced a functional score predicting the CD8 T cell antitumor activity. Another advantage is the identification of both TCRα and β chain that will be further used to transduce naïve PBMCs in order to perform ACT or to study TCR-pMHC interactions. However, this assay will require many technical developments to ensure its reproducibility and clearly define the clonotype frequency variations required to identify clinically relevant TCRs. Indeed, the main limitation of this assay is the identification of under-represented highly relevant TCRs (for example derived from PBLs). The difference of the TCR frequency between two repertoires might not be tangible and single cell sequencing methods will require an extension of the number of single cells treated. However, its high potency is related to its simplicity of implementation, as opposed to other available methods measuring the functionality of single CD8 T cells. Unlike the highly specific devices allowing single cell calcium release measurement, cytokine release assessment, or trogocytosis evaluation (*366-369*), which require anyhow single cell TCR sequencing, our method would only imply Ag-specific CD8 cell sorting followed by single cell TCR sequencing. Besides freeing from costly and highly specific device, the overall overview of a TCR repertoire would reduce the bias inherent to every single cell measurement. Finally, due to the cell stimulation required for the implementation of others cutting edge technologies, cell apoptosis might be induced on cells of interest, preventing high quality single cell TCR sequencing. Thus, our subtraction assay might be an easy and rapid solution allowing the identification of high interest TCR.

References

1. D. J. Laydon, C. R. Bangham, B. Asquith, Estimating T-cell repertoire diversity: limitations of classical estimators and a new approach. *Philos Trans R Soc Lond B Biol Sci* **370**, (2015).
2. M. Mamonkin, *Transcriptional Regulation of CD8+ T Cell Differentiation (PhD Thesis)*. (2015).
3. B. E. Russ, J. E. Prier, S. Rao, S. J. Turner, T cell immunity as a tool for studying epigenetic regulation of cellular differentiation. *Front Genet* **4**, 218 (2013).
4. R. N. Germain, T-cell development and the CD4-CD8 lineage decision. *Nat Rev Immunol* **2**, 309-322 (2002).
5. K. E. Pauken, E. J. Wherry, Overcoming T cell exhaustion in infection and cancer. *Trends Immunol* **36**, 265-276 (2015).
6. Z. Pancer, M. D. Cooper, The evolution of adaptive immunity. *Annu Rev Immunol* **24**, 497-518 (2006).
7. C. A. Janeway, Jr., R. Medzhitov, Innate immune recognition. *Annu Rev Immunol* **20**, 197-216 (2002).
8. S. N. Mueller, T. Gebhardt, F. R. Carbone, W. R. Heath, Memory T Cell Subsets, Migration Patterns, and Tissue Residence. *Annual Review of Immunology, Vol 31* **31**, 137-161 (2013).
9. M. A. Markiewicz *et al.*, Long-term T cell memory requires the surface expression of self-peptide major histocompatibility complex molecules. *P Natl Acad Sci USA* **95**, 3065-3070 (1998).
10. G. W. Litman *et al.*, Phylogenetic Diversification of Immunoglobulin Genes and the Antibody Repertoire. *Mol Biol Evol* **10**, 60-72 (1993).
11. B. Heyman, Complement and Fc-receptors in regulation of the antibody response. *Immunol Lett* **54**, 195-199 (1996).
12. A. M. Silverstein, Cellular versus humoral immunology: a century-long dispute. *Nat Immunol* **4**, 425-428 (2003).
13. C. A. Janeway, *Immunobiology the immune system in health and disease*. (Churchill Livingstone ; Garland Pub., Edinburgh; New York, 2001).
14. F. A. Bonilla, H. C. Oettgen, Adaptive immunity. *Journal of Allergy and Clinical Immunology* **125**, S33-S40 (2010).
15. D. D. Chaplin, Overview of the immune response. *The Journal of allergy and clinical immunology* **125**, S3-S23 (2010).
16. S. L. Swain, K. K. McKinstry, T. M. Strutt, Expanding roles for CD4(+) T cells in immunity to viruses. *Nat Rev Immunol* **12**, 136-148 (2012).
17. R. Clark, T. Kupper, Old Meets New: The Interaction Between Innate and Adaptive Immunity. *Journal of Investigative Dermatology* **125**, 629-637 (2005).
18. S. Lederman *et al.*, Identification of a novel surface protein on activated CD4+ T cells that induces contact-dependent B cell differentiation (help). *J Exp Med* **175**, 1091-1101 (1992).
19. S. Lederman *et al.*, T-BAM/CD40-L on helper T lymphocytes augments lymphokine-induced B cell Ig isotype switch recombination and rescues B cells from programmed cell death. *J Immunol* **152**, 2163-2171 (1994).
20. E. M. Shevach, Mechanisms of foxp3+ T regulatory cell-mediated suppression. *Immunity* **30**, 636-645 (2009).

21. M. Wieczorek *et al.*, Major Histocompatibility Complex (MHC) Class I and MHC Class II Proteins: Conformational Plasticity in Antigen Presentation. *Front Immunol* **8**, 292 (2017).
22. A. Townsend, J. Trowsdale, The transporters associated with antigen presentation. *Semin Cell Biol* **4**, 53-61 (1993).
23. K. Murphy, P. Travers, M. Walport, C. Janeway, *Janeway's immunobiology*. (Garland Science, New York, 2008).
24. J. A. Villadangos, P. Schnorrer, Intrinsic and cooperative antigen-presenting functions of dendritic-cell subsets in vivo. *Nat Rev Immunol* **7**, 543-555 (2007).
25. N. Zhang, M. J. Bevan, CD8(+) T cells: foot soldiers of the immune system. *Immunity* **35**, 161-168 (2011).
26. M. S. Abdel-Hakeem, N. H. Shoukry, Protective immunity against hepatitis C: many shades of gray. *Front Immunol* **5**, (2014).
27. A. Wilson, H. R. MacDonald, F. Radtke, Notch 1-deficient common lymphoid precursors adopt a B cell fate in the thymus. *J Exp Med* **194**, 1003-1012 (2001).
28. D. I. Godfrey, J. Kennedy, T. Suda, A. Zlotnik, A developmental pathway involving four phenotypically and functionally distinct subsets of CD3-CD4-CD8- triple-negative adult mouse thymocytes defined by CD44 and CD25 expression. *J Immunol* **150**, 4244-4252 (1993).
29. I. Aifantis, J. Feinberg, H. J. Fehling, J. P. Di Santo, H. von Boehmer, Early T cell receptor beta gene expression is regulated by the pre-T cell receptor-CD3 complex. *J Exp Med* **190**, 141-144 (1999).
30. E. Robey, B. J. Fowlkes, Selective events in T cell development. *Annu Rev Immunol* **12**, 675-705 (1994).
31. M. Attaf, E. Huseby, A. K. Sewell, αβ T cell receptors as predictors of health and disease. *Cellular And Molecular Immunology* **12**, 391 (2015).
32. S. D. Fugmann, A. I. Lee, P. E. Shockett, I. J. Villey, D. G. Schatz, The RAG proteins and V(D)J recombination: complexes, ends, and transposition. *Annu Rev Immunol* **18**, 495-527 (2000).
33. S. M. Haeryfar *et al.*, Terminal deoxynucleotidyl transferase establishes and broadens antiviral CD8+ T cell immunodominance hierarchies. *J Immunol* **181**, 649-659 (2008).
34. A. K. Sewell, Why must T cells be cross-reactive? *Nature Reviews Immunology* **12**, 669 (2012).
35. M. A. Daniels *et al.*, Thymic selection threshold defined by compartmentalization of Ras/MAPK signalling. *Nature* **444**, 724-729 (2006).
36. C.-S. Hsieh, H.-M. Lee, C.-W. J. Lio, Selection of regulatory T cells in the thymus. *Nature Reviews Immunology* **12**, 157 (2012).
37. M. K. Jenkins, J. J. Moon, Response to Comment on "The Role of Naive T Cell Precursor Frequency and Recruitment in Dictating Immune Response Magnitude". *Journal of Immunology* **190**, 1896-1896 (2013).
38. C. C. Brinkman, S. J. Rouhani, N. Srinivasan, V. H. Engelhard, Peripheral tissue homing receptors enable T cell entry into lymph nodes and affect the anatomical distribution of memory cells (vol 191, pg 2412, 2013). *Journal of Immunology* **191**, 6292-6292 (2013).
39. C. R. Sousa, Essay - Dendritic cells in a mature age. *Nature Reviews Immunology* **6**, 476-483 (2006).

40. L. P. Chen, D. B. Flies, Molecular mechanisms of T cell co-stimulation and co-inhibition (vol 13, pg 27, 2013). *Nature Reviews Immunology* **13**, (2013).
41. K. N. Pollizzi, J. D. Powell, Integrating canonical and metabolic signalling programmes in the regulation of T cell responses. *Nature Reviews Immunology* **14**, 435-446 (2014).
42. R. Obst, The timing of T cell priming and cycling. *Front Immunol* **6**, (2015).
43. Y. Yamashita *et al.*, *Perforin and granzyme expression in cytotoxic T-cell lymphomas*. (1998), vol. 11, pp. 313-323.
44. V. Kalia, S. Sarkar, R. Ahmed, CD8 T-Cell Memory Differentiation during Acute and Chronic Viral Infections. *Adv Exp Med Biol* **684**, 79-95 (2010).
45. A. J. Darmon, M. J. Pinkoski, R. C. Bleackley, in *Apoptosis: Biology and Mechanisms,* S. Kumar, Ed. (Springer Berlin Heidelberg, Berlin, Heidelberg, 1999), pp. 103-125.
46. N. Hagimoto *et al.*, Essential roles of the Fas-Fas ligand pathway in the development of pulmonary fibrosis. *Am J Resp Crit Care* **159**, A214-A214 (1999).
47. C. D. Surh, J. Sprent, Homeostasis of naive and memory T cells. *Immunity* **29**, 848-862 (2008).
48. F. Sallusto, D. Lenig, R. Forster, M. Lipp, A. Lanzavecchia, Two subsets of memory T lymphocytes with distinct homing potentials and effector functions. *Nature* **401**, 708-712 (1999).
49. B. Youngblood, J. S. Hale, R. Ahmed, Memory CD8 T cell transcriptional plasticity. *F1000Prime Rep* **7**, 38 (2015).
50. M. A. Williams, A. J. Tyznik, M. J. Bevan, Interleukin-2 signals during priming are required for secondary expansion of CD8+ memory T cells. *Nature* **441**, 890-893 (2006).
51. X. Jiang *et al.*, Skin infection generates non-migratory memory CD8+ T(RM) cells providing global skin immunity. *Nature* **483**, 227-231 (2012).
52. W. W. Agace, J. M. Higgins, B. Sadasivan, M. B. Brenner, C. M. Parker, T-lymphocyte-epithelial-cell interactions: integrin alpha(E)(CD103)beta(7), LEEP-CAM and chemokines. *Curr Opin Cell Biol* **12**, 563-568 (2000).
53. L. Gattinoni *et al.*, A human memory T cell subset with stem cell-like properties. *Nat Med* **17**, 1290-1297 (2011).
54. A. Ballesteros-Tato, B. Leon, B. O. Lee, F. E. Lund, T. D. Randall, Epitope-specific regulation of memory programming by differential duration of antigen presentation to influenza-specific CD8(+) T cells. *Immunity* **41**, 127-140 (2014).
55. C. S. Guy, D. A. A. Vignali, Organization of proximal signal initiation at the TCR:CD3 complex. *Immunological Reviews* **232**, 7-21 (2009).
56. P. A. van der Merwe, S. J. Davis, A. S. Shaw, M. L. Dustin, Cytoskeletal polarization and redistribution of cell-surface molecules during T cell antigen recognition. *Semin Immunol* **12**, 5-21 (2000).
57. S. J. Davis, P. A. van der Merwe, The kinetic-segregation model: TCR triggering and beyond. *Nat Immunol* **7**, 803-809 (2006).
58. H. P. Wang *et al.*, ZAP-70: An Essential Kinase in T-cell Signaling. *Csh Perspect Biol* **2**, (2010).
59. W. G. Zhang, J. Sloan-Lancaster, J. Kitchen, R. P. Trible, L. E. Samelson, LAT: The ZAP-70 tyrosine kinase substrate that links T cell receptor to cellular activation. *Cell* **92**, 83-92 (1998).
60. M. O. Li, A. Y. Rudensky, T cell receptor signalling in the control of regulatory T cell differentiation and function. *Nature Reviews Immunology* **16**, 220-233 (2016).

61. O. Acuto, V. Di Bartolo, F. Michel, Tailoring T-cell receptor signals by proximal negative feedback mechanisms. *Nat Rev Immunol* **8**, 699-712 (2008).
62. E. J. Wherry, T cell exhaustion. *Nat Immunol* **12**, 492 (2011).
63. L. Baitsch *et al.*, Exhaustion of tumor-specific CD8(+) T cells in metastases from melanoma patients. *J Clin Invest* **121**, 2350-2360 (2011).
64. S. M. Kahan, E. J. Wherry, A. J. Zajac, T cell exhaustion during persistent viral infections. *Virology* **479**, 180-193 (2015).
65. D. T. Utzschneider *et al.*, T cells maintain an exhausted phenotype after antigen withdrawal and population reexpansion. *Nat Immunol* **14**, 603-+ (2013).
66. Y. Jiang, Y. Li, B. Zhu, T-cell exhaustion in the tumor microenvironment. *Cell Death Dis* **6**, e1792 (2015).
67. Y. Agata *et al.*, Expression of the PD-1 antigen on the surface of stimulated mouse T and B lymphocytes. *Int Immunol* **8**, 765-772 (1996).
68. R. V. Parry *et al.*, CTLA-4 and PD-1 receptors inhibit T-cell activation by distinct mechanisms. *Mol Cell Biol* **25**, 9543-9553 (2005).
69. J. Chen *et al.*, Interferon-gamma-induced PD-L1 surface expression on human oral squamous carcinoma via PKD2 signal pathway. *Immunobiology* **217**, 385-393 (2012).
70. M. Muhlbauer *et al.*, PD-L1 is induced in hepatocytes by viral infection and by interferon-alpha and -gamma and mediates T cell apoptosis. *J Hepatol* **45**, 520-528 (2006).
71. D. L. Barber *et al.*, Restoring function in exhausted CD8 T cells during chronic viral infection. *Nature* **439**, 682-687 (2006).
72. S. J. Lee *et al.*, Interferon regulatory factor-1 is prerequisite to the constitutive expression and IFN-gamma-induced upregulation of B7-H1 (CD274). *FEBS Lett* **580**, 755-762 (2006).
73. A. T. Parsa *et al.*, Loss of tumor suppressor PTEN function increases B7-H1 expression and immunoresistance in glioma. *Nat Med* **13**, 84-88 (2007).
74. H. Kuipers *et al.*, Contribution of the PD-1 ligands/PD-1 signaling pathway to dendritic cell-mediated CD4+ T cell activation. *Eur J Immunol* **36**, 2472-2482 (2006).
75. S. J. Im *et al.*, Defining CD8(+) T cells that provide the proliferative burst after PD-1 therapy. *Nature* **537**, 417-+ (2016).
76. D. T. Utzschneider *et al.*, T Cell Factor 1-Expressing Memory-like CD8(+) T Cells Sustain the Immune Response to Chronic Viral Infections. *Immunity* **45**, 415-427 (2016).
77. Y. Xing, K. A. Hogquist, T-Cell Tolerance: Central and Peripheral. *Csh Perspect Biol* **4**, (2012).
78. S. Feau, R. Arens, S. Togher, S. P. Schoenberger, Autocrine IL-2 is required for secondary population expansion of CD8+ memory T cells. *Nat Immunol* **12**, 908 (2011).
79. L. E. Cheng, C. Öhlén, B. H. Nelson, P. D. Greenberg, Enhanced signaling through the IL-2 receptor in CD8⁺ T cells regulated by antigen recognition results in preferential proliferation and expansion of responding CD8⁺ T cells rather than promotion of cell death. *Proceedings of the National Academy of Sciences* **99**, 3001 (2002).
80. H. Suzuki *et al.*, Deregulated T cell activation and autoimmunity in mice lacking interleukin-2 receptor beta. *Science* **268**, 1472-1476 (1995).
81. M. F. Bachmann, P. Wolint, S. Walton, K. Schwarz, A. Oxenius, Differential role of IL-2R signaling for CD8+ T cell responses in acute and chronic viral infections. *Eur J Immunol* **37**, 1502-1512 (2007).

82. L. O'Connor *et al.*, Bim: a novel member of the Bcl-2 family that promotes apoptosis. *The EMBO journal* **17**, 384-395 (1998).
83. D. Tischner, C. Woess, E. Ottina, A. Villunger, Bcl-2-regulated cell death signalling in the prevention of autoimmunity. *Cell Death Dis* **1**, e48 (2010).
84. A. Strasser, M. Pellegrini, T-lymphocyte death during shutdown of an immune response. *Trends Immunol* **25**, 610-615 (2004).
85. S. Gallucci, M. Lolkema, P. Matzinger, Natural adjuvants: endogenous activators of dendritic cells. *Nat Med* **5**, 1249-1255 (1999).
86. A. E. Morelli, A. W. Thomson, Tolerogenic dendritic cells and the quest for transplant tolerance. *Nat Rev Immunol* **7**, 610-621 (2007).
87. M. K. Jenkins, D. M. Pardoll, J. Mizuguchi, H. Quill, R. H. Schwartz, T-cell unresponsiveness in vivo and in vitro: fine specificity of induction and molecular characterization of the unresponsive state. *Immunol Rev* **95**, 113-135 (1987).
88. H. Quill, R. H. Schwartz, Stimulation of normal inducer T cell clones with antigen presented by purified Ia molecules in planar lipid membranes: specific induction of a long-lived state of proliferative nonresponsiveness. *J Immunol* **138**, 3704-3712 (1987).
89. B. Beverly, S. M. Kang, M. J. Lenardo, R. H. Schwartz, Reversal of in vitro T cell clonal anergy by IL-2 stimulation. *Int Immunol* **4**, 661-671 (1992).
90. C. Kurts *et al.*, CD8 T cell ignorance or tolerance to islet antigens depends on antigen dose. *P Natl Acad Sci USA* **96**, 12703-12707 (1999).
91. C. F. Barker, R. E. Billingham, Immunologically Privileged Sites. *Adv Immunol* **25**, 1-54 (1977).
92. S. Hong, L. Van Kaer, Immune privilege: Keeping an eye on natural killer T cells. *J Exp Med* **190**, 1197-1200 (1999).
93. J. Abramson, M. Giraud, C. Benoist, D. Mathis, Aire's partners in the molecular control of immunological tolerance. *Cell* **140**, 123-135 (2010).
94. M. S. Anderson, M. A. Su, AIRE expands: new roles in immune tolerance and beyond. *Nature Reviews Immunology* **16**, 247-258 (2016).
95. F. F. Huo *et al.*, Deficiency of autoimmune regulator impairs the immune tolerance effect of bone marrow-derived dendritic cells in mice. *Autoimmunity* **51**, 10-17 (2018).
96. W. F. Zhu *et al.*, Overexpressing autoimmune regulator regulates the expression of toll-like receptors by interacting with their promoters in RAW264.7 cells. *Cell Immunol* **270**, 156-163 (2011).
97. B. J. Zhao, L. Chang, H. Y. Fu, G. Y. Sun, W. Yang, The Role of Autoimmune Regulator (AIRE) in Peripheral Tolerance. *J Immunol Res*, (2018).
98. D. B. Li *et al.*, Transplantation of Aire-overexpressing bone marrow-derived dendritic cells delays the onset of type 1 diabetes. *Int Immunopharmacol* **49**, 13-20 (2017).
99. L. W. Collison *et al.*, The inhibitory cytokine IL-35 contributes to regulatory T-cell function. *Nature* **450**, 566-U519 (2007).
100. L. S. K. Walker, A. Chodos, M. Eggena, H. Dooms, A. K. Abbas, Antigen-dependent proliferation of CD4(+) CD25(+) regulatory T cells in vivo. *J Exp Med* **198**, 249-258 (2003).
101. S. K. Lathrop, N. A. Santacruz, D. Pham, J. Q. Luo, C. S. Hsieh, Antigen-specific peripheral shaping of the natural regulatory T cell population. *J Exp Med* **205**, 3105-3117 (2008).
102. K. A. Weissler, A. J. Caton, The role of T-cell receptor recognition of peptide:MHC complexes in the formation and activity of Foxp3(+) regulatory T cells. *Immunological Reviews* **259**, 11-22 (2014).

103. D. C. Gondek, L. F. Lu, S. A. Quezada, S. Sakaguchi, R. J. Noelle, Cutting edge: Contact-mediated suppression by CD4(+)-CD25(+) regulatory cells involves a granzyme B-dependent, perforin-independent mechanism. *Journal of Immunology* **174**, 1783-1786 (2005).
104. L. S. K. Walker, D. M. Sansom, The emerging role of CTLA4 as a cell-extrinsic regulator of T cell responses. *Nature Reviews Immunology* **11**, 852-863 (2011).
105. P. Puccetti, U. Grohmann, IDO and regulatory T cells: a role for reverse signalling and non-canonical NF-kappa B activation. *Nature Reviews Immunology* **7**, 817-823 (2007).
106. X. Yu *et al.*, The surface protein TIGIT suppresses T cell activation by promoting the generation of mature immunoregulatory dendritic cells. *Nat Immunol* **10**, 48-57 (2009).
107. J. J. Kobie *et al.*, T regulatory and primed uncommitted CD4 T cells express CD73, which suppresses effector CD4 T cells by converting 5 '-adenosine monophosphate to adenosine. *Journal of Immunology* **177**, 6780-6786 (2006).
108. C. T. Huang *et al.*, Role of LAG-3 in regulatory T cells. *Immunity* **21**, 503-513 (2004).
109. S. Sakaguchi, T. Yamaguchi, T. Nomura, M. Ono, Regulatory T cells and immune tolerance. *Cell* **133**, 775-787 (2008).
110. P. Pandiyan, L. X. Zheng, S. Ishihara, J. Reed, M. J. Lenardo, CD4(+) CD25(+) Foxp3(+) regulatory T cells induce cytokine deprivation -mediated apoptosis of effector CD4(+) T cells. *Nat Immunol* **8**, 1353-1362 (2007).
111. M. Caridade, L. Graca, R. M. Ribeiro, Mechanisms Underlying CD4+ Treg Immune Regulation in the Adult: From Experiments to Models. *Front Immunol* **4**, 378 (2013).
112. K. Hemminki, M. Koskinen, H. Rajaniemi, C. Y. Zhao, DNA adducts, mutations, and cancer 2000. *Regul Toxicol Pharm* **32**, 264-275 (2000).
113. C. Carrillo-Infante, G. Abbadessa, L. Bagella, A. Giordano, Viral infections as a cause of cancer (Review). *Int J Oncol* **30**, 1521-1528 (2007).
114. R. Meinert, U. Kaletsch, P. Kaatsch, J. Schuz, J. Michaelis, Associations between childhood cancer and ionizing radiation: Results of a population-based case-control study in Germany. *Cancer Epidem Biomar* **8**, 793-799 (1999).
115. E. Piemonte *et al.*, Oral cancer associated with chronic mechanical irritation of the oral mucosa. *Med Oral Patol Oral* **23**, E151-E160 (2018).
116. L. B. Alexandrov, M. R. Stratton, Mutational signatures: the patterns of somatic mutations hidden in cancer genomes. *Curr Opin Genet Dev* **24**, 52-60 (2014).
117. D. Hanahan, R. A. Weinberg, Hallmarks of Cancer: The Next Generation. *Cell* **144**, 646-674 (2011).
118. F. R. Balkwill, M. Capasso, T. Hagemann, The tumor microenvironment at a glance. *J Cell Sci* **125**, 5591-5596 (2012).
119. A. F. Chambers, A. C. Groom, I. C. MacDonald, Dissemination and growth of cancer cells in metastatic sites. *Nat Rev Cancer* **2**, 563-572 (2002).
120. D. Mittal, M. M. Gubin, R. D. Schreiber, M. J. Smyth, New insights into cancer immunoediting and its three component phases--elimination, equilibrium and escape. *Curr Opin Immunol* **27**, 16-25 (2014).
121. M. J. Smyth, D. I. Godfrey, J. A. Trapani, A fresh look at tumor immunosurveillance and immunotherapy. *Nat Immunol* **2**, 293 (2001).
122. V. Shankaran *et al.*, IFNgamma and lymphocytes prevent primary tumour development and shape tumour immunogenicity. *Nature* **410**, 1107-1111 (2001).

123. M. J. Smyth, NK cells and NKT cells collaborate in host protection from methylcholanthrene-induced fibrosarcoma. *Int Immunol* **20**, 631 (2008).
124. M. R. Zaidi, G. Merlino, The two faces of interferon-gamma in cancer. *Clin Cancer Res* **17**, 6118-6124 (2011).
125. J. S. Weber, S. A. Rosenberg, Modulation of murine tumor major histocompatibility antigens by cytokines in vivo and in vitro. *Cancer Res* **48**, 5818-5824 (1988).
126. M. B. Fuertes *et al.*, Host type I IFN signals are required for antitumor CD8+ T cell responses through CD8{alpha}+ dendritic cells. *J Exp Med* **208**, 2005-2016 (2011).
127. C. Blank *et al.*, PD-L1/B7H-1 inhibits the effector phase of tumor rejection by T cell receptor (TCR) transgenic CD8+ T cells. *Cancer Res* **64**, 1140-1145 (2004).
128. K. Abiko *et al.*, IFN-gamma from lymphocytes induces PD-L1 expression and promotes progression of ovarian cancer. *Br J Cancer* **112**, 1501-1509 (2015).
129. I. M. Svane *et al.*, Chemically induced sarcomas from nude mice are more immunogenic than similar sarcomas from congenic normal mice. *Eur J Immunol* **26**, 1844-1850 (1996).
130. G. P. Dunn, A. T. Bruce, H. Ikeda, L. J. Old, R. D. Schreiber, Cancer immunoediting: from immunosurveillance to tumor escape. *Nat Immunol* **3**, 991-998 (2002).
131. G. P. Dunn, L. J. Old, R. D. Schreiber, The three Es of cancer immunoediting. *Annu Rev Immunol* **22**, 329-360 (2004).
132. G. P. Dunn, C. M. Koebel, R. D. Schreiber, Interferons, immunity and cancer immunoediting. *Nat Rev Immunol* **6**, 836-848 (2006).
133. R. Kim, M. Emi, K. Tanabe, Cancer immunoediting from immune surveillance to immune escape. *Immunology* **121**, 1-14 (2007).
134. D. Gabrilovich, Mechanisms and functional significance of tumour-induced dendritic-cell defects. *Nat Rev Immunol* **4**, 941-952 (2004).
135. D. Marvel, D. I. Gabrilovich, Myeloid-derived suppressor cells in the tumor microenvironment: expect the unexpected. *J Clin Invest* **125**, 3356-3364 (2015).
136. D. A. A. Vignali, L. W. Collison, C. J. Workman, How regulatory T cells work. *Nature Reviews Immunology* **8**, 523 (2008).
137. Y. Iwai, J. Hamanishi, K. Chamoto, T. Honjo, Cancer immunotherapies targeting the PD-1 signaling pathway. *J Biomed Sci* **24**, 26 (2017).
138. G. T. Motz *et al.*, Tumor endothelium FasL establishes a selective immune barrier promoting tolerance in tumors. *Nat Med* **20**, 607-615 (2014).
139. H. O. Sjogren, I. Hellstrom, S. C. Bansal, G. A. Warner, K. E. Hellstrom, Elution of "blocking factors" from human tumors, capable of abrogating tumor-cell destruction by specifically immune lymphocytes. *Int J Cancer* **9**, 274-283 (1972).
140. R. Khanna, Tumour surveillance: missing peptides and MHC molecules. *Immunol Cell Biol* **76**, 20-26 (1998).
141. W. Y. Lei *et al.*, Total HLA Class I Antigen Loss with the Downregulation of Antigen-Processing Machinery Components in Two Newly Established Sarcomatoid Hepatocellular Carcinoma Cell Lines. *J Immunol Res* **2018**, 8363265 (2018).
142. N. Vigneron, B. J. Van den Eynde, Insights into the processing of MHC class I ligands gained from the study of human tumor epitopes. *Cell Mol Life Sci* **68**, 1503-1520 (2011).
143. P. G. Coulie, B. J. Van den Eynde, P. van der Bruggen, T. Boon, Tumour antigens recognized by T lymphocytes: at the core of cancer immunotherapy. *Nat Rev Cancer* **14**, 135-146 (2014).

144. V. Brichard *et al.*, The Tyrosinase Gene Codes for an Antigen Recognized by Autologous Cytolytic T-Lymphocytes on Hla-A2 Melanomas. *J Exp Med* **178**, 489-495 (1993).
145. N. Vigneron *et al.*, A peptide derived from melanocytic protein gp100 and presented by HLA-B35 is recognized by autologous cytolytic T lymphocytes on melanoma cells. *Tissue Antigens* **65**, 156-162 (2005).
146. P. G. Coulie *et al.*, A New Gene Coding for a Differentiation Antigen Recognized by Autologous Cytolytic T-Lymphocytes on Hla-A2 Melanomas. *J Exp Med* **180**, 35-42 (1994).
147. M. J. W. Visseren *et al.*, Ctl Specific for the Tyrosinase Autoantigen Can Be Induced from Healthy Donor Blood to Lyse Melanoma-Cells. *Journal of Immunology* **154**, 3991-3998 (1995).
148. J. J. Nordlund *et al.*, Vitiligo in Patients with Metastatic Melanoma - a Good Prognostic Sign. *J Am Acad Dermatol* **9**, 689-696 (1983).
149. N. Vigneron, V. Stroobant, B. J. Van den Eynde, P. van der Bruggen, Database of T cell-defined human tumor antigens: the 2013 update. *Cancer Immun* **13**, 15 (2013).
150. H. Ikeda *et al.*, Characterization of an antigen that is recognized on a melanoma showing partial HLA loss by CTL expressing an NK inhibitory receptor. *Immunity* **6**, 199-208 (1997).
151. M. R. Parkhurst *et al.*, T cells targeting carcinoembryonic antigen can mediate regression of metastatic colorectal cancer but induce severe transient colitis. *Mol Ther* **19**, 620-626 (2011).
152. D. Iacovides, S. Michael, C. Achilleos, K. Strati, Shared mechanisms in stemness and carcinogenesis: lessons from oncogenic viruses. *Front Cell Infect Microbiol* **3**, 66 (2013).
153. S. Lucas *et al.*, Identification of a new MAGE gene with tumor-specific expression by representational difference analysis. *Cancer Research* **58**, 743-752 (1998).
154. Y. T. Chen *et al.*, A testicular antigen aberrantly expressed in human cancers detected by autologous antibody screening. *P Natl Acad Sci USA* **94**, 1914-1918 (1997).
155. P. van der Bruggen *et al.*, A gene encoding an antigen recognized by cytolytic T lymphocytes on a human melanoma (Reprinted from Science vol 254, 13 December 1991). *Journal of Immunology* **178**, 2617-2621 (2007).
156. J. Weber *et al.*, Expression of the Mage-1 Tumor-Antigen Is up-Regulated by the Demethylating Agent 5-Aza-2'-Deoxycytidine. *Cancer Research* **54**, 1766-1771 (1994).
157. G. G. Haas, O. J. Dcruz, L. E. Debault, Distribution of Human-Leukocyte Antigen-Abc and Antigen-D/Dr Antigens in the Unfixed Human Testis. *Am J Reprod Immunol* **18**, 47-51 (1988).
158. Y. Guilloux *et al.*, A peptide recognized by human cytolytic T lymphocytes on HLA-A2 melanomas is encoded by an intron sequence of the N-acetylglucosaminyltransferase V gene. *J Exp Med* **183**, 1173-1183 (1996).
159. B. Van den Eynde *et al.*, A new antigen recognized by cytolytic T lymphocytes on a human kidney tumor results from reverse strand transcription. *J Exp Med* **190**, 1793-1799 (1999).
160. S. Ochsenreither *et al.*, Cyclin-A1 represents a new immunogenic targetable antigen expressed in acute myeloid leukemia stem cells with characteristics of a cancer-testis antigen. *Blood* **119**, 5492-5501 (2012).
161. N. Renkvist, C. Castelli, P. F. Robbins, G. Parmiani, A listing of human tumor antigens recognized by T cells. *Cancer Immunol Immun* **50**, 3-15 (2001).

162. R. F. Wang, S. A. Rosenberg, Human tumor antigens for cancer vaccine development. *Immunological Reviews* **170**, 85-100 (1999).
163. M. Linnebacher *et al.*, Frameshift peptide-derived T-cell epitopes: a source of novel tumor-specific antigens. *International Journal of Cancer* **93**, 6-11 (2001).
164. B. Linard *et al.*, A ras-mutated peptide targeted by CTL infiltrating a human melanoma lesion. *J Immunol* **168**, 4802-4808 (2002).
165. D. Ito *et al.*, Immunological characterization of missense mutations occurring within cytotoxic T cell-defined p53 epitopes in HLA-A*0201(+) squamous cell carcinomas of the head and neck. *International Journal of Cancer* **120**, 2618-2624 (2007).
166. D. Gfeller, M. Bassani-Sternberg, J. Schmidt, I. F. Luescher, Current tools for predicting cancer-specific T cell immunity. *Oncoimmunology* **5**, e1177691 (2016).
167. D. Sims, I. Sudbery, N. E. Ilott, A. Heger, C. P. Ponting, Sequencing depth and coverage: key considerations in genomic analyses. *Nat Rev Genet* **15**, 121-132 (2014).
168. P. Leone *et al.*, MHC Class I Antigen Processing and Presenting Machinery: Organization, Function, and Defects in Tumor Cells. *Jnci-J Natl Cancer I* **105**, 1172-1187 (2013).
169. M. Nielsen *et al.*, Reliable prediction of T-cell epitopes using neural networks with novel sequence representations. *Protein Sci* **12**, 1007-1017 (2003).
170. M. Nielsen, O. Lund, NN-align. An artificial neural network-based alignment algorithm for MHC class II peptide binding prediction. *Bmc Bioinformatics* **10**, (2009).
171. R. Vita *et al.*, The Immune Epitope Database (IEDB): 2018 update. *Nucleic Acids Res* **47**, D339-D343 (2019).
172. A. Fridman *et al.*, An efficient T-cell epitope discovery strategy using in silico prediction and the iTopia assay platform. *Oncoimmunology* **1**, 1258-1270 (2012).
173. M. Harndahl *et al.*, Peptide-MHC class I stability is a better predictor than peptide affinity of CTL immunogenicity. *Eur J Immunol* **42**, 1405-1416 (2012).
174. C. R. Berkers *et al.*, Definition of Proteasomal Peptide Splicing Rules for High-Efficiency Spliced Peptide Presentation by MHC Class I Molecules. *Journal of Immunology* **195**, 4085-4095 (2015).
175. A. Dalet *et al.*, An antigenic peptide produced by reverse splicing and double asparagine deamidation. *P Natl Acad Sci USA* **108**, E323-E331 (2011).
176. E. Caron *et al.*, Analysis of Major Histocompatibility Complex (MHC) Immunopeptidomes Using Mass Spectrometry. *Mol Cell Proteomics* **14**, 3105-3117 (2015).
177. J. Cox, M. Mann, MaxQuant enables high peptide identification rates, individualized p.p.b.-range mass accuracies and proteome-wide protein quantification. *Nature Biotechnology* **26**, 1367-1372 (2008).
178. D. P. Granados *et al.*, MHC I-associated peptides preferentially derive from transcripts bearing miRNA response elements. *Blood* **119**, E181-E191 (2012).
179. M. Bassani-Sternberg, S. Pletscher-Frankild, L. J. Jensen, M. Mann, Mass Spectrometry of Human Leukocyte Antigen Class I Peptidomes Reveals Strong Effects of Protein Abundance and Turnover on Antigen Presentation. *Mol Cell Proteomics* **14**, 658-673 (2015).
180. T. N. Schumacher, R. D. Schreiber, Neoantigens in cancer immunotherapy. *Science* **348**, 69-74 (2015).
181. T. C. Wirth, F. Kuhnel, Neoantigen Targeting-Dawn of a New Era in Cancer Immunotherapy? *Front Immunol* **8**, 1848 (2017).

182. T. D. Prickett *et al.*, Durable Complete Response from Metastatic Melanoma after Transfer of Autologous T Cells Recognizing 10 Mutated Tumor Antigens. *Cancer Immunol Res* **4**, 669-678 (2016).
183. V. Lennerz *et al.*, The response of autologous T cells to a human melanoma is dominated by mutated neoantigens. *Proc Natl Acad Sci U S A* **102**, 16013-16018 (2005).
184. J. Zhou, M. E. Dudley, S. A. Rosenberg, P. F. Robbins, Persistence of multiple tumor-specific T-cell clones is associated with complete tumor regression in a melanoma patient receiving adoptive cell transfer therapy. *J Immunother* **28**, 53-62 (2005).
185. E. Stronen *et al.*, Targeting of cancer neoantigens with donor-derived T cell receptor repertoires. *Science*, (2016).
186. N. A. Rizvi *et al.*, Cancer immunology. Mutational landscape determines sensitivity to PD-1 blockade in non-small cell lung cancer. *Science* **348**, 124-128 (2015).
187. N. McGranahan *et al.*, Clonal neoantigens elicit T cell immunoreactivity and sensitivity to immune checkpoint blockade. *Science* **351**, 1463-1469 (2016).
188. M. Schuster, A. Nechansky, R. Kircheis, Cancer immunotherapy. *Biotechnology Journal* **1**, 138-147 (2006).
189. C. L. Ventola, Cancer Immunotherapy, Part 3: Challenges and Future Trends. *P & T : a peer-reviewed journal for formulary management* **42**, 514-521 (2017).
190. A. Karlitepe, O. Ozalp, C. B. Avci, New approaches for cancer immunotherapy. *Tumour Biol* **36**, 4075-4078 (2015).
191. L. M. Weiner, Cancer immunology for the clinician. *Clin Adv Hematol Oncol* **13**, 299-306 (2015).
192. N. S. Lipman, L. R. Jackson, L. J. Trudel, F. Weis-Garcia, Monoclonal versus polyclonal antibodies: distinguishing characteristics, applications, and information resources. *ILAR J* **46**, 258-268 (2005).
193. A. M. Scott, J. D. Wolchok, L. J. Old, Antibody therapy of cancer. *Nat Rev Cancer* **12**, 278-287 (2012).
194. C. S. Karapetis *et al.*, K-ras mutations and benefit from cetuximab in advanced colorectal cancer. *N Engl J Med* **359**, 1757-1765 (2008).
195. C. L. Vogel *et al.*, Efficacy and safety of trastuzumab as a single agent in first-line treatment of HER2-overexpressing metastatic breast cancer. *J Clin Oncol* **20**, 719-726 (2002).
196. D. Przepiorka *et al.*, FDA Approval: Blinatumomab. *Clin Cancer Res* **21**, 4035-4039 (2015).
197. U. Reusch *et al.*, A novel tetravalent bispecific TandAb (CD30/CD16A) efficiently recruits NK cells for the lysis of CD30+ tumor cells. *MAbs* **6**, 728-739 (2014).
198. B. Husain, D. Ellerman, Expanding the Boundaries of Biotherapeutics with Bispecific Antibodies. *BioDrugs* **32**, 441-464 (2018).
199. R. Ahamadi-Fesharaki *et al.*, Single-Chain Variable Fragment-Based Bispecific Antibodies: Hitting Two Targets with One Sophisticated Arrow. *Mol Ther Oncolytics* **14**, 38-56 (2019).
200. F. S. Hodi *et al.*, Improved survival with ipilimumab in patients with metastatic melanoma. *N Engl J Med* **363**, 711-723 (2010).
201. J. D. Wolchok *et al.*, Nivolumab plus ipilimumab in advanced melanoma. *N Engl J Med* **369**, 122-133 (2013).
202. M. Ahmadzadeh *et al.*, Tumor antigen-specific CD8 T cells infiltrating the tumor express high levels of PD-1 and are functionally impaired. *Blood* **114**, 1537-1544 (2009).

203. C. Robert *et al.*, Nivolumab in previously untreated melanoma without BRAF mutation. *N Engl J Med* **372**, 320-330 (2015).
204. N. C. Institute, Clinical Trials Using Pembrolizumab. (2019).
205. J. Schachter *et al.*, Pembrolizumab versus ipilimumab for advanced melanoma: final overall survival results of a multicentre, randomised, open-label phase 3 study (KEYNOTE-006). *Lancet* **390**, 1853-1862 (2017).
206. A. Ribas *et al.*, Pembrolizumab versus investigator-choice chemotherapy for ipilimumab-refractory melanoma (KEYNOTE-002): a randomised, controlled, phase 2 trial. *Lancet Oncol* **16**, 908-918 (2015).
207. M. A. Postow *et al.*, Nivolumab and ipilimumab versus ipilimumab in untreated melanoma. *N Engl J Med* **372**, 2006-2017 (2015).
208. S. S. Joshi, S. B. Maron, D. V. Catenacci, Pembrolizumab for treatment of advanced gastric and gastroesophageal junction adenocarcinoma. *Future Oncol* **14**, 417-430 (2018).
209. O. Bylicki, N. Paleiron, G. Rousseau-Bussac, C. Chouaid, New PDL1 inhibitors for non-small cell lung cancer: focus on pembrolizumab. *Onco Targets Ther* **11**, 4051-4064 (2018).
210. S. Tomassetti, R. Chen, S. Dandapani, The role of pembrolizumab in relapsed/refractory primary mediastinal large B-cell lymphoma. *Ther Adv Hematol* **10**, 2040620719841591 (2019).
211. J. E. Rosenberg *et al.*, Atezolizumab in patients with locally advanced and metastatic urothelial carcinoma who have progressed following treatment with platinum-based chemotherapy: a single-arm, multicentre, phase 2 trial. *Lancet* **387**, 1909-1920 (2016).
212. T. N. P. organisation. (2018).
213. V. Gopalakrishnan *et al.*, Gut microbiome modulates response to anti-PD-1 immunotherapy in melanoma patients. *Science* **359**, 97-103 (2018).
214. L. E. Kandalaft *et al.*, A Phase I vaccine trial using dendritic cells pulsed with autologous oxidized lysate for recurrent ovarian cancer. *J Transl Med* **11**, 149 (2013).
215. U. Sahin *et al.*, Personalized RNA mutanome vaccines mobilize poly-specific therapeutic immunity against cancer. *Nature* **547**, 222-226 (2017).
216. P. A. Ott *et al.*, An immunogenic personal neoantigen vaccine for patients with melanoma. *Nature* **547**, 217-221 (2017).
217. D. Apter *et al.*, Efficacy of human papillomavirus 16 and 18 (HPV-16/18) AS04-adjuvanted vaccine against cervical infection and precancer in young women: final event-driven analysis of the randomized, double-blind PATRICIA trial. *Clin Vaccine Immunol* **22**, 361-373 (2015).
218. R. E. Hollingsworth, K. Jansen, Turning the corner on therapeutic cancer vaccines. *NPJ Vaccines* **4**, 7 (2019).
219. S. R. Pedersen, M. R. Sorensen, S. Buus, J. P. Christensen, A. R. Thomsen, Comparison of vaccine-induced effector CD8 T cell responses directed against self- and non-self-tumor antigens: implications for cancer immunotherapy. *J Immunol* **191**, 3955-3967 (2013).
220. P. Romero *et al.*, The Human Vaccines Project: A roadmap for cancer vaccine development. *Sci Transl Med* **8**, 334ps339 (2016).
221. S. H. T. Jorritsma, E. J. Gowans, B. Grubor-Bauk, D. K. Wijesundara, Delivery methods to increase cellular uptake and immunogenicity of DNA vaccines. *Vaccine* **34**, 5488-5494 (2016).

222. P. W. Kantoff *et al.*, Overall survival analysis of a phase II randomized controlled trial of a Poxviral-based PSA-targeted immunotherapy in metastatic castration-resistant prostate cancer. *J Clin Oncol* **28**, 1099-1105 (2010).
223. C. L. Trimble *et al.*, Safety, efficacy, and immunogenicity of VGX-3100, a therapeutic synthetic DNA vaccine targeting human papillomavirus 16 and 18 E6 and E7 proteins for cervical intraepithelial neoplasia 2/3: a randomised, double-blind, placebo-controlled phase 2b trial. *Lancet* **386**, 2078-2088 (2015).
224. M. Diken, L. M. Kranz, S. Kreiter, U. Sahin, mRNA: A Versatile Molecule for Cancer Vaccines. *Curr Issues Mol Biol* **22**, 113-128 (2017).
225. K. Lundstrom, Replicon RNA Viral Vectors as Vaccines. *Vaccines (Basel)* **4**, (2016).
226. L. M. Kranz *et al.*, Systemic RNA delivery to dendritic cells exploits antiviral defence for cancer immunotherapy. *Nature* **534**, 396-401 (2016).
227. M. A. Neller, J. A. Lopez, C. W. Schmidt, Antigens for cancer immunotherapy. *Semin Immunol* **20**, 286-295 (2008).
228. S. Srivatsan *et al.*, Allogeneic tumor cell vaccines: the promise and limitations in clinical trials. *Hum Vaccin Immunother* **10**, 52-63 (2014).
229. P. W. Kantoff *et al.*, Sipuleucel-T immunotherapy for castration-resistant prostate cancer. *N Engl J Med* **363**, 411-422 (2010).
230. B. Mastelic-Gavillet, K. Balint, C. Boudousquie, P. O. Gannon, L. E. Kandalaft, Personalized Dendritic Cell Vaccines-Recent Breakthroughs and Encouraging Clinical Results. *Front Immunol* **10**, 766 (2019).
231. L. H. Butterfield *et al.*, Adenovirus MART-1-engineered autologous dendritic cell vaccine for metastatic melanoma. *J Immunother* **31**, 294-309 (2008).
232. G. Alatrash, H. Jakher, P. D Stafford, E. Mittendorf, *Cancer immunotherapies, their safety and toxicity*. (2013), vol. 12.
233. J. L. Tanyi *et al.*, Personalized cancer vaccine effectively mobilizes antitumor T cell immunity in ovarian cancer. *Sci Transl Med* **10**, (2018).
234. D. J. Schwartzentruber *et al.*, gp100 peptide vaccine and interleukin-2 in patients with advanced melanoma. *N Engl J Med* **364**, 2119-2127 (2011).
235. E. Quoix *et al.*, TG4010 immunotherapy and first-line chemotherapy for advanced non-small-cell lung cancer (TIME): results from the phase 2b part of a randomised, double-blind, placebo-controlled, phase 2b/3 trial. *Lancet Oncol* **17**, 212-223 (2016).
236. P. Klener, Jr., P. Otahal, L. Lateckova, P. Klener, Immunotherapy Approaches in Cancer Treatment. *Curr Pharm Biotechnol* **16**, 771-781 (2015).
237. S. Turcotte, S. A. Rosenberg, Immunotherapy for metastatic solid cancers. *Adv Surg* **45**, 341-360 (2011).
238. W. Lasek, R. Zagozdzon, M. Jakobisiak, Interleukin 12: still a promising candidate for tumor immunotherapy? *Cancer Immunol Immunother* **63**, 419-435 (2014).
239. M. Sadelain, R. Brentjens, I. Riviere, The basic principles of chimeric antigen receptor design. *Cancer Discov* **3**, 388-398 (2013).
240. M. Kalos *et al.*, T cells with chimeric antigen receptors have potent antitumor effects and can establish memory in patients with advanced leukemia. *Sci Transl Med* **3**, 95ra73 (2011).
241. H. Dai, Y. Wang, X. Lu, W. Han, Chimeric Antigen Receptors Modified T-Cells for Cancer Therapy. *J Natl Cancer Inst* **108**, (2016).
242. J. N. Brudno, J. N. Kochenderfer, Recent advances in CAR T-cell toxicity: Mechanisms, manifestations and management. *Blood Rev* **34**, 45-55 (2019).

243. A. N. Miliotou, L. C. Papadopoulou, CAR T-cell Therapy: A New Era in Cancer Immunotherapy. *Curr Pharm Biotechnol* **19**, 5-18 (2018).
244. S. A. Rosenberg, Cell transfer immunotherapy for metastatic solid cancer--what clinicians need to know. *Nat Rev Clin Oncol* **8**, 577-585 (2011).
245. S. A. Rosenberg, N. P. Restifo, J. C. Yang, R. A. Morgan, M. E. Dudley, Adoptive cell transfer: a clinical path to effective cancer immunotherapy. *Nat Rev Cancer* **8**, 299-308 (2008).
246. M. E. Dudley, S. A. Rosenberg, Adoptive-cell-transfer therapy for the treatment of patients with cancer. *Nat Rev Cancer* **3**, 666-675 (2003).
247. S. A. Rosenberg *et al.*, Durable complete responses in heavily pretreated patients with metastatic melanoma using T-cell transfer immunotherapy. *Clin Cancer Res* **17**, 4550-4557 (2011).
248. S. Kelderman *et al.*, Antigen-specific TIL therapy for melanoma: A flexible platform for personalized cancer immunotherapy. *European journal of immunology*, (2016).
249. C. Linnemann *et al.*, High-throughput epitope discovery reveals frequent recognition of neo-antigens by CD4+ T cells in human melanoma. *Nat Med* **21**, 81-85 (2015).
250. S. Kreiter *et al.*, Mutant MHC class II epitopes drive therapeutic immune responses to cancer. *Nature* **520**, 692-696 (2015).
251. E. Tran *et al.*, Cancer immunotherapy based on mutation-specific CD4+ T cells in a patient with epithelial cancer. *Science* **344**, 641-645 (2014).
252. M. Ruella, M. Kalos, Adoptive immunotherapy for cancer. *Immunol Rev* **257**, 14-38 (2014).
253. C. S. Hinrichs *et al.*, Adoptively transferred effector cells derived from naive rather than central memory CD8+ T cells mediate superior antitumor immunity. *Proc Natl Acad Sci U S A* **106**, 17469-17474 (2009).
254. C. Bonini, A. Mondino, Adoptive T-cell therapy for cancer: The era of engineered T cells. *Eur J Immunol* **45**, 2457-2469 (2015).
255. S. A. Feldman, Y. Assadipour, I. Kriley, S. L. Goff, S. A. Rosenberg, Adoptive Cell Therapy--Tumor-Infiltrating Lymphocytes, T-Cell Receptors, and Chimeric Antigen Receptors. *Semin Oncol* **42**, 626-639 (2015).
256. N. P. Restifo, M. E. Dudley, S. A. Rosenberg, Adoptive immunotherapy for cancer: harnessing the T cell response. *Nat Rev Immunol* **12**, 269-281 (2012).
257. D. Hammerl, D. Rieder, J. W. M. Martens, Z. Trajanoski, R. Debets, Adoptive T Cell Therapy: New Avenues Leading to Safe Targets and Powerful Allies. *Trends Immunol* **39**, 921-936 (2018).
258. R. A. Morgan *et al.*, Cancer regression in patients after transfer of genetically engineered lymphocytes. *Science* **314**, 126-129 (2006).
259. L. Duval *et al.*, Adoptive transfer of allogeneic cytotoxic T lymphocytes equipped with a HLA-A2 restricted MART-1 T-cell receptor: a phase I trial in metastatic melanoma. *Clin Cancer Res* **12**, 1229-1236 (2006).
260. L. A. Johnson *et al.*, Gene therapy with human and mouse T-cell receptors mediates cancer regression and targets normal tissues expressing cognate antigen. *Blood* **114**, 535-546 (2009).
261. C. Fournier *et al.*, Trial Watch: Adoptively transferred cells for anticancer immunotherapy. *Oncoimmunology* **6**, e1363139 (2017).
262. Y. Ping, C. Liu, Y. Zhang, T-cell receptor-engineered T cells for cancer treatment: current status and future directions. *Protein Cell* **9**, 254-266 (2018).

263. P. F. Robbins *et al.*, A pilot trial using lymphocytes genetically engineered with an NY-ESO-1-reactive T-cell receptor: long-term follow-up and correlates with response. *Clin Cancer Res* **21**, 1019-1027 (2015).
264. R. Yossef *et al.*, Enhanced detection of neoantigen-reactive T cells targeting unique and shared oncogenes for personalized cancer immunotherapy. *Jci Insight* **3**, (2018).
265. E. Stronen *et al.*, Targeting of cancer neoantigens with donor-derived T cell receptor repertoires. *Science* **352**, 1337-1341 (2016).
266. P. Malekzadeh *et al.*, Neoantigen screening identifies broad TP53 mutant immunogenicity in patients with epithelial cancers. *J Clin Invest* **129**, 1109-1114 (2019).
267. P. A. Beavis *et al.*, Reprogramming the tumor microenvironment to enhance adoptive cellular therapy. *Semin Immunol* **28**, 64-72 (2016).
268. L. Cherkassky *et al.*, Human CAR T cells with cell-intrinsic PD-1 checkpoint blockade resist tumor-mediated inhibition. *J Clin Invest* **126**, 3130-3144 (2016).
269. E. K. Moon *et al.*, Blockade of Programmed Death 1 Augments the Ability of Human T Cells Engineered to Target NY-ESO-1 to Control Tumor Growth after Adoptive Transfer. *Clin Cancer Res* **22**, 436-447 (2016).
270. D. A. Mahvi *et al.*, Ctla-4 blockade plus adoptive T-cell transfer promotes optimal melanoma immunity in mice. *J Immunother* **38**, 54-61 (2015).
271. A. Sukari, N. Abdallah, M. Nagasaka, Unleash the power of the mighty T cells-basis of adoptive cellular therapy. *Crit Rev Oncol Hematol* **136**, 1-12 (2019).
272. R. M. Teague *et al.*, Interleukin-15 rescues tolerant CD8(+) T cells for use in adoptive immunotherapy of established tumors. *Nature Medicine* **12**, 335-341 (2006).
273. Z. Q. Zhu *et al.*, High-Avidity T Cells Are Preferentially Tolerized in the Tumor Microenvironment (Retraction of vol 73, pg 595, 2013). *Cancer Research* **76**, 2491-2491 (2016).
274. C. H. June, R. S. O'Connor, O. U. Kawalekar, S. Ghassemi, M. C. Milone, CAR T cell immunotherapy for human cancer. *Science* **359**, 1361-1365 (2018).
275. B. Wolf *et al.*, Safety and Tolerability of Adoptive Cell Therapy in Cancer. *Drug Safety* **42**, 315-334 (2019).
276. M. Casucci, R. E. Hawkins, G. Dotti, A. Bondanza, Overcoming the toxicity hurdles of genetically targeted T cells. *Cancer Immunol Immun* **64**, 123-130 (2015).
277. H. E. Heslop *et al.*, Long-term outcome of EBV-specific T-cell infusions to prevent or treat EBV-related lymphoproliferative disease in transplant recipients. *Blood* **115**, 925-935 (2010).
278. J. Scholler *et al.*, Decade-long safety and function of retroviral-modified chimeric antigen receptor T cells. *Sci Transl Med* **4**, 132ra153 (2012).
279. C. Phetsouphanh, J. J. Zaunders, A. D. Kelleher, Detecting Antigen-Specific T Cell Responses: From Bulk Populations to Single Cells. *Int J Mol Sci* **16**, 18878-18893 (2015).
280. L. S. De Clerck, C. H. Bridts, A. M. Mertens, M. M. Moens, W. J. Stevens, Use of fluorescent dyes in the determination of adherence of human leucocytes to endothelial cells and the effect of fluorochromes on cellular function. *J Immunol Methods* **172**, 115-124 (1994).
281. A. C. Karlsson *et al.*, Comparison of the ELISPOT and cytokine flow cytometry assays for the enumeration of antigen-specific T cells. *Journal of Immunological Methods* **283**, 141-153 (2003).

282. H. A. Pass, S. L. Schwarz, J. R. Wunderlich, S. A. Rosenberg, Immunization of patients with melanoma peptide vaccines: immunologic assessment using the ELISPOT assay. *Cancer J Sci Am* **4**, 316-323 (1998).
283. A. Schmittel *et al.*, Application of the IFN-gamma ELISPOT assay to quantify T cell responses against proteins. *J Immunol Methods* **247**, 17-24 (2001).
284. J. D. Altman *et al.*, Phenotypic analysis of antigen-specific T lymphocytes. *Science* **274**, 94-96 (1996).
285. P. Guillaume, D. Dojcinovic, I. F. Luescher, Soluble MHC-peptide complexes: tools for the monitoring of T cell responses in clinical trials and basic research. *Cancer Immun* **9**, 7 (2009).
286. M. Magnin, P. Guillaume, G. Coukos, A. Harari, J. Schmidt, in *Methods in Enzymology*. (Academic Press, 2019).
287. M. Plebanski, M. Katsara, K. C. Sheng, S. D. Xiang, V. Apostolopoulos, Methods to measure T-cell responses. *Expert Rev Vaccines* **9**, 595-600 (2010).
288. S. Kuerten *et al.*, Dissociated production of perforin, granzyme B, and IFN-gamma by HIV-specific CD8(+) cells in HIV infection. *AIDS Res Hum Retroviruses* **24**, 62-71 (2008).
289. S. Vigano *et al.*, Functional avidity: a measure to predict the efficacy of effector T cells? *Clin Dev Immunol* **2012**, 153863 (2012).
290. A. Harari *et al.*, An HIV-1 clade C DNA prime, NYVAC boost vaccine regimen induces reliable, polyfunctional, and long-lasting T cell responses. *J Exp Med* **205**, 63-77 (2008).
291. S. Zhong *et al.*, T-cell receptor affinity and avidity defines antitumor response and autoimmunity in T-cell immunotherapy. *P Natl Acad Sci USA* **110**, 6973-6978 (2013).
292. M. E. Dudley, M. I. Nishimura, A. K. C. Holt, S. A. Rosenberg, Antitumor immunization with a minimal peptide epitope (G9-209-2M) leads to a functionally heterogeneous CTL response. *Journal of Immunotherapy* **22**, 288-298 (1999).
293. M. Hebeisen *et al.*, Identifying Individual T Cell Receptors of Optimal Avidity for Tumor Antigens. *Front Immunol* **6**, 582 (2015).
294. M. A. AlexanderMiller, G. R. Leggatt, J. A. Berzofsky, Selective expansion of high- or low-avidity cytotoxic T lymphocytes and efficacy for adoptive immunotherapy. *P Natl Acad Sci USA* **93**, 4102-4107 (1996).
295. A. J. Ozga *et al.*, pMHC affinity controls duration of CD8+ T cell-DC interactions and imprints timing of effector differentiation versus expansion. *J Exp Med* **213**, 2811-2829 (2016).
296. D. Presotto *et al.*, Fine-Tuning of Optimal TCR Signaling in Tumor-Redirected CD8 T Cells by Distinct TCR Affinity-Mediated Mechanisms. *Front Immunol* **8**, 1564 (2017).
297. M. Irving *et al.*, Interplay between T cell receptor binding kinetics and the level of cognate peptide presented by major histocompatibility complexes governs CD8+ T cell responsiveness. *J Biol Chem* **287**, 23068-23078 (2012).
298. E. Palmer, D. Naeher, Affinity threshold for thymic selection through a T-cell receptor-co-receptor zipper. *Nature Reviews Immunology* **9**, 206-212 (2009).
299. D. J. Schwartzentruber *et al.*, In-Vitro Predictors of Therapeutic Response in Melanoma Patients Receiving Tumor-Infiltrating Lymphocytes and Interleukin-2. *Journal of Clinical Oncology* **12**, 1475-1483 (1994).
300. D. Zehn, C. King, M. J. Bevan, E. Palmer, TCR signaling requirements for activating T cells and for generating memory. *Cell Mol Life Sci* **69**, 1565-1575 (2012).
301. M. P. Tan *et al.*, T cell receptor binding affinity governs the functional profile of cancer-specific CD8+ T cells. *Clin Exp Immunol* **180**, 255-270 (2015).

302. M. Allard *et al.*, TCR-ligand dissociation rate is a robust and stable biomarker of CD8+ T cell potency. *JCI Insight* **2**, (2017).
303. M. Nauerth *et al.*, TCR-ligand koff rate correlates with the protective capacity of antigen-specific CD8+ T cells for adoptive transfer. *Sci Transl Med* **5**, 192ra187 (2013).
304. J. Galvez, J. J. Galvez, P. Garcia-Penarrubia, Is TCR/pMHC Affinity a Good Estimate of the T-cell Response? An Answer Based on Predictions From 12 Phenotypic Models. *Front Immunol* **10**, (2019).
305. R. Bos, K. L. Marquardt, J. Cheung, L. A. Sherman, Functional differences between low- and high-affinity CD8(+) T cells in the tumor environment. *Oncoimmunology* **1**, 1239-1247 (2012).
306. O. Y. Borbulevych, S. M. Santhanagopolan, M. Hossain, B. M. Baker, TCRs Used in Cancer Gene Therapy Cross-React with MART-1/Melan-A Tumor Antigens via Distinct Mechanisms. *Journal of Immunology* **187**, 2453-2463 (2011).
307. C. N. Janicki, S. R. Jenkinson, N. A. Williams, D. J. Morgan, Loss of CTL function among high-avidity tumor-specific CD8(+) T cells following tumor infiltration. *Cancer Research* **68**, 2993-3000 (2008).
308. G. Y. Liu *et al.*, Low avidity recognition of self-antigen by T cells permits escape from central tolerance. *Immunity* **3**, 407-415 (1995).
309. N. Woller *et al.*, Viral Infection of Tumors Overcomes Resistance to PD-1-immunotherapy by Broadening Neoantigenome-directed T-cell Responses. *Molecular Therapy* **23**, 1630-1640 (2015).
310. D. A. Schmid *et al.*, Evidence for a TCR affinity threshold delimiting maximal CD8 T cell function. *J Immunol* **184**, 4936-4946 (2010).
311. E. Corse, R. A. Gottschalk, M. Krogsgaard, J. P. Allison, Attenuated T Cell Responses to a High-Potency Ligand In Vivo. *Plos Biol* **8**, (2010).
312. S. Tian, R. Maile, E. J. Collins, J. A. Frelinger, CD8(+) T cell activation is governed by TCR-Peptide/MHC affinity, not dissociation rate. *Journal of Immunology* **179**, 2952-2960 (2007).
313. N. van Rooij *et al.*, Tumor exome analysis reveals neoantigen-specific T-cell reactivity in an ipilimumab-responsive melanoma. *J Clin Oncol* **31**, e439-442 (2013).
314. C. Iseli, G. Ambrosini, P. Bucher, C. V. Jongeneel, Indexing Strategies for Rapid Searches of Short Words in Genome Sequences. *Plos One* **2**, (2007).
315. A. Leimgruber *et al.*, TCRep 3D: An Automated In Silico Approach to Study the Structural Properties of TCR Repertoires. *Plos One* **6**, (2011).
316. W. Giudicelli, D. Chaume, M. P. Lefranc, IMGT/GENE-DB: a comprehensive database for human and mouse immunoglobulin and T cell receptor genes. *Nucleic Acids Res* **33**, D256-D261 (2005).
317. U. Pieper *et al.*, MODBASE: a database of annotated comparative protein structure models and associated resources. *Nucleic Acids Res* **34**, D291-D295 (2006).
318. P. W. Rose *et al.*, The RCSB Protein Data Bank: redesigned web site and web services. *Nucleic Acids Res* **39**, D392-D401 (2011).
319. R. C. Edgar, MUSCLE: multiple sequence alignment with high accuracy and high throughput. *Nucleic Acids Res* **32**, 1792-1797 (2004).
320. V. Zoete, O. Michielin, Comparison between computational alanine scanning and per-residue binding free energy decomposition for protein-protein association using MM-GBSA: Application to the TCR-p-MHC complex. *Proteins* **67**, 1026-1047 (2007).

321. V. Zoete, M. Irving, M. Ferber, M. A. Cuendet, O. Michielin, Structure-based, rational design of T cell receptors. *Front Immunol* **4**, (2013).
322. E. F. Pettersen *et al.*, UCSF chimera - A visualization system for exploratory research and analysis. *J Comput Chem* **25**, 1605-1612 (2004).
323. A. M. Bjerregaard *et al.*, An Analysis of Natural T Cell Responses to Predicted Tumor Neoepitopes. *Front Immunol* **8**, (2017).
324. S. Bobisse *et al.*, Sensitive and frequent identification of high avidity neo-epitope specific CD8 (+) T cells in immunotherapy-naive ovarian cancer. *Nat Commun* **9**, 1092 (2018).
325. J. J. A. Calis *et al.*, Properties of MHC Class I Presented Peptides That Enhance Immunogenicity. *Plos Comput Biol* **9**, (2013).
326. D. Weiskopf *et al.*, Insights into HLA-Restricted T Cell Responses in a Novel Mouse Model of Dengue Virus Infection Point toward New Implications for Vaccine Design. *Journal of Immunology* **187**, 4268-4279 (2011).
327. D. Gfeller, M. Bassani-Sternberg, Predicting Antigen Presentation - What Could We Learn From a Million Peptides? *Front Immunol* **9**, (2018).
328. V. Jurtz *et al.*, NetMHCpan-4.0: Improved Peptide-MHC Class I Interaction Predictions Integrating Eluted Ligand and Peptide Binding Affinity Data. *J Immunol* **199**, 3360-3368 (2017).
329. M. Nielsen, C. Lundegaard, O. Lund, C. Kesmir, The role of the proteasome in generating cytotoxic T-cell epitopes: insights obtained from improved predictions of proteasomal cleavage. *Immunogenetics* **57**, 33-41 (2005).
330. J. Schmidt *et al.*, Reversible major histocompatibility complex I-peptide multimers containing Ni(2+)-nitrilotriacetic acid peptides and histidine tags improve analysis and sorting of CD8(+) T cells. *J Biol Chem* **286**, 41723-41735 (2011).
331. K. W. Jorgensen, M. Rasmussen, S. Buus, M. Nielsen, NetMHCstab - predicting stability of peptide-MHC-I complexes; impacts for cytotoxic T lymphocyte epitope discovery. *Immunology* **141**, 18-26 (2014).
332. M. Rasmussen *et al.*, Pan-Specific Prediction of Peptide-MHC Class I Complex Stability, a Correlate of T Cell Immunogenicity. *Journal of Immunology* **197**, 1517-1524 (2016).
333. E. Lanitis, D. Dangaj, M. Irving, G. Coukos, Mechanisms regulating T-cell infiltration and activity in solid tumors. *Annals of Oncology* **28**, 18-32 (2017).
334. V. Zoete, M. B. Irving, O. Michielin, MM-GBSA binding free energy decomposition and T cell receptor engineering. *J Mol Recognit* **23**, 142-152 (2010).
335. D. A. Price *et al.*, Avidity for antigen shapes clonal dominance in CD8+ T cell populations specific for persistent DNA viruses. *J Exp Med* **202**, 1349-1361 (2005).
336. S. M. Peng *et al.*, Sensitive Detection and Analysis of Neoantigen-Specific T Cell Populations from Tumors and Blood. *Cell Rep* **28**, 2728-+ (2019).
337. Y. C. Lu, P. F. Robbins, Cancer immunotherapy targeting neoantigens. *Semin Immunol* **28**, 22-27 (2016).
338. J. Schmidt *et al.*, In silico and cell-based analyses reveal strong divergence between prediction and observation of T cell recognized tumor antigen T cell epitopes. *J Biol Chem*, (2017).
339. A. K. Bentzen *et al.*, T cell receptor fingerprinting enables in-depth characterization of the interactions governing recognition of peptide-MHC complexes. *Nat Biotechnol*, (2018).

340. A. Schietinger, P. D. Greenberg, Tolerance and exhaustion: defining mechanisms of T cell dysfunction. *Trends Immunol* **35**, 51-60 (2014).
341. C. M. Fu, A. M. Jiang, Dendritic Cells and CD8 T Cell Immunity in Tumor Microenvironment. *Front Immunol* **9**, (2018).
342. M. Hebeisen *et al.*, Identification of Rare High-Avidity, Tumor-Reactive CD8+ T Cells by Monomeric TCR-Ligand Off-Rates Measurements on Living Cells. *Cancer Res* **75**, 1983-1991 (2015).
343. P. O. Gannon *et al.*, Quantitative TCR:pMHC Dissociation Rate Assessment by NTAmers Reveals Antimelanoma T Cell Repertoires Enriched for High Functional Competence. *J Immunol* **195**, 356-366 (2015).
344. A. P. Conley *et al.*, MAGE-A3 Is a Clinically Relevant Target in Undifferentiated Pleomorphic Sarcoma/Myxofibrosarcoma. *Cancers* **11**, (2019).
345. E. V. Rothenberg, J. L. A. Zhang, T-Cell Identity and Epigenetic Memory. *Curr Top Microbiol* **356**, 117-143 (2012).
346. A. Schietinger, J. J. Delrow, R. S. Basom, J. N. Blattman, P. D. Greenberg, Rescued Tolerant CD8 T Cells Are Preprogrammed to Reestablish the Tolerant State. *Science* **335**, 723-727 (2012).
347. P. Newton, G. O'Boyle, Y. Jenkins, S. Ali, J. A. Kirby, T cell extravasation: Demonstration of synergy between activation of CXCR3 and the T cell receptor. *Mol Immunol* **47**, 485-492 (2009).
348. M. Mokrani, J. Klibi, D. Bluteau, G. Bismuth, F. Mami-Chouaib, Smad and NFAT Pathways Cooperate To Induce CD103 Expression in Human CD8 T Lymphocytes. *Journal of Immunology* **192**, 2471-2479 (2014).
349. C. Y. Slaney, M. H. Kershaw, P. K. Darcy, Trafficking of T Cells into Tumors. *Cancer Research* **74**, 7168-7174 (2014).
350. N. Mukaida, S. Sasaki, T. Baba, Chemokines in Cancer Development and Progression and Their Potential as Targeting Molecules for Cancer Treatment. *Mediat Inflamm*, (2014).
351. T. W. Mckeithan, Kinetic Proofreading in T-Cell Receptor Signal-Transduction. *P Natl Acad Sci USA* **92**, 5042-5046 (1995).
352. S. Valitutti, S. Muller, M. Cella, E. Padovan, A. Lanzavecchia, Serial Triggering of Many T-Cell Receptors by a Few Peptide-Mhc Complexes. *Nature* **375**, 148-151 (1995).
353. A. M. Kalergis *et al.*, Efficient T cell activation requires an optimal dwell-time of interaction between the TCR and the pMHC complex. *Nat Immunol* **2**, 229-234 (2001).
354. O. Dushek, P. A. van der Merwe, An induced rebinding model of antigen discrimination. *Trends Immunol* **35**, 153-158 (2014).
355. Y. Chen, L. Ju, M. Rushdi, C. Ge, C. Zhu, Receptor-mediated cell mechanosensing. *Mol Biol Cell* **28**, 3134-3155 (2017).
356. M. Saitakis *et al.*, Different TCR-induced T lymphocyte responses are potentiated by stiffness with variable sensitivity. *Elife* **6**, (2017).
357. Y. N. Feng, E. L. Reinherz, M. J. Lang, alpha beta T Cell Receptor Mechanosensing Forces out Serial Engagement. *Trends Immunol* **39**, 596-609 (2018).
358. K. H. Hu, M. J. Butte, T cell activation requires force generation. *J Cell Biol* **213**, 535-542 (2016).
359. B. Liu *et al.*, 2D TCR-pMHC-CD8 kinetics determines T-cell responses in a self-antigen-specific TCR system. *Eur J Immunol* **44**, 239-250 (2014).

360. L. Ju, Y. Chen, M. N. Rushdi, W. Chen, C. Zhu, Two-Dimensional Analysis of Cross-Junctional Molecular Interaction by Force Probes. *Methods Mol Biol* **1584**, 231-258 (2017).
361. B. Liu, W. Chen, B. D. Evavold, C. Zhu, Accumulation of dynamic catch bonds between TCR and agonist peptide-MHC triggers T cell signaling. *Cell* **157**, 357-368 (2014).
362. L. V. Sibener *et al.*, Isolation of a Structural Mechanism for Uncoupling T Cell Receptor Signaling from Peptide-MHC Binding. *Cell* **174**, 672-+ (2018).
363. G. Dolton *et al.*, Optimized Peptide-MHC Multimer Protocols for Detection and Isolation of Autoimmune T-Cells. *Front Immunol* **9**, (2018).
364. P. Guillaume, P. Baumgaertner, G. S. Angelov, D. Speiser, I. F. Luescher, Fluorescence-activated cell sorting and cloning of bona fide CD8+ CTL with reversible MHC-peptide and antibody Fab' conjugates. *J Immunol* **177**, 3903-3912 (2006).
365. J. Neudorfer *et al.*, Reversible HLA multimers (Streptamers) for the isolation of human cytotoxic T lymphocytes functionally active against tumor- and virus-derived antigens. *Journal of Immunological Methods* **320**, 119-131 (2007).
366. H. P. Arrol, L. D. Church, P. A. Bacon, S. P. Young, Intracellular calcium signalling patterns reflect the differentiation status of human T cells. *Clin Exp Immunol* **153**, 86-95 (2008).
367. P. Zhao *et al.*, Clickable Multifunctional Dumbbell Particles for in Situ Multiplex Single-Cell Cytokine Detection. *ACS Appl Mater Interfaces* **9**, 32482-32488 (2017).
368. X. An *et al.*, Single-cell profiling of dynamic cytokine secretion and the phenotype of immune cells. *PLoS One* **12**, e0181904 (2017).
369. R. Uzana *et al.*, Trogocytosis Is a Gateway to Characterize Functional Diversity in Melanoma-Specific CD8(+) T Cell Clones. *Journal of Immunology* **188**, 632-640 (2012).

High-throughput identification of human antigen-specific CD8$^+$ and CD4$^+$ T cells using soluble pMHC multimers

Morgane Magnin[a,b], Philippe Guillaume[a,b], George Coukos[a,b,*], Alexandre Harari[a,b], Julien Schmidt[a,b]

[a]Ludwig Institute for Cancer Research, University of Lausanne, Lausanne, Switzerland
[b]Department of Oncology, University Hospital of Lausanne, Lausanne, Switzerland
*Corresponding author: e-mail address: george.coukos@chuv.ch

Contents

1. Introduction 2
2. Monitoring of antigen-specific CD8$^+$ and CD4$^+$ T cells with soluble pMHC I & II 3
   2.1 Improved pMHC monomer quality 3
   2.2 Choosing the best multimeric scaffold 4
   2.3 An improved staining protocol 6
3. Staining of antigen-specific CD8$^+$ and CD4$^+$ T cells: Materials and methods 8
   3.1 Materials 8
4. High dimensional T-cell staining 11
   4.1 High-throughput pMHC monomer synthesis 11
   4.2 Fluorochrome-based combinatorial staining 12
   4.3 Heavy-metal ions-based combinatorial staining 13
   4.4 DNA-barcoded pMHC multimers 13
5. Reversible pMHC multimer for comprehensive analysis of antigen-specific T cells 15
   5.1 Isolation of "untouched" antigen-specific CD8 T cells 16
   5.2 Measurement of pMHC-TCR monomeric dissociation rates 16
6. Conclusion 17
References 18

Abstract

Peptide major histocompatibility complex (pMHC) multimers have been used since decades to identify, isolate and analyze antigen-specific T cells by flow (and more recently mass) cytometry. Yet well established as a standard technology, improvements are still required to face the growing needs of personalized immune monitoring. Here we review the latest developments about (i) the quality of pMHC class I and II

Methods in Enzymology
ISSN 0076-6879
https://doi.org/10.1016/bs.mie.2019.05.019

monomers, (ii) the importance of the multimeric scaffold, (iii) the staining conditions and (iv) the high-throughput synthesis of pMHC monomers. Finally, innovative multiplexed, combinatorial strategies for parallel detection of antigen-specific T cells in a single sample are discussed.

1. Introduction

$CD8^+$ and $CD4^+$ T lymphocytes are main actors of adaptive cellular immunity and play a central role in protecting individuals against pathogen infections and neoplastic transformations (Gorska & Alam, 2003). While $CD8^+$ T cells mainly differentiate in cytotoxic T lymphocytes with killing capacities toward target cells displaying pMHC class I complexes, $CD4^+$ T cells differentiate in T helper cells (e.g., Th1, Th2) or regulatory T cells (Treg) and recognize cell surface pMHC class II complexes (Fooksman et al., 2010).

Detection, isolation and analysis of antigen-specific $CD8^+$ and $CD4^+$ T cells is of major importance to monitor disease progression as well as for the development of vaccines and personalized immunotherapies (Bobisse et al., 2018; Tanyi et al., 2018).

While initially determined by limiting dilution and assessment of frequencies of T cells mediating functional responses, antigen-specific $CD8^+$ and $CD4^+$ T cells are now routinely determined by using soluble pMHC multimers, labeled either with fluorescent dyes or isotopes, by flow and mass cytometry, respectively (Brett, Kingston, & Colston, 1987; Schmidt, Dojcinovic, Guillaume, & Luescher, 2013; Sharrock, Kaminski, & Man, 1990). These methods have the advantage of being highly sensitive and not dependent on any functional capacity of T cells. However, besides requiring a detailed knowledge of HLA typing and antigen restriction, pMHC multimers can also failed to detect cells bearing very low-affinity TCRs. In 1992, Garboczi et al. published the first refolded peptide-HLA-A0201 complex (Garboczi, Hung, & Wiley, 1992) and in 1996, Altman and colleagues reported the first soluble pMHC tetramer for direct identification and enumeration of antigen-specific $CD8^+$ T cells (Altman et al., 1996).

Peptide-MHC class I monomers can be obtained by a simple, cost efficient procedure that consists of refolding denatured heavy and light (beta-2-microglobulin, β2m) chains in the presence of an 8–11 residue long, synthetic peptide of interest. On the other hand, pMHC class II monomers

are more difficult to obtain in reasonable yields by refolding or by mammalian expressions systems. Indeed, folding conditions of pMHC class II have to be optimized individually for each allotype (Vollers & Stern, 2008). The most commonly adopted strategy is the expression of "empty" MHC class II molecules expressed by insect cells (such as Drosophila S2 or SF9 cells) and further loaded with synthetic peptides of 10–16 residues (Frayser, Sato, Xu, & Stern, 1999; Fremont, Hendrickson, Marrack, & Kappler, 1996). This method relies on the lack of antigen processing and loading machinery in insect cells and the recovery of stable pure MHC class II proteins without any peptide.

Due to the low affinity of pMHC class I/II monomers for T-cell receptors (TCR), multimeric structures are required to enable efficient staining of antigen-specific T-cell populations. Enzymatic biotinylation of pMHC monomers allows multimerization thanks to fluorescent streptavidin conjugates, increasing their overall avidity for TCRs. Performances of pMHC class II multimers are worse than their class I counterparts and can be accounted for (i) the lower affinity TCR expressed by $CD4^+$ T cells, (ii) the lack of contribution of the CD4 coreceptor in stabilizing the binding to pMHC class II, (iii) the high conformational diversity of pMHC complexes and (iv) the poor quality of pMHC class II reagents. Over the last decade, many advances have been made to improve the quality of pMHC class I/II multimers, the staining protocols and the developments of high dimensional detection strategies.

2. Monitoring of antigen-specific $CD8^+$ and $CD4^+$ T cells with soluble pMHC I & II

Optimal detection of antigen-specific $CD8^+$ and $CD4^+$ T cell is mainly driven by the binding strength between multimeric pMHC and their cognate TCRs (Rius et al., 2018). Several parameters can be optimized to increase the avidity of pMHC multimers.

2.1 Improved pMHC monomer quality

Following the refolding of peptides with heavy and light chains, pMHC class I monomers are purified by size exclusion chromatography, eliminating unfolded proteins. Production yields as well as stability of pMHC class I complexes are correlated with the peptide binding affinity for a given HLA molecule. While some pMHC class I complexes have half-lives of several hours at 37 °C, others are highly unstable (Schmidt et al., 2017).

Great care should be taken when using low stability pMHC multimers. Lowering working temperature as well as addition of free β2m and synthetic peptides can help preserving pMHC integrity (Wooldridge et al., 2009).

Peptide binding affinity to MHC class II also correlates with peptide loading efficiency of "empty" MHC class II molecules (Frayser et al., 1999). The fraction of peptide loaded complexes cannot be separated from "empty" monomers by means of size exclusion chromatography. Resulting pMHC class II multimers contain a fraction of active monomers, thus precluding efficient staining of low affinity antigen-specific $CD4^+$ T cells (Ayyoub, Pignon, et al., 2010; Gebe et al., 2003). Purification of peptide-containing complexes can be achieved by careful ion exchange chromatography but remains very challenging. Alternatively, Luescher et al. have reported the use of molecularly defined pMHC class II multimers restoring staining of NY-ESO-I-specific $CD4^+$ T cells that were not detected with conventional multimers (Ayyoub, Dojcinovic, et al., 2010). Molecularly defined pMHC class II monomers are produced with long peptides carrying a specific tag (i.e., Histag) enabling the tag-purification of peptide-containing monomers and subsequent assembly of pMHC multimers composed of fully loaded monomers. As it has been reported that flanking residues can lead to unwanted side effects (Carson, Vignali, Woodland, & Vignali, 1997; Sant'Angelo, Robinson, Janeway, & Denzin, 2002), introduction of a photocleavable residue allows efficient tag removal. If the gain in staining efficiency remains marginal for high avidity $CD4^+$ T cells, it becomes dramatic for low affinity ones, typically tumor-specific T cells (Carson et al., 1997; Sant'Angelo et al., 2002).

Another hurdle in the preparation of pMHC class I/II monomers is the biotinylation step needed for further multimerization using streptavidin-dyes conjugates. Routinely performed using the BirA enzyme, with overnight exposure at room temperature in the presence of biotin and ATP, this step can lead to degradation of unstable complexes. To circumvent this, it is possible to perform biotinylation directly in bacteria by co-transformation with the BirA enzyme and a given HLA leading directly to biotinylated inclusion bodies readily usable for refolding (Leisner et al., 2008). Working with highly pure, molecularly defined pMHC class I/II monomers is a prerequisite for further building of improved quality multimers.

2.2 Choosing the best multimeric scaffold

The dissociation constant (K_D) of pMHC-TCR is in the range of 1–1000 μM (Boniface et al., 1998), precluding staining of T cells with

soluble monomeric complexes. Increasing pMHC valency by multimerization with streptavidin (SA) conjugates leads to increased pMHC-TCR avidity and allows the effective detection of antigen-specific T cells by flow cytometry (Altman et al., 1996). However, it has been shown that, in addition to the number of pMHC monomers displayed by multimeric scaffolds, their spatial arrangement is also an important parameter.

Elegant studies using synthetic linkers of different length and flexibility shown that maximal binding avidity is obtained with very short linkers (<20 Å) and gradually decreases with the spacer length. Similarly, binding avidity is also increasing with valency, octamers being better binders than tetramers and than dimers (Angelov et al., 2006; Cebecauer, Guillaume, Mark, et al., 2005).

So-called pMHC tetramers are usually made by reacting biotinylated pMHC class I/II monomers with heterogenous streptavidin-PE (or APC) and should therefore be considered as multimers. A PE (or APC)-labeled multimer carries in average 8–12 pMHC monomers making allowing highly efficient binding to antigen-specific T cells. Conversely, true tetrameric pMHC complexes can be obtained using a tetra-grade PE (with equimolar ratio PE/SA) (Hugues, Malherbe, Filippi, & Glaichenhaus, 2002). The latter exhibit much lower binding avidities compared to conventional multimers. This is also true when using SA labeled with small molecular weight fluorochromes (i.e., FITC, Alexa Fluor or Cyanine derivatives). The choice of the multimeric scaffold is therefore important to avoid inefficient staining of low affinity T cells.

Conventional pMHC multimers made of SA-PE (or -APC) are available from different companies or academic core facilities but other multimeric scaffolds have emerged and are extensively used nowadays (Fig. 1). Pro-Immune is commercializing MHC class I and II "Pentamers" made of a coiled coil protein carrying five PE and five pMHC monomers (Leisner et al., 2008). "Dextramers" are available from Immudex and are built on a dextran polymer carrying multiple fluorochromes and up to 12 pMHC monomers (Batard et al., 2006). More recently, "Dodecamers" were reported (Huang et al., 2016). They are molecularly well defined and display 12 pMHC monomers but unfortunately are not commercially available. "Dodecamers," "Dextramers" and conventional multimers confer the highest and comparable staining efficiencies, with a slight advantage for "dodecamers." They outperform "Pentamers" and true tetramers, which is accounted for lower valency of these latter (Dolton et al., 2014; Schmidt et al., 2011).

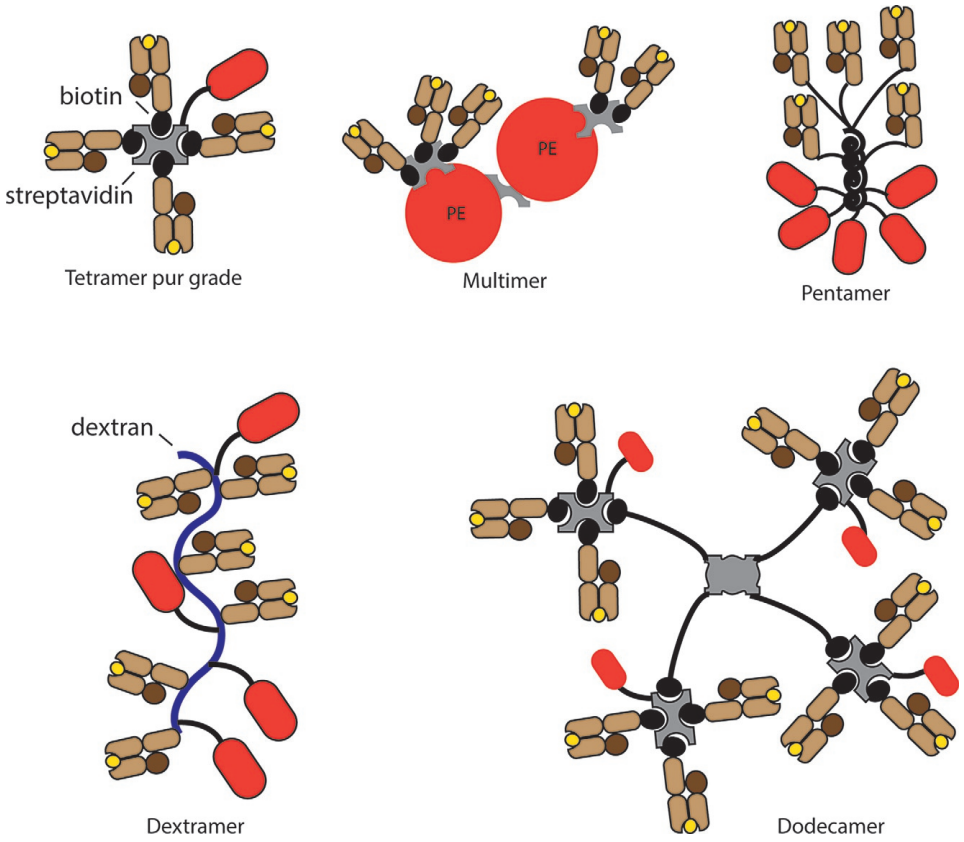

Fig. 1 Representation of the most commonly used soluble pMHC-based reagents. Cartoons of pMHC oligomers and their multimeric scaffolds. Red circles represent PE fluorochromes.

2.3 An improved staining protocol

Despite all efforts to improve the quality of pMHC multimers, they can still fail to detect relevant functional T-cell clonotypes. Several reports highlighted discrepancies between frequencies of antigen-specific $CD8^+$ and $CD4^+$ T cells determined by functional assays (ELISpot and ICS) and by multimer staining (Rius et al., 2018; Rubio-Godoy et al., 2001). This is mainly due to the difficulty to stain T cells bearing TCRs of low affinity for cognate antigen as pMHC-TCR binding strength needed for efficient staining is superior to the one needed for T-cell activation (Laugel et al., 2007).

Several optimizations in staining protocols have led to improved methodology for detection of very low affinity T cells such as $CD4^+$ T cells or

those directed against self-antigens (i.e., anticancer and autoimmune). First, the use of the protein kinase inhibitor Dasatinib improves the physical detection of $CD8^+$ T cells by inhibiting TCR downregulation pathways preventing TCR internalization, therefore increasing cell surface TCR presentation (Lissina et al., 2009; Weichsel et al., 2008). However, it cannot be used for functional profiling assays as it inhibits cellular activation. Second, the use of an anti-PE monoclonal antibody targeting cell surface bound pMHC multimers helps stabilizing their binding. This anti-PE can directly be coupled to magnetic beads allowing at the same time antigen-specific $CD8^+$ T cells enrichment (Dolton et al., 2018).

Staining of antigen-specific $CD4^+$ T cells can be improved, first by using molecularly defined pMHC class II multimers lowering the affinity threshold of detectable clones and second by using glycoside hydrolase enzymes, like neuraminidase (i.e., from *Vibrio cholerae*), as staining efficiency critically depends on $CD4^+$ T cells surface glycosylation (Massilamany, Gangaplara, Chapman, Rose, & Reddy, 2011; Reddy et al., 2003).

It is important to point out that effect of Dasatinib and/or neuraminidase on T cell viability, proliferation or functional analysis has never been clearly investigated and even they provide a significant gain in staining efficiency, care should be considered for T cell sorting and cloning.

Temperature is also an important parameter influencing staining efficiencies. It has been reported that the binding of pMHC class I multimers to antigen-specific $CD8^+$ T cells can strongly induce cell activation, sometimes leading to apoptosis. This TCR-induced cell death is directly correlated to and increases with TCR affinity. This negative effect can be circumvented by the use of dasatinib and manipulation of cells at 4 °C (Dolton et al., 2018). On the other side, staining of antigen-specific $CD4^+$ T cells is better when performed at 37 °C and it has never been reported any TCR-induced cell death of these latter with soluble pMHC class II multimers.

The choice of anti-CD8 and/or anti-CD4 antibodies can also affect multimer staining. Generally, these anti-coreceptor antibodies can be disruptive and should therefore be used in a second step after cells were stained with multimers (Wooldridge et al., 2006).

Finally, it is important to highlight that both pMHC class I and II multimers can be aliquoted and frozen. A comparative study showed they can be cryopreserved for at least 6 months, which is advantageous for low stability pMHC complexes and better reliability (Hadrup et al., 2015).

3. Staining of antigen-specific $CD8^+$ and $CD4^+$ T cells: Materials and methods

The protocol described below is intended for the detection of a single antigen-specific $CD8^+$ T cell and a single antigen-specific $CD4^+$ T cell population in a given sample of PBMCs. Detection of multiple pMHC specificities in one sample is discussed later in this chapter. This protocol can also be adapted for detection of only $CD8^+$ or $CD4^+$ antigen-specific T cells.

General recommendations before starting are (i) work fast with freshly-prepared reagents and solutions and (ii) avoid light-exposure for all reagents containing fluorochromes. Indicated volumes are intended for 10^7 T cells but can be adapted for other cell numbers.

3.1 Materials

3.1.1 Chemicals and reagents

1. Pan human T cell isolation kit, ref# 130-096-535, Miltenyi
2. Alexa Fluor 488 anti-human CD8 antibody, clone SK1, ref# 344716, Biolegend
3. PE/Cy7 anti-human CD4 antibody, clone A161A1, ref# 357409, Biolegend
4. PE-labeled pMHC class I multimer
5. APC-labeled pMHC class II multimer
6. Mouse anti-PE primary unconjugated monoclonal antibody, clone PE001, ref# 408101, BioLegend
7. Mouse anti-APC primary unconjugated monoclonal antibody, clone APC003, ref# 408001, BioLegend
8. Live/Dead cell marker (4′,6-diamidino-2-phenylindole, DAPI), ref# D1306, ThermoFisher Scientific
9. Dasatinib, ref# 1392, Axon Medchem
10. Neuraminidase, ref# 11585886001, Sigma-Aldrich

3.1.2 Instruments and software

1. Flow cytometer LSR II, Becton Dickinson
2. FlowJo software, Tristar
3. Centrifuge 5810R, Eppendorf

3.1.3 Solutions

1. FACS buffer: PBS pH 7.2, 0.5% BSA, 2 mM EDTA, 0.02% NaN_3.
2. Dasatinib: 1 mM single use DMSO stocks at −80 °C. Final experimental concentration is 50 nM in PBS.
3. Neuraminidase: final experimental concentration is 0.2 U/mL in PBS.
4. pMHC class I/II multimers: stock solution at 200 nM. Final experimental concentration is usually 4 nM in FACS buffer but should be determined by titration if possible.
5. Mouse anti-PE (or APC) antibody: final experimental concentration is 10 μg/mL in FACS buffer.
6. Anti-CD8 and anti-CD4 antibodies: final experimental concentration should be determined by titration.
7. DAPI: 1 mg/mL H_2O stocks at 4 °C. Final experimental concentration is 1 μg/mL FACS buffer.

3.1.4 Methods

1. T cells isolation from PBMCs using Pan T cell isolation kit
   - Count PBMCs with trypan blue.
   - Centrifuge PBMCs 5 min at 400*g*. Discard supernatant and resuspend pellet in 40 μL of FACS buffer per 10^7 cells.
   - Add 10 μL of Pan T cell biotin-antibody cocktail per 10^7 cells.
   - Mix well and incubate for 5 min at 4 °C in the refrigerator.
   - Add 30 μL of FACS buffer per 10^7 cells.
   - Add 20 μL of Pan T cell microbead cocktail per 10^7 cells.
   - Mix well and incubate for 10 min at 4 °C in the refrigerator.
   - Proceed to subsequent magnetic cell separation. A minimum volume of 500 μL is required. If needed add FACS buffer to the cell suspension.
   - Place LS column in the magnetic field of a suitable MACS Separator.
   - Wash column three times with 3 mL of FACS buffer.
   - Apply cell suspension and collect flow-through containing unlabeled cells, representing the enriched T cells in a 15 mL Falcon tube.
   - Rinse column with 3 mL of FACS buffer and keep collecting in the same Falcon tube.
   - Count T cells with trypan blue.
2. Staining of antigen-specific $CD8^+$ and $CD4^+$ T cells
   - Centrifuge T cells 5 min at 400*g*, discard supernatant and resuspend pellet in 1 mL of dasatinib/neuraminidase solution per 10^7 cells.
   - Incubate 30 min at 37 °C.

- Add 5 mL of FACS buffer and centrifuge 5 min at 400*g*.
- Discard supernatant and resuspend pellet in 100 μL of pMHC class I/II multimer solution per 10^7 cells.
- Mix well and incubate 40 min at 4 °C in the refrigerator.
- Add 5 mL of FACS buffer and centrifuge 5 min at 400*g*.
- Discard supernatant and resuspend pellet in 100 μL of anti-PE and anti-APC antibodies.
- Mix well and incubate 20 min at 4 °C in the refrigerator.
- Add 5 mL of FACS buffer and centrifuge 5 min at 400*g*.
- Discard supernatant and resuspend pellet in 100 μL of antibody cocktail solution per 10^7 cells.
- Mix well and incubate 20 min at 4 °C in the refrigerator.
- Add 5 mL of FACS buffer and centrifuge 5 min at 400*g*.
- Add 5 mL of FACS buffer and centrifuge 5 min at 400*g*.
- Discard supernatant and resuspend pellet in 200 μL of DAPI solution.
- Keep sample on ice and proceed immediately with FACS analysis.

3. Flow cytometer acquisition and analysis

- Calibrate the flow cytometer using reference beads.
- Using unstained control cells and single-color stained samples adjust the location of viable lymphocyte gate (FSC vs SSC) as well as single color signals (by changing voltages).
- Automatically calculate compensations.
- Run negative control samples using irrelevant cells (alternatively irrelevant pMHC multimers) stained identically.
- Acquire data by collecting events of each sample tube and negative control tube.
- Gating strategy and analysis
  - Import FCS files and open them with FlowJo. Start analyzing a negative control sample.
  - Plot FSC-A vs SSC-A and draw a gate around live lymphocytes.
  - Plot FSC-A vs FSC-H and gate on single cells.
  - Plot SSC-H vs SSC-A and gate on single cells.
  - Plot FSC-A vs DAPI and gate on live, DAPI negative cells.
  - Plot CD8 vs CD4 and draw gates around $CD8^+$ and $CD4^+$ populations.
  - Plot separately CD8 vs pMHC class I multimer and CD4 vs pMHC class II multimer and set quadrant boundaries according to multimer backgrounds determined with the negative irrelevant sample tubes.
  - Analyze all samples without changing gates.

4. High dimensional T-cell staining

Developments of personalized immunotherapies call for a growing need for high-throughput, multiple screening of T-cell specificities in limited samples. Recently, innovative combinatorial staining strategies using pMHC class I multimers were made possible to screen for >1000 specificities in a single sample, better mapping immune responses at a genome-wide level (Bentzen & Hadrup, 2017).

4.1 High-throughput pMHC monomer synthesis

Generation of pMHC class I monomers is tedious and time-consuming. Because empty MHC class I molecules are unstable, each new pMHC complex has to be individually refolded and purified before multimerization, limiting their use to only few selected epitopes at one time. This prompted the development of new methods for multiplexed parallel synthesis of pMHC class I monomers. Strategies are based on the large-scale production of a single pMHC class I complex used for subsequent peptide exchange with peptides of interest. Rodenko et al. reported an elegant way of high-throughput synthesis using a pMHC class I complex refolded with a photocleavable peptide that is cleaved upon UV irradiation (Rodenko et al., 2006). Addition of a "rescue" peptide in the solution, if of sufficient affinity, can restore the pMHC complex by displacing cleaved fragments from the binding groove. In situ-produced pMHC monomers can then be multimerized and directly used for staining purposes. This UV-conditional approach allows as well the quantification of peptide binding to a given MHC molecule thanks to the use of a conformational antibody and has facilitated the fast discovery of multiple epitopes. Such UV-conditional peptides have now been designed for a large number of MHC class I alleles, of both human and murine origin. However, this approach requires the use of a specific photocleavable peptide for each MHC allele. UV exposure can also damage MHC molecules and "rescue" peptides, create nitroso reactive species and lead to sample evaporation due to overheating. A similar approach used a chemically-cleavable peptide to generate pMHC that this time is cleaved by addition of periodate or dithionite and replaced by a peptide of interest (Rodenko et al., 2009). Again, the need to find an efficient conditional peptide for each MHC allele and the possible chemical side effects have limited its widespread use. Dipeptides can also act as catalysts and facilitate the folding reaction and peptide exchange by binding to the F pocket of MHC class I

molecules but have never been applied in high-throughput generation of pMHC multimers (Saini et al., 2015). More recently the thermo-labile production of pMHC class I monomers was introduced (Luimstra et al., 2018). A pMHC class I complex is refolded with a peptide having a low off-rate at 4 °C. Because complexes undergo conformational changes at a certain temperature leading to full peptide dissociation, increasing temperature will promote exchange with higher affinity peptides creating new stable pMHC complexes. This strategy does not require the use of specific, non-natural amino acids nor deleterious triggers and can be applied directly after pMHC multimer formation. Even if the design of thermo-labile peptides is not trivial and only reported so far for H-2K^b and HLA-A0201 in monitoring viral responses, there is no doubt that this principle will be expanded. Thanks to these different methods the synthesis of pMHC class I monomers is no longer a time limiting factor.

4.2 Fluorochrome-based combinatorial staining

Parallel identification of multiple antigen-specific CD8$^+$ and CD4$^+$ T cells with conventional pMHC multimers is limited by the low number of streptavidin-conjugated fluorochromes available. In 2009, two innovative strategies using fluorescent multidimensional encoding of pMHC class I multimers were reported.

Assuming that a single T cell will only bind one pMHC complex, distinct color-coding can be assigned to each specific pMHC multimer. Hadrup et al. reported a dual-color coding, where each antigen-specific population is stained using a unique combination of two specific pMHC multimers, providing a detection limit of 0.002% in terms of frequency (Hadrup et al., 2009). In the meantime, Newell et al. reported the use of multivalent color coding, using combinations of one to four colors to stain individual antigen-specific populations (Newell, Klein, Yu, & Davis, 2009). If the multivalent color-coding strategy theoretically provides a higher number of color combinations, it has the disadvantage of reducing staining intensity as the number of colors is increasing. The dual-color coding, thus, provides a lower number of unique combinations but a better staining intensity and a lower background as any T cell not matching the color combination is gated out and recorded as a background event. This approach has also been successfully tested with pMHC class II multimers directly ex vivo (Uchtenhagen et al., 2016).

4.3 Heavy-metal ions-based combinatorial staining

With the advent of mass cytometry, using heavy metal ions, the number of parallel labels detectable increased dramatically (Chen & Weng, 2012). Newell et al. reported the screening of 109 different antigen-specificities in a single sample combined with phenotype and functional analysis (Newell, Sigal, Bendall, Nolan, & Davis, 2012). Combinatorial staining by mass cytometry offers higher order of combinations and simplifies the analysis as no/little compensations are required, each metal ion being detectable in a single channel. Yet this technology has several drawbacks including low resolution and processing speed, high instrument and reagents costs and the lack of cell recovery as cells are nebulized during the process.

4.4 DNA-barcoded pMHC multimers

More recently, Bentzen et al. have reported the use of DNA-barcoded pMHC multimers (Bentzen et al., 2016) (Fig. 2). These reagents are made of a polysaccharide dextran backbone (like Dextramers) carrying a high number of SA and PE. Biotinylated pMHC as well as biotinylated DNA barcodes can be coupled to free SA binding sites generating high avidity reagents with a unique combination of theoretically up to 10^{10} single DNA barcodes. After combinatorial staining of a single sample (with >1000 pMHC specificities), antigen-specific $CD8^+$ T cells can be sorted by means of the PE signal and subsequently, DNA barcodes amplified and identified by high-throughput sequencing. The number of reads for a specific DNA barcode assigned to a given pMHC correlates with the frequency of antigen-specific T cells within the sorted population. Even if TCR expression and affinity might introduce a bias to be fully quantitative, comparison between fluorochrome-based and DNA barcode combinatorial determination of T-cell frequencies showed high correlation ($r^2 > 0.9$ across 10 healthy donors and 11 melanoma patients looking at 32 and 15 T-cell responses, respectively). Moreover, even cells labeled with low levels of DNA-barcodes will be detected and counted as positives after DNA amplification where fluorescent labeled would not have provided sufficient separation of multimer positive and negative cells. This is of particular interest for low affinity clones like $CD4^+$ T cells.

The invaluable advantage of DNA barcoded pMHC multimers is the possibility to screen an unprecedented number of antigens in a single, often limited sample. Due to higher sensitivity and lower detection limits compared to other previous methodologies, it enables earlier screening of

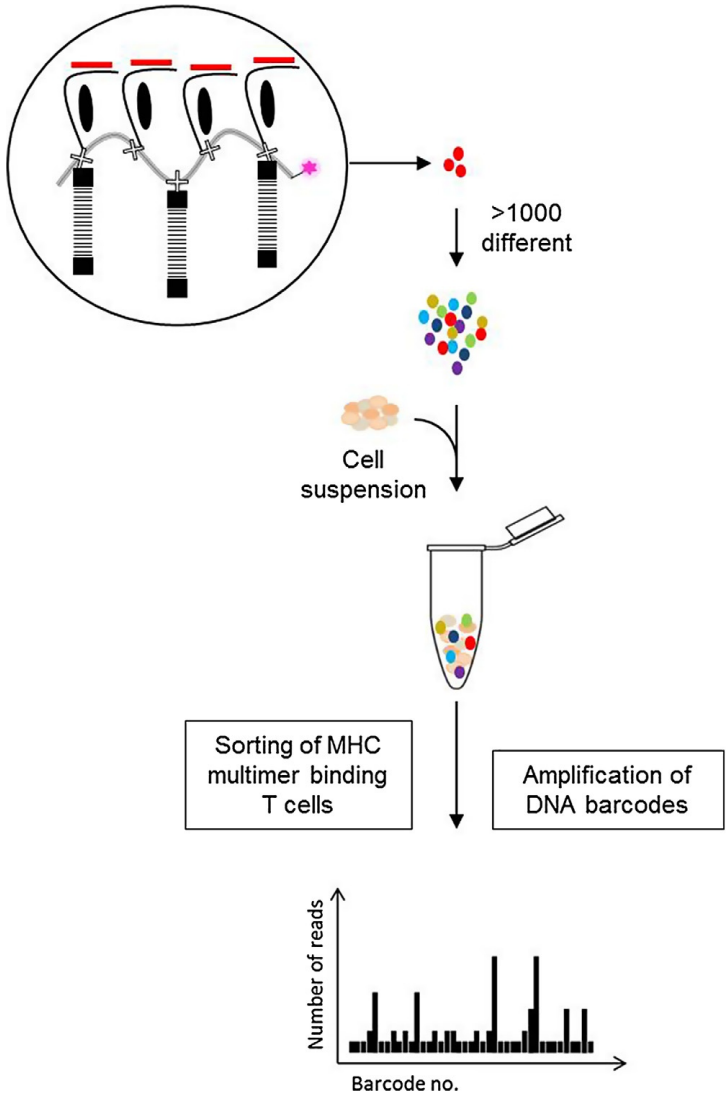

Fig. 2 Detection of antigen-responsive T cells using the DNA barcode-labeled MHC multimer methodology. A PE-labeled dextran backbone carrying a number of SA binding sites (illustrated as an X) is applied to co-attach biotinylated molecules; DNA barcodes and pMHCs. Thus, >1000 pMHC multimers can be generated, each carrying a different DNA barcode. All MHC multimer binding T cells are sorted based on the common fluorescent label and the associated DNA barcodes are amplified and sequenced. The relative numbers of DNA barcode reads are used to determine the composition of antigen-responsive T cells in the sample. *Reproduced from Bentzen, A. K., & Hadrup, S. R. (2017). Evolution of MHC-based technologies used for detection of antigen-responsive T cells.* Cancer Immunology, Immunotherapy, 66*(5), 657–666. doi:10.1007/s00262-017-1971-5, according to the terms of the Creative Commons Attribution 4.0 International License (http://creativecommons.org/licenses/by/4.0/).*

PBMCs or TILS that could be less expanded and then less prone to cell culture bias. The possibility for high dimensional screening in a sample allows unbiased interpretation of antigen-specific T-cell frequencies as all precursor T cells will be in presence of the entire pMHC library. The DNA-barcoded methodology has been applied in both peripheral blood and tissue biopsies (Bentzen et al., 2016). However, even if in theory the combination of DNA barcodes would be sufficient to cover antigens at a genome-wide level, many limitations are still to be addressed. First, this strategy does not allow, as for the mass cytometry approach, recovery of viable cells since cells are lyzed during processing. Second, the manufacturing of such large libraries is limited by the inherent production costs and turnover times of synthetic peptides that are incompressible. Also, as one pMHC can be recognized by several TCRs, cross-reactivity cannot be evaluated by this approach as the number of reads cannot be associated with any visual assessment. Very recently, it has been applied at the single cell level enabling integration of transcriptome, cell-surface protein, immune repertoire and TCR-antigen specificity measurements. Combining DNA-barcoded pMHC dextramers (Immudex) with single cell immune profiling (10× Genomics) allows direct correlation between TCR sequences and their antigen specificity at unprecedented resolution. This high-throughput, highly sensitive and unbiased methodology will rapidly increase our understanding of T-cell recognition. Finally, the group of Hadrup showed the feasibility of applying the DNA-barcoded multimers strategy to determine TCR cross-recognition patterns, which they termed the TCR fingerprinting (Bentzen et al., 2018). The authors investigated the recognition pattern of two distinct TCRs recognizing each a 10mer epitope derived from Merkel cell polyomavirus. They mutated each position of the two epitopes with all possible amino acid available and used these large peptides variants libraries for high-throughput generation of DNA-barcoded multimers. By measuring the relative affinity of TCRs to libraries of barcoded pMHC variants it is possible to determine the TCR fingerprinting and to fully characterize TCR cross-recognition. Even if the study was only extended to a limited number of TCRs, the power of this approach is invaluable in evaluating potential clinical risks of cross-reactivity in TCR-based therapies.

5. Reversible pMHC multimer for comprehensive analysis of antigen-specific T cells

Reversible pMHC multimers are reagents in which pMHC monomers can be disrupted from the multimeric scaffold upon addition of a

specific stimulus. Because of the weak affinity of pMHC monomers for TCRs, staining with reversible multimers allows the removal of all pMHC monomers from the cell surface.

5.1 Isolation of "untouched" antigen-specific CD8 T cells

It is known that staining of antigen-specific $CD8^+$ T cells with pMHC multimers can lead to TCR-mediated activation and even in some cases to TCR-induced cell death (Cebecauer, Guillaume, Hozak, et al., 2005). In 2002, Knabel et al. reported the use of *Streptamers*, reversible pMHC class I multimers commercially available from IBA Life Science (Knabel et al., 2002). *Streptamers* are built on an optimized streptactin-streptag scaffold mimicking the streptavidin-biotin interaction. Because streptactin binds more avidly biotin than streptag, addition of free biotin allows the dissociation of pMHC monomers from the multimeric scaffold. More recently, reversible multimers built on Ni^{2+}-NTA-Histag chelates complexes that can be disrupted upon addition of imidazole (so-called NTAmers) were described (Schmidt et al., 2011). If NTAmers appear more stable and provide better staining efficiencies than *Streptamers*, both reversible reagents showed similar advantages for isolation of "untouched" antigen-specific $CD8^+$ T cells. Sorting of antigen-specific $CD8^+$ T cells with NTAmers or *Streptamers* leads to better cloning efficiencies by preventing the loss of high affinity T cell clones that can fully undergo TCR-induced apoptosis when conventional multimers are used (Neudorfer et al., 2007; Schmidt et al., 2011). This approach then allows the analysis of complete TCR repertoires of antigen-specific $CD8^+$ T cells. Even applicable to antigen-specific $CD4^+$ T cells, reversible sorting of $CD4^+$ T cells has not been yet fully evaluated.

5.2 Measurement of pMHC-TCR monomeric dissociation rates

A major advantage of reversible multimers is the measurement of pMHC-TCR dissociation kinetics. By addition of a fluorescent label on the β2m (i.e., Cy5), it is possible to follow over time the dissociation of pMHC monomers from the engaged TCR after dissociation of the multimeric scaffold. Briefly, antigen-specific $CD8^+$ T cells are stained in the cold to avoid internalization and cell-associated PE (multimeric scaffold) and Cy5 (pMHC monomers) fluorescence are recorded before and after the addition of the disruptive stimulus. Nauerth et al. used *Streptamers* in real-time microscopic-based assay to measure monomeric pMHC-TCR dissociation

kinetics on live virus-specific $CD8^+$ T cells and showed a correlation between off-rates and T cell responsiveness in vitro as well as a better protection capacity in vivo (Nauerth et al., 2013). More recently, similar work was performed on self tumor-specific $CD8^+$ T cells using NTAmers, as these reagents, due to faster decay under the monomeric form upon addition of imidazole, allow measurement of lower affinity T cells (Hebeisen et al., 2015). Allard et al. have used the NTAmer technology for a comprehensive analysis of structural and functional avidities of virus and tumor-specific $CD8^+$ T cells (Allard et al., 2017). They showed a strong correlation between pMHC-TCR off-rates and cytokine production, polyfunctionality, cell proliferation, activating/inhibitory receptor expression and in vivo tumor control. Moreover, the pMHC-TCR off-rate is a more stable and more reliable parameter than conventional functional assays that depend on the T cell's shape and activation state.

The use of reversible pMHC multimers has proven its importance in sorting "untouched" $CD8^+$ T cells and characterization of their TCR structural affinities. Despite several drawbacks, like the need to clone and expand specific T cells before affinity measurements or their restriction to $CD8^+$ T cells analysis as $CD4^+$ T cells display too weak affinity TCR precluding their efficient use, they remain a useful tool for rapid screening of functionally relevant $CD8^+$ T cells.

6. Conclusion

Technical advances have been recently made to identify and isolate antigen-specific $CD8^+$ and $CD4^+$ T cells using soluble pMHC class I and II multimers. Detection of low avidity T cells, especially self-reactive and $CD4^+$ T cells, has been dramatically improved using molecularly defined pMHC class II monomers and optimized staining protocols. Developments of high-throughput pMHC class I synthesis as well as combinatorial strategies allow rapid and parallel screening of thousands of antigen specificities in a precious and limited blood sample or tissue biopsies. Finally, developments of reversible pMHC class I multimers allow high-throughput screening of functionally relevant viral or self tumor-specific T cell clones. Application of these methodologies at the single cell level will greatly improve our understanding of mechanisms governing T cell recognition. Future developments will be needed to reduce costs and automate processes.

References

Allard, M., Couturaud, B., Carretero-Iglesia, L., Duong, M. N., Schmidt, J., Monnot, G. C., et al. (2017). TCR-ligand dissociation rate is a robust and stable biomarker of CD8+ T cell potency. *JCI Insight*, *2*(14). https://doi.org/10.1172/jci.insight.92570.

Altman, J. D., Moss, P. A., Goulder, P. J., Barouch, D. H., McHeyzer-Williams, M. G., Bell, J. I., et al. (1996). Phenotypic analysis of antigen-specific T lymphocytes. *Science*, *274*(5284), 94–96.

Angelov, G. S., Guillaume, P., Cebecauer, M., Bosshard, G., Dojcinovic, D., Baumgaertner, P., et al. (2006). Soluble MHC-peptide complexes containing long rigid linkers abolish CTL-mediated cytotoxicity. *Journal of Immunology*, *176*(6), 3356–3365.

Ayyoub, M., Dojcinovic, D., Pignon, P., Raimbaud, I., Schmidt, J., Luescher, I., et al. (2010). Monitoring of NY-ESO-1 specific CD4+ T cells using molecularly defined MHC class II/His-tag-peptide tetramers. *Proceedings of the National Academy of Sciences of the United States of America*, *107*(16), 7437–7442. https://doi.org/10.1073/pnas.1001322107.

Ayyoub, M., Pignon, P., Dojcinovic, D., Raimbaud, I., Old, L. J., Luescher, I., et al. (2010). Assessment of vaccine-induced CD4 T cell responses to the 119-143 immunodominant region of the tumor-specific antigen NY-ESO-1 using DRB1*0101 tetramers. *Clinical Cancer Research*, *16*(18), 4607–4615. https://doi.org/10.1158/1078-0432.CCR-10-1485.

Batard, P., Peterson, D. A., Devevre, E., Guillaume, P., Cerottini, J. C., Rimoldi, D., et al. (2006). Dextramers: New generation of fluorescent MHC class I/peptide multimers for visualization of antigen-specific CD8+ T cells. *Journal of Immunological Methods*, *310*(1–2), 136–148. https://doi.org/10.1016/j.jim.2006.01.006.

Bentzen, A. K., & Hadrup, S. R. (2017). Evolution of MHC-based technologies used for detection of antigen-responsive T cells. *Cancer Immunology, Immunotherapy*, *66*(5), 657–666. https://doi.org/10.1007/s00262-017-1971-5.

Bentzen, A. K., Marquard, A. M., Lyngaa, R., Saini, S. K., Ramskov, S., Donia, M., et al. (2016). Large-scale detection of antigen-specific T cells using peptide-MHC-I multimers labeled with DNA barcodes. *Nature Biotechnology*, *34*(10), 1037–1045. https://doi.org/10.1038/nbt.3662.

Bentzen, A. K., Such, L., Jensen, K. K., Marquard, A. M., Jessen, L. E., Miller, N. J., et al. (2018). T cell receptor fingerprinting enables in-depth characterization of the interactions governing recognition of peptide-MHC complexes. *Nature Biotechnology*, *36*, 1191–1196. https://doi.org/10.1038/nbt.4303.

Bobisse, S., Genolet, R., Roberti, A., Tanyi, J. L., Racle, J., Stevenson, B. J., et al. (2018). Sensitive and frequent identification of high avidity neo-epitope specific CD8 (+) T cells in immunotherapy-naive ovarian cancer. *Nature Communications*, *9*(1), 1092. https://doi.org/10.1038/s41467-018-03301-0.

Boniface, J. J., Rabinowitz, J. D., Wulfing, C., Hampl, J., Reich, Z., Altman, J. D., et al. (1998). Initiation of signal transduction through the T cell receptor requires the multivalent engagement of peptide/MHC ligands [corrected]. *Immunity*, *9*(4), 459–466.

Brett, S. J., Kingston, A. E., & Colston, M. J. (1987). Limiting dilution analysis of the human T cell response to mycobacterial antigens from BCG vaccinated individuals and leprosy patients. *Clinical and Experimental Immunology*, *68*(3), 510–520.

Carson, R. T., Vignali, K. M., Woodland, D. L., & Vignali, D. A. (1997). T cell receptor recognition of MHC class II-bound peptide flanking residues enhances immunogenicity and results in altered TCR V region usage. *Immunity*, *7*(3), 387–399.

Cebecauer, M., Guillaume, P., Hozak, P., Mark, S., Everett, H., Schneider, P., et al. (2005). Soluble MHC-peptide complexes induce rapid death of CD8+ CTL. *Journal of Immunology*, *174*(11), 6809–6819.

Cebecauer, M., Guillaume, P., Mark, S., Michielin, O., Boucheron, N., Bezard, M., et al. (2005). CD8+ cytotoxic T lymphocyte activation by soluble major histocompatibility complex-peptide dimers. *The Journal of Biological Chemistry*, *280*(25), 23820–23828. https://doi.org/10.1074/jbc.M500654200.

Chen, G., & Weng, N. P. (2012). Analyzing the phenotypic and functional complexity of lymphocytes using CyTOF (cytometry by time-of-flight). *Cellular & Molecular Immunology*, *9*(4), 322–323. https://doi.org/10.1038/cmi.2012.16.

Dolton, G., Lissina, A., Skowera, A., Ladell, K., Tungatt, K., Jones, E., et al. (2014). Comparison of peptide-major histocompatibility complex tetramers and dextramers for the identification of antigen-specific T cells. *Clinical and Experimental Immunology*, *177*(1), 47–63. https://doi.org/10.1111/cei.12339.

Dolton, G., Zervoudi, E., Rius, C., Wall, A., Thomas, H. L., Fuller, A., et al. (2018). Optimized peptide-MHC multimer protocols for detection and isolation of autoimmune T-Cells. *Frontiers in Immunology*, *9*, 1378. https://doi.org/10.3389/fimmu.2018.01378.

Fooksman, D. R., Vardhana, S., Vasiliver-Shamis, G., Liese, J., Blair, D. A., Waite, J., et al. (2010). Functional anatomy of T cell activation and synapse formation. *Annual Review of Immunology*, *28*, 79–105. https://doi.org/10.1146/annurev-immunol-030409-101308.

Frayser, M., Sato, A. K., Xu, L., & Stern, L. J. (1999). Empty and peptide-loaded class II major histocompatibility complex proteins produced by expression in *Escherichia coli* and folding in vitro. *Protein Expression and Purification*, *15*(1), 105–114. https://doi.org/10.1006/prep.1998.0987.

Fremont, D. H., Hendrickson, W. A., Marrack, P., & Kappler, J. (1996). Structures of an MHC class II molecule with covalently bound single peptides. *Science*, *272*(5264), 1001–1004.

Garboczi, D. N., Hung, D. T., & Wiley, D. C. (1992). Hla-A2-peptide complexes—Refolding and crystallization of molecules expressed in *Escherichia coli* and complexed with single antigenic peptides. *Proceedings of the National Academy of Sciences of the United States of America*, *89*(8), 3429–3433. https://doi.org/10.1073/pnas.89.8.3429.

Gebe, J. A., Falk, B. A., Rock, K. A., Kochik, S. A., Heninger, A. K., Reijonen, H., et al. (2003). Low-avidity recognition by CD4+ T cells directed to self-antigens. *European Journal of Immunology*, *33*(5), 1409–1417. https://doi.org/10.1002/eji.200323871.

Gorska, M. M., & Alam, R. (2003). Signaling molecules as therapeutic targets in allergic diseases. *Journal of Allergy and Clinical Immunology*, *112*(2), 241–250. https://doi.org/10.1067/mai.2003.1667.

Hadrup, S. R., Bakker, A. H., Shu, C. J., Andersen, R. S., van Veluw, J., Hombrink, P., et al. (2009). Parallel detection of antigen-specific T-cell responses by multidimensional encoding of MHC multimers. *Nature Methods*, *6*(7), 520–526. https://doi.org/10.1038/nmeth.1345.

Hadrup, S. R., Maurer, D., Laske, K., Frosig, T. M., Andersen, S. R., Britten, C. M., et al. (2015). Cryopreservation of MHC multimers: Recommendations for quality assurance in detection of antigen specific T cells. *Cytometry. Part A*, *87*(1), 37–48. https://doi.org/10.1002/cyto.a.22575.

Hebeisen, M., Schmidt, J., Guillaume, P., Baumgaertner, P., Speiser, D. E., Luescher, I., et al. (2015). Identification of rare high-avidity, tumor-reactive CD8+ T cells by monomeric TCR-ligand off-rates measurements on living cells. *Cancer Research*, *75*(10), 1983–1991. https://doi.org/10.1158/0008-5472.CAN-14-3516.

Huang, J., Zeng, X., Sigal, N., Lund, P. J., Su, L. F., Huang, H., et al. (2016). Detection, phenotyping, and quantification of antigen-specific T cells using a peptide-MHC dodecamer. *Proceedings of the National Academy of Sciences of the United States of America*, *113*(13), E1890–E1897. https://doi.org/10.1073/pnas.1602488113.

Hugues, S., Malherbe, L., Filippi, C., & Glaichenhaus, N. (2002). Generation and use of alternative multimers of peptide/MHC complexes. *Journal of Immunological Methods*, *268*(1), 83–92.

Knabel, M., Franz, T. J., Schiemann, M., Wulf, A., Villmow, B., Schmidt, B., et al. (2002). Reversible MHC multimer staining for functional isolation of T-cell populations and effective adoptive transfer. *Nature Medicine*, *8*(6), 631–637. https://doi.org/10.1038/nm0602-631.

Laugel, B., van den Berg, H. A., Gostick, E., Cole, D. K., Wooldridge, L., Boulter, J., et al. (2007). Different T cell receptor affinity thresholds and CD8 coreceptor dependence govern cytotoxic T lymphocyte activation and tetramer binding properties. *The Journal of Biological Chemistry*, *282*(33), 23799–23810. https://doi.org/10.1074/jbc.M700976200.

Leisner, C., Loeth, N., Lamberth, K., Justesen, S., Sylvester-Hvid, C., Schmidt, E. G., et al. (2008). One-pot, mix-and-read peptide-MHC tetramers. *PLoS One*, *3*(2), e1678. https://doi.org/10.1371/journal.pone.0001678.

Lissina, A., Ladell, K., Skowera, A., Clement, M., Edwards, E., Seggewiss, R., et al. (2009). Protein kinase inhibitors substantially improve the physical detection of T-cells with peptide-MHC tetramers. *Journal of Immunological Methods*, *340*(1), 11–24. https://doi.org/10.1016/j.jim.2008.09.014.

Luimstra, J. J., Garstka, M. A., Roex, M. C. J., Redeker, A., Janssen, G. M. C., van Veelen, P. A., et al. (2018). A flexible MHC class I multimer loading system for large-scale detection of antigen-specific T cells. *The Journal of Experimental Medicine*, *215*(5), 1493–1504. https://doi.org/10.1084/jem.20180156.

Massilamany, C., Gangaplara, A., Chapman, N., Rose, N., & Reddy, J. (2011). Detection of cardiac myosin heavy chain-alpha-specific CD4 cells by using MHC class II/IA (k) tetramers in A/J mice. *Journal of Immunological Methods*, *372*(1–2), 107–118. https://doi.org/10.1016/j.jim.2011.07.004.

Nauerth, M., Weissbrich, B., Knall, R., Franz, T., Dossinger, G., Bet, J., et al. (2013). TCR-ligand koff rate correlates with the protective capacity of antigen-specific CD8+ T cells for adoptive transfer. *Science Translational Medicine*, *5*(192), 192ra187. https://doi.org/10.1126/scitranslmed.3005958.

Neudorfer, J., Schmidt, B., Huster, K. M., Anderl, F., Schiemann, M., Holzapfel, G., et al. (2007). Reversible HLA multimers (streptamers) for the isolation of human cytotoxic T lymphocytes functionally active against tumor- and virus-derived antigens. *Journal of Immunological Methods*, *320*(1–2), 119–131. https://doi.org/10.1016/j.jim.2007.01.001.

Newell, E. W., Klein, L. O., Yu, W., & Davis, M. M. (2009). Simultaneous detection of many T-cell specificities using combinatorial tetramer staining. *Nature Methods*, *6*(7), 497–499. https://doi.org/10.1038/nmeth.1344.

Newell, E. W., Sigal, N., Bendall, S. C., Nolan, G. P., & Davis, M. M. (2012). Cytometry by time-of-flight shows combinatorial cytokine expression and virus-specific cell niches within a continuum of CD8+ T cell phenotypes. *Immunity*, *36*(1), 142–152. https://doi.org/10.1016/j.immuni.2012.01.002.

Reddy, J., Bettelli, E., Nicholson, L., Waldner, H., Jang, M. H., Wucherpfennig, K. W., et al. (2003). Detection of autoreactive myelin proteolipid protein 139-151-specific T cells by using MHC II (IAs) tetramers. *Journal of Immunology*, *170*(2), 870–877.

Rius, C., Attaf, M., Tungatt, K., Bianchi, V., Legut, M., Bovay, A., et al. (2018). Peptide-MHC class I tetramers can fail to detect relevant functional T cell clonotypes and underestimate antigen-reactive T cell populations. *Journal of Immunology*, *200*(7), 2263–2279. https://doi.org/10.4049/jimmunol.1700242.

Rodenko, B., Toebes, M., Celie, P. H., Perrakis, A., Schumacher, T. N., & Ovaa, H. (2009). Class I major histocompatibility complexes loaded by a periodate trigger. *Journal of the American Chemical Society*, *131*(34), 12305–12313. https://doi.org/10.1021/ja9037565.

Rodenko, B., Toebes, M., Hadrup, S. R., van Esch, W. J., Molenaar, A. M., Schumacher, T. N., et al. (2006). Generation of peptide-MHC class I complexes through UV-mediated ligand exchange. *Nature Protocols*, *1*(3), 1120–1132. https://doi.org/10.1038/nprot.2006.121.

Rubio-Godoy, V., Dutoit, V., Rimoldi, D., Lienard, D., Lejeune, F., Speiser, D., et al. (2001). Discrepancy between ELISPOT IFN-gamma secretion and binding of A2/peptide multimers to TCR reveals interclonal dissociation of CTL effector function from TCR-peptide/MHC complexes half-life. *Proceedings of the National Academy of Sciences of the United States of America*, *98*(18), 10302–10307. https://doi.org/10.1073/pnas.181348898.

Saini, S. K., Schuster, H., Ramnarayan, V. R., Rammensee, H. G., Stevanovic, S., & Springer, S. (2015). Dipeptides catalyze rapid peptide exchange on MHC class I molecules. *Proceedings of the National Academy of Sciences of the United States of America*, *112*(1), 202–207. https://doi.org/10.1073/pnas.1418690112.

Sant'Angelo, D. B., Robinson, E., Janeway, C. A., Jr., & Denzin, L. K. (2002). Recognition of core and flanking amino acids of MHC class II-bound peptides by the T cell receptor. *European Journal of Immunology*, *32*(9), 2510–2520. https://doi.org/10.1002/1521-4141(200209)32:9<2510::AID-IMMU2510>3.0.CO;2-Q.

Schmidt, J., Dojcinovic, D., Guillaume, P., & Luescher, I. (2013). Analysis, isolation, and activation of antigen-specific CD4(+) and CD8(+) T cells by soluble MHC-peptide complexes. *Frontiers in Immunology*, *4*, 218. https://doi.org/10.3389/fimmu.2013.00218.

Schmidt, J., Guillaume, P., Dojcinovic, D., Karbach, J., Coukos, G., & Luescher, I. (2017). In silico and cell-based analyses reveal strong divergence between prediction and observation of T-cell-recognized tumor antigen T-cell epitopes. *The Journal of Biological Chemistry*, *292*(28), 11840–11849. https://doi.org/10.1074/jbc.M117.789511.

Schmidt, J., Guillaume, P., Irving, M., Baumgaertner, P., Speiser, D., & Luescher, I. F. (2011). Reversible major histocompatibility complex I-peptide multimers containing Ni(2+)-nitrilotriacetic acid peptides and histidine tags improve analysis and sorting of CD8(+) T cells. *The Journal of Biological Chemistry*, *286*(48), 41723–41735. https://doi.org/10.1074/jbc.M111.283127.

Sharrock, C. E., Kaminski, E., & Man, S. (1990). Limiting dilution analysis of human T cells: A useful clinical tool. *Immunology Today*, *11*(8), 281–286.

Tanyi, J. L., Bobisse, S., Ophir, E., Tuyaerts, S., Roberti, A., Genolet, R., et al. (2018). Personalized cancer vaccine effectively mobilizes antitumor T cell immunity in ovarian cancer. *Science Translational Medicine*, *10*(436). https://doi.org/10.1126/scitranslmed.aao5931.

Uchtenhagen, H., Rims, C., Blahnik, G., Chow, I. T., Kwok, W. W., Buckner, J. H., et al. (2016). Efficient ex vivo analysis of CD4+ T-cell responses using combinatorial HLA class II tetramer staining. *Nature Communications*, *7*, 12614. https://doi.org/10.1038/ncomms12614.

Vollers, S. S., & Stern, L. J. (2008). Class II major histocompatibility complex tetramer staining: Progress, problems, and prospects. *Immunology*, *123*(3), 305–313. https://doi.org/10.1111/j.1365-2567.2007.02801.x.

Weichsel, R., Dix, C., Wooldridge, L., Clement, M., Fenton-May, A., Sewell, A. K., et al. (2008). Profound inhibition of antigen-specific T-cell effector functions by dasatinib. *Clinical Cancer Research*, *14*(8), 2484–2491. https://doi.org/10.1158/1078-0432.CCR-07-4393.

Wooldridge, L., Lissina, A., Cole, D. K., van den Berg, H. A., Price, D. A., & Sewell, A. K. (2009). Tricks with tetramers: How to get the most from multimeric peptide-MHC. *Immunology*, *126*(2), 147–164. https://doi.org/10.1111/j.1365-2567.2008.02848.x.

Wooldridge, L., Scriba, T. J., Milicic, A., Laugel, B., Gostick, E., Price, D. A., et al. (2006). Anti-coreceptor antibodies profoundly affect staining with peptide-MHC class I and class II tetramers. *European Journal of Immunology*, *36*(7), 1847–1855. https://doi.org/10.1002/eji.200635886.